Small Scale Methanol Production

Process modelling and design of an autonomous, renewable container sized methanol plant

Marnix L. de Jong

Technische Universiteit Delft

Small Scale Methanol Production

Process modelling and design of an autonomous, renewable container sized methanol plant

By

M.L. de Jong

in partial fulfilment of the requirements for the degree of

Master of Science
in Sustainable Process and Energy Technologies

at the Delft University of Technology,

to be defended publicly on Wednesday April 4, 2018 at 11:00 AM.

Supervisor:	Prof. dr. ir. W. de Jong	TU Delft
Thesis committee:	Dr. ir. G. Korevaar	TU Delft
	Ir. T. Woudstra	TU Delft
	Ir. J. van Kranendonk	ZEF

TU Delft

Preface

Great are the works of the LORD, studied by all who delight in them.
Psalm 111:2

This master thesis is a report of all my efforts of the past year. More than that however, it is the conclusion to my time as a student at the TU Delft. For seven and a half years I have worked to obtain this degree. At times vigorously and focused, at other times more as a side project to other undertaken activities, but almost always with an, as the Dutch like to call it 'frisse portie tegenzin' which roughly translates to 'a healthy amount of reluctance'. Still, in the end I look back with satisfaction and an appropriate amount of pride at this achievement.

I would like to thank several people for their support in writing this master thesis. Wiebren, thank you for always finding some time in your very busy schedule to provide my work with constructive criticism and ideas to improve the academic quality. Jan, thank you very much for always being able to meet on very short notice, giving helpful advice on managing the project, providing me with useful literature and maybe most importantly always being almost instantly available to help me find the bug in my code. Gijsbert and Theo, thank you for taking the time to read through my entire report by taking place in my graduation committee.

Also, I would like to thank my parents, whom have supported me morally and financially through my whole education. Their unconditional love and support has been the basis for my achievements. Thank you very much! Thanks to all my friends who took interest in my work and giving me motivation. Thanks to my fellow students who kept me from working on my thesis during our numerous breaks.

Carine, thank you for believing in me, for always being there to cheer me up, for always offering to help me and designing the front cover. Finally, thank you God for giving me life and energy to perform daily and for creating this amazing world for us all to investigate and discover.

Marnix de Jong, Delft, 21-3-2018

Abstract

At the United Nations Climate Change Conference held in Paris in 2015, ambitious goals for the worldwide CO_2 emissions were set. To achieve these goals, a huge reduction in CO_2 emissions must be realized. For the energy market, the current aim is to use renewable electricity instead of fossil fuels. However, there are multiple sectors where electricity is not a suitable form of energy, due to storage issues. For example, the chemical industry is heavily based on fossil fuels as a resource to synthesize chemicals. It is therefore useful to investigate the feasibility of renewable synthetic fuels.

The goal of this thesis is to design a process that converts the hydrocarbon fuel combustion products CO_2 and H_2O into a fuel that is a liquid at atmospheric conditions. Methanol is selected as the liquid fuel because of its basic molecule structure. It requires much more energy to obtain methanol from CO_2 and H_2O than it does from natural gas. The process is determined to be container-sized to become cost competitive through mass production. The technical feasibility of a mass produced, autonomous, renewable and container-sized methanol production plant is studied in this thesis. The whole process is divided into sub processes. H_2O is obtained from desalination of seawater. The H_2O is split into H_2 and O_2 using alkaline electrolysis. The CO_2 is adsorbed from the air and recovered using pressure and temperature swing. The required energy is obtained using solar PV and solar thermal. The H_2 and CO_2 are finally converted to methanol in the methanol synthesis sub process. The intermittent character of solar energy yields a dynamically operated process. The methanol synthesis sub process is studied further because of the small scale and dynamic operation that are new concepts for this technology. The other sub processes are considered as black boxes with fixed in- and outputs. The steady state operation of the whole process is modeled using Aspen Plus™ and the distillation process is modelled in MATLAB®. Using the results from Aspen, pinch analysis is performed for optimal use of the available heat.

From the results of the model, it is found that an autonomous container-sized methanol production plant is technically feasible. 140 kg of methanol can be produced daily with a purity of at least 96.6 %, using a set-up of three 40 feet sea containers, two of which are dedicated to the capture of CO_2. 288 kW of electrical power and 24 kW of heat is required for the operation. This is equal to a solar park with an area of 1663 m^2 assuming an average 6 hours of solar irradiance. Using the LHV of methanol in the calculation, the total efficiency of the process is estimated at 45 %. The results from the MATLAB® model of the distillation cannot be validated because the used equation of state of REFPROP underestimates the concentration of methanol in each iteration, yielding an invalid mass balance. Fixing this issue results in an invalid energy balance. It is therefore concluded that REFPROP is not suitable for iterative calculations of distillation columns.

Table of Contents

List of figures

List of tables

Nomenclature

Sign	Name	Unit
A	area	m^2
C_{aq}	molal concentration of dissolved O_2 in H_2O	mol kg^{-1}
CP	specific heat	W $°C^{-1}$
D	diameter	m
D_p	particle diameter	m
E	joint efficiency	-
f_s	storage factor	-
F	feed flow	mol h^{-1}
g	gravitational constant	m s^{-2}
H	enthalpy	J kg^{-1}
i	cell number	-
j	iteration number	-
k	kinetic pre-factor for reaction rate	kmol kg_{cat}^{-1} s^{-1} driving $force^{-1}$
K	equilibrium constant	-
$K_{a/b/c}$	adsorption constant	- or Pa^n
K_p	equilibrium constant for partial pressure	Pa or Pa^2
L	liquid flow	mol h^{-1}
m	mass	kg
$\dot{m}$	mass flow	kg s^{-1}
m_{corr}	mass correction factor	-
M	molar mass	kg mol^{-1}
n	amount of	-
p	partial pressure	Pa
P	pressure	Pa
P	power	kW
q	quality of liquid-vapor mixture	-
Q	heat	J
Q	heat flow	kJ h^{-1}
r	reaction rate	mol kg_{cat}^{-1} s^{-1}
$rflx$	reflux	-
R	universal gas constant	J K^{-1} mol^{-1}
R	inside shell radius	mm
Re_D	Reynolds number	-
S	maximum allowable stress	MPa
t	wall thickness	mm
T	temperature	K
u	velocity	m s^{-1}
U	superficial velocity	m s^{-1}
U	energy	J
v	velocity	m s^{-1}
V	vapor flow	mol h^{-1}
w	mass fraction	-
W	work	J
x	liquid composition	-
y	vapor composition	-
z	feed composition	-
z	reactor length	m
z	height	m
α	vapor to feed ratio	-
ϵ	void fraction	-
η	efficiency	-
κ	isentropic exponent	-
μ	fluid viscosity	Pa s
ρ	density	kg m^{-3}
ϕ_s	particle shape factor	-

Index	Name
act	actual
$evap$	evaporator
ex	external
i	component i
int	interval
$isen$	isentropic
$MeOH$	methanol
$rflx$	reflux
$RWGS$	reverse water-gas shift

Abbreviations

Abbreviation	Meaning
AEL	alkaline electrolysis
AHP	absorption heat pump
BoD	basis of design
COP	coefficient of performance
COS	continuously operated scenario
DAC	direct air capture
DOS	dynamically operated scenario
DS	determined scenario
ECS	extended corresponding states
FBR	fixed bed reactor
HETP	height equivalent to a theoretical plate
HHV	higher heating value
HIDIC	heat integrated distillation column
IoT	internet of things
LHHW	Langmuir-Hinshelwood-Hougen-Watson
LHV	lower heating value
MESH	mass, equilibrium, summation and heat
MR	membrane reactor
mtf	mass transfer factor
MVR	mechanical vapor recompression
NRTL	non-random two-liquid model
NRTL-RK	non-random two-liquid model Redlich-Kwong
PEM	proton exchange membrane
ppm	parts per million
PR	Peng-Robinson
PV	photovoltaic
RK-ASPEN	Redlich-Kwong-Aspen
RKSMHV2	Redlich-Kwong-Soave with modified Huron-Vidal mixing rules
RWGS	reverse water gas shift
SOEC	solid oxide electrolyser cell
SRK	Soave-Redlich-Kwong
STP	standard pressure and temperature
TBR	trickle bed reactors
TVR	thermal vapor recompression
SL	slurry reactors
UNIFAC	universal quasichemical functional group activity coefficients

1 Introduction

The fossil-based economy has a limited lifespan. Although new resources are still found, there is a worldwide movement away from an economy based on fossil fuels, as evidenced by the Paris climate agreement of 2016. To secure future energy supply and avoid the harmful effects of climate change on the environment and the economy, a transition to a sustainable and renewable economy is required. Because the current economy heavily relies on liquid fuels and a highly developed infrastructure is present, it makes sense to move to renewable forms of energy, substituting the current fossil fuels by renewable synthetic fuels to smooth the transition. (König, Baucks, Dietrich, & Wörner, 2015) Another advantage of synthetic liquid fuels is the high energy density and ease of storage, which make it a suitable form of energy storage. This thesis researches the feasibility of a process to produce a completely renewable liquid fuel.

Renewable synthetic fuels are currently produced from biomass. However, the large-scale use of biomass to produce synthetic fuels has some disadvantages: an increase in food price and availability, tropical deforestation and loss of biodiversity (Jefferson, 2008). Fuel from biomass uses CO_2 indirectly. It is therefore interesting to investigate a direct synthesis from CO_2 to fuels which captures the CO_2 directly from the air, avoiding the negative side-effects of biomass as a source.

Processes to convert CO_2 together with hydrogen into synthetic fuels are not new. Different routes to produce synthetic fuels from CO_2 are known. Methanol is selected as liquid fuel because of its simple molecule structure. The process to synthesize methanol from renewable syngas is currently not economically feasible because of the low prices of oil and natural gas. (Graves, Ebbesen, Mogensen, & Lacknera, 2011) In order to become economically feasible, a different approach is proposed. Instead of benefitting from economies of scale, which has always been the philosophy of the chemical industry, the cost reduction is obtained using mass production. This scale-down approach is in line with the characteristics of renewables. Renewable sources are available in low concentrations compared to fossil resources but widespread. A local scaled down approach is therefore very suitable.

The size of the plant is brought down to the scale of one 40 feet sea container. There are additional advantages to a container sized plant. A plant inside a container is not limited in its use to one location, but very flexible. Provided that the production of the required energy is included in the process, the plant can easily be relocated to a different location. It can for example be used in refugee camps or be relocated to a more profitable location. Another advantage is the possibility for autonomous operation. This is not possible for large plants and further reduces costs.

1.1 Main question

The main question to be answered by this master thesis is:

To what extent is it possible to operate an autonomous container sized methanol production plant with significant production volume, using only naturally abundantly available resources?

Several parts of this research question have already been briefly mentioned in the introduction. The question is explained and justified in more detail in this section.

1.1.1 Autonomous operation

The design approach of container-sized synthesis gives room for another concept: autonomous operation. Because of safety and practical reasons, autonomous operation is not possible for large plants. There are two main advantages to autonomous operation. First, there are reduced operational costs to the plant. For large plants, operation of the plant is a significant part of the costs. The elimination of this part greatly reduces overall costs and therefore enhances economic feasibility. Second, there is no expertise required in the operation. The plant can be operated with minimal to no training. This is ideal for the application in remote locations such as for example refugee camps where infrastructure is weak, and knowledge is lacking.

There are some implications of autonomous operation that need to be considered in designing the plant. First, the plant will need to have a startup procedure that can either be controlled from a remote location

via an internet connection or by simply pushing a button. Second, the system will need to consist of components that inherently require low maintenance. This is a requirement that will be explored further in the basis of design chapter.

1.1.2 Container sized

In the chemical industry, the general idea has always been that bigger is better. Through upscaling, processes became more efficient and cheaper. Nowadays, there is a paradigm shift occurring towards small scale processes. The economy of scale is then obtained by increasing the number of plants instead of the capacity (i.e. mass production). The advantage of having a container-sized plant is that the supply of product can be located much closer to the demand. This way, either the cost for transport is reduced or transport losses are avoided. Another advantage is the ability to relocate the plant to another location if the profitability is jeopardized due to changes in the market.

There are some implications of the container scale that need to be considered in designing the plant. First, the process dynamics are different from large reactors. Some processes that might work on large scale don't work on small scale. Another implication is that all the equipment will have to fit into one container, geometrically. This is a requirement that will be explored further in the basis of design chapter. Finally, the separate components should be as small as possible for a certain production rate. Because the smaller a component is, the higher the total capacity of the process can become.

1.1.3 Methanol

This section elaborates on the advantages and disadvantages of methanol as product of the process.

Advantages

Methanol is one of the most basic hydrocarbons available, making the synthesis of it straightforward. An advantage of methanol compared to other basic organic chemicals such as methane and formic acid, is the high volumetric energy density and the excellent storage properties. Methanol is versatile since it can be used as a precursor to all sorts of chemicals and can also be used directly as a fuel. Methanol has a low volatility (EPA, 1982). Because of its low volatility compared to gasoline, it is less explosive and therefore safer. Also, methanol fires can be easily extinguished using water. Environmentally, methanol is also superior to gasoline, because methanol is biodegradable in low concentrations. Furthermore, methanol emits less NO_x and no particle matter or sulphur during engine combustion, making it less polluting (EPA, 1982). Finally, there is currently an existing and growing market for methanol, facilitating market entry (IGP Energy).

Disadvantages

There are some downsides to using methanol as a fuel. Methanol shows more acidic behavior than for example gasoline. Since oxygen molecules are present in the fuel, engine parts will corrode more easily. Also, the energy density of methanol is much lower than that of gasoline, so more fuel is required per unit of power. A considerable safety issue is the fact that methanol flames are hardly visible in daylight. Fire detection is an issue. This can however easily be resolved by dissolving agents that promote fire visibility. The lower volatility compared to gasoline is also a disadvantage because it is therefore harder to start an engine, especially in cold weather. This can be addressed by pre-heating the fuel prior to injection. (EPA, 1982)

1.1.4 Significant production volume

The significant volume of methanol produced is defined by the amount of methanol required for a specific application. In refugee camps for example, because the main advantage of the concept of containers is that it is extremely easy to scale. If a higher production volume is required, more containers can be transferred to that location. According to (Lehne, Blyth, Lahn, Bazilian, & Grafham, 2016), a total of 3.9 million tons of oil equivalent was used by forcibly displaced people in 2014. This is equal to 163 PJ/year or 447 TJ/day, which is equal to 22.71 kton methanol per day if the energy supply of all the forcibly displaced people is supplied by methanol production. Another application could be the energy and fuel supply in remote locations, where infrastructure is lacking. This container concept could in theory also replace traditional methanol production if the cost per liter methanol produced and delivered becomes lower. Multiple containers connected to a large scale solar PV farm could be a potential future form of renewable chemical and fuel production.

1.1.5 Naturally abundantly available resources

The *Naturally abundantly available resources* that are mentioned in the main question are further specified in this section. Obviously, air, (sea)water, sand, rock and biomass are examples of these resources. Technically speaking, oil and coal is also naturally abundantly available. But the difference with the other resources is the circular characteristic that is lacking with oil and coal. If for example, methanol is produced using carbon dioxide and water, then these inputs will be retrieved in the combustion of methanol. The required oxygen for this oxidation is produced in the process of creating methanol, making it a fully circular process, element-wise (not energy-wise!). This circularity is also a prerequisite for the process to be developed: the resources will need to remain abundantly available, also in the long term.

The potential resources for methanol synthesis will need to have carbon, oxygen and hydrogen atoms. Rock and sand are therefore discarded as possible resources since they mainly consist of silicon. Biomass is suitable, but the main issue with biomass is that the atoms are captured in complex molecules, that the structure of biomass differs per type, and that the degree of abundance is much smaller than air and seawater. Also, biomass that is currently commercially exploited requires land use, which competes with the food industry. Research is carried out to algae, where the land use is no issue. This is however still in developmental phase and hard to combine with autonomous operation.

From the carbon dioxide in the air together with the H_2O from the (sea)water, a methanol synthesis is possible. The enthalpy of the reaction of CO_2 and H_2O to methanol is negative, so additional energy is required for this process. The source of this energy also needs to meet the set requirements. It therefore must be renewable energy, regarding the circularity requirement. The implication of using renewable energy is that the capital costs of the design become an important design criterion in the likely case that the nature of the renewable energy source is intermittent.

The intermittency of the power source poses an interesting dilemma between two options. The methanol production process can be operated continuously if an energy storage device is added to the plant or the process can be operated dynamically, only operating when power is available. In the continuously operated scenario (COS), the share of the capital costs is relatively smaller, since more methanol is produced using the same equipment. Additional energy storage equipment is required however. The dynamically operated scenario (DOS) is characterized by its higher share of capital costs because of part-time operation. The additional costs for energy storage equipment is however saved. The implications of both scenarios are investigated in the basis of design (BoD).

1.2 Methodology

This paragraph describes the methodology of this master thesis. The BoD is composed first and is based on a review of literature. The scope of the thesis is defined since a complete, detailed design of the entire process is not feasible in the given time. Second, the capacity of the plant is determined using the size of one container as reference. The capacity is restricted by the sizes of the individual components. The in- and outputs of the process are determined and quantified with the calculated capacity and the product quality is determined. The process is then divided into sub processes with each a separate function and the mode of operation of all the components is determined. The basis of design is finalized, and a review of literature is performed to determine the realization of the selected sub processes. These selected sub processes are modeled using a flowsheeting software package in Aspen Plus™ (further referred to as Aspen) and MATLAB® (further referred to as Matlab) to describe a steady state methanol production process. The results from the models are interpreted and discussed.

Chapter 2 contains the review of the studied literature and acts as a ground for the BoD in chapter 3. In chapter 3, the information gathered in the literature review was considered and a selection of appropriate technologies was made, using criteria based on the elaboration of the main question. This selection of technologies is presented and at the end of the chapter, a demarcation of the processes that are studied more extensively is made. The mode of operation is determined. Chapter 4 elaborates on the models. The entire process is modelled in Aspen, except for the distillation which is modelled in Matlab. The way of modelling is described in this chapter, including the selected process conditions. Chapter 5 explores the implications of the small scale of the design, which is special for this design. Chapter 6 shows the results the models produced and reflects on these results with respect to the BoD. The conclusions and recommendations are listed in Chapter 7, where the results are viewed in the light of the main question posed in the beginning.

2 Literature Review

In this chapter, the available literature that is required to determine the realization of the design is described. On some aspects, the amount of literature reviewed was limited and incorporated in the basis of design in chapter 3.

2.1 Carbon capture

The type of carbon capture that is investigated is direct air capture (DAC). Other types of capture of CO_2 from a stack or from minerals is not investigated since this source of CO_2 would add additional CO_2 to the atmosphere which conflicts with the circularity requirement.

There are three types of carbon capture: wet absorption, dry adsorption and membrane filtration. The wet route uses a sodium hydroxide solution or equivalent to absorb carbon dioxide from the air into the solution. The carbon dioxide is then recovered by letting the sodium carbonate react with lime (calcium hydroxide) to retrieve sodium hydroxide and calcium carbonate. The process of releasing CO_2 from the calcium carbonate happens at high temperatures and is energy intensive (Mahmoudkhani & Keith, 2009). The dry route uses a catalyst-like material such as zeolites or activated carbon to adsorb the carbon dioxide onto the surface. The carbon dioxide is then released from the surface using pressure and temperature swing. Membrane filtration is the third option. This is however discarded since huge volumes of air must pass through the membrane due to the very low concentration of CO_2 in air. Also, a high pressure difference is required over the membrane. This high pressure combined with a large volume flow will require significant amounts of power (Yang, et al., 2008).

From one dry-route patent that was filed by Climeworks (Jain, 2010), the data in table 1 was obtained. The examples mentioned in the patent are concerning carbon capture from flue gas.

Table 1 – Flue gas carbon capture by Climeworks

	I	II	III	IV
CO2 concentration	12.5%	12.5%	3.4%	12.8%
Adsorption material	Zeolite 5A	Zeolite 13X	Zeolite 5A	Zeolite 5A
Cycle time	36 min	36 min	36 min	10 min
Output purity	99.8 %	98.5%	91%	81.6%
Recovery	85.8 %	78%	86%	25.4%

It becomes clear from this data that a lower concentration of carbon dioxide in the input stream is not correlated to the recovery or output purity. This is backed by data from a later patent, also filed by Climeworks (Jones, 2016), in which a direct air capture of CO_2 is described. Using a refinement step after the initial capture, a purity of 98.32% can be obtained. Extending the refinement step can further increase the purity to 99.96%.

As mentioned before, the dry route of carbon capture can make use of waste heat generated in the process, since a temperature of approximately 100 degrees is required for the release of the captured carbon dioxide. In a patent filed by the company Antecy (O'Connor, 2016), the excess heat of a methanol synthesis is coupled to the carbon capture, effectively reducing the energy requirement of the carbon capture. The total heat requirement is currently in the order of 7500 KJ/kg CO_2. According to Antecy experts, this can be brought down to below 5000 KJ/kg CO_2 upon further optimization. Industrial amine systems are currently operating below 4000 KJ/kg CO_2 (P. O'Connor, personal communication, 16 May 2017)

2.2 Electrolysis

The process to produce methanol requires hydrogen. Water is split into hydrogen and oxygen by electrolysis. There are other processes to split water such as thermal decomposition, but they are all less effective and less developed than electrolysis. There are three different types of electrolysis: alkaline electrolysis (AEL), proton exchange membrane (PEM) electrolysis and solid oxide electrolysis cell (SOEC). AEL and PEM have currently reached commercialization whereas SOECs are still in the research phase. (Kjartansdóttir & Møller, 2014).

The electrolysis cell in AEL consists of an anode and a cathode that are immersed in a liquid alkaline. They are separated from each other by an ionic conducting diaphragm. The diaphragm further serves as a boundary to prevent the hydrogen and oxygen gas from mixing. When a voltage is applied to the electrodes, the water decomposes in hydrogen and hydroxyl molecules at the cathode. The charge carrier in this type of electrolyser is the OH^- ion, which migrates through the diaphragm and forms water and oxygen at the anode.

In PEM electrolysis, the cell consists of an acidic solid membrane, enclosed by an anode and a cathode on each side. Due to the current applied, the water that is fed to the anode side decomposes into oxygen and hydrogen. The hydrogen atom migrates through the membrane (hence the name of the process) because of the presence of sulfonic acid in the membrane. Because of the acidity of the membrane, noble element catalysts such as palladium or iridium are required, significantly increasing the cost of this type of electrolyser.

With SOEC, the electrolyte consists of a ceramic material that conducts oxygen ions. The high temperatures required are caused by the ionic conductivity characteristics of the membrane. At the cathode, water is split into hydrogen and oxygen atoms. The oxygen atoms migrate through the electrolyte and form oxygen gas at the anode. The hydrogen atoms form hydrogen gas at the cathode and are collected there. Because of the severe operating conditions, expensive materials are required such as yttrium and zirconium, which drastically increase the cost of the electrolyser.

In table 2, an overview is given of the performance and the characteristics of the three types of electrolysers.

Table 2 – Electrolysis characteristics [1]

Type of electrolysis	**AEL**	**PEM**	**SOEC**
Temperature	40 – 90 °C	20 – 100 °C	700 – 1000 °C
Pressure	4 – 60 bar	30 – 200 bar	1 bar
Electrolyte	Liquid alkaline KOH	Solid acid polymer	Ceramic metal compound
Anode material	Ni	Ti, Ir (catalyst)	Ni doped YSZ[1]
Cathode material	Stainless steel mesh	Carbon, Pt (catalyst)	LSM[2]
Charge carrier	OH^-	H^+	O^{2-}
Life-time	50,000 – 100,000 hours [2]	<40,000 hours [2]	1,000 – 5,000 hours

[1]Yttria-stabilized-zirconia
[2]Lanthanum strontium manganate
[1] (Smolinka, 2014)
[2] (Gandia, Arzamedi, & Dieguez, 2013)

2.3 Methanol Synthesis

2.3.1 Carbon dioxide pretreatment

This section addresses the possibility to reduce the carbon dioxide to carbon monoxide, prior to the methanol synthesis. From the stoichiometry reaction

$$CO_2 + 3H_2 \leftrightarrow CH_3OH + H_2O \quad (2.1)$$

It is known that carbon dioxide and hydrogen can be synthesized to methanol in a single step. The carbon dioxide can however also first be reduced to carbon monoxide using the reverse water gas shift (RWGS) reaction shown in equation 2.2.

$$CO_2 + H_2 \leftrightarrow CO + H_2O \quad (2.2)$$

Carbon monoxide can be synthesized together with hydrogen to form methanol in the reaction shown in equation 2.3:

$$CO + 2H_2 \leftrightarrow CH_3OH \quad (2.3)$$

Since the RWGS reaction is an equilibrium reaction, only a part of the carbon dioxide is reduced to carbon monoxide. In the subsequent methanol synthesis, less water is formed compared to a feed containing only carbon dioxide. This is beneficial for the downstream process since less water has to be separated from the methanol. The required hydrogen for the methanol synthesis also decreases, but the increase of hydrogen required for the RWGS reaction is equal. The main question is whether the reduced water content in the produced methanol outweighs the extra energy required for the carbon dioxide reduction.

In order to determine whether a pre-treatment step in the form of a reverse water gas shift reaction to convert the CO2 to CO is desirable, a comparison of the economic performances of the two options is made. (B. Anicic, 2014) compared the two technologies using only carbon dioxide and hydrogen as initial raw materials. Their study resulted in the following costs for the processes.

Table 3 – Capital cost of CO and CO2 process for a large-scale plant (B. Anicic, 2014)

Process/unit	**Costs CO route (M$)**	**Costs CO_2 route (M$)**
Water electrolysis	45.93	51.61
RWGS	17.29	0
Methanol reactor 1	24.93	19.49
Methanol reactor 2	0	16.18
Methanol distillation	5.01	5.46
PSA	0.07	0.19
Combustion unit	13.61	0
Compressors	0.85	0.45
Total	**84.18**	**72.94**

From tables 3 and 4, it becomes clear that the CO_2 route is more economic than the CO route. (B. Anicic, 2014) however, based their scenario on a large-scale methanol production facility. The exact production size was not mentioned. For a container sized autonomous process, these values will differ. In a container-sized design, the second methanol reactor can be replaced by a larger recycle stream. This will increase the costs of the first reactor, but not by more than the cost of the second reactor. The costs of the other processes are assumed to remain the same, relative to each other.

Table 4 – Operational cost of CO and CO2 process for a large-scale plant (B. Anicic, 2014)

		CO route	CO_2 route
Electric power required	CO_2 capture (MW)	8.263	7.956
	H_2 production (MW)	295.2	309.3
	Compressors (MW)	2.20	1.07
Electricity required per kg of produced methanol (kWh/kg)		10.63	11.07

Regarding the electricity costs, the operating costs are slightly higher for the CO_2 route. However, the paper does not consider the cost of catalyst of the RWGS reaction. Also, no energy requirement of the

RWGS is mentioned, so it is unknown whether these costs are considered. The RWGS process is assumed to be more expensive for the container-sized design than for the large-scale plant. Because no cheap sources of heat such as natural gas are available for heating, all the heat required will have to come from electricity. The RWGS reaction is endothermic and operates at a temperature of 800 °C, and therefore requires high grade heat. Due to the high temperature, waste heat integration will not mitigate these extra costs significantly.

2.3.2 Methanol synthesis reactor

There are three categories of reactors to synthesize methanol from syngas: dry, wet and membrane reactors. (Bozzano & Manenti, 2016) Each of these is investigated in further detail and the advantages and disadvantages are listed.

Dry synthesis

The first and most prominent one is the dry synthesis. A gaseous feed stream enters the reactor and reacts over the solid catalyst to form a gaseous product. There are two types of dry synthesis reactors: adiabatic and isothermal. The difference between the two is the temperature control. In adiabatic reactors, the reagents heat up due to the reaction heat of the exothermic methanol synthesis. Adiabatic reactors are often designed in stages, where the cooling of the process is performed between the stages. Isothermal reactors have continuous cooling. The heat of the reaction is transferred to an evaporating liquid. The pressure of the coolant is chosen so that the boiling point matches the ideal reaction temperature. Table 5 lists all the different types of adiabatic and isothermal reactors. (Bozzano & Manenti, 2016) Do not mention disadvantages for certain types of reactors. These entries are therefore left open.

Table 5 – Methanol synthesis reactor types (Bozzano & Manenti, 2016)

Reactor	Description	Advantages	Disadvantages
		Adiabatic	
ICI quench converter	Multiple adiabatic beds in series in a pressurized shell	+ simple and reliable configuration + easy construction and loading of catalyst + upgraded concepts available	- irregular temperature distribution - large recycle stream - low heat recovery - little performance tuning
Kellogg, Brown and Root reactor	Series of spherical reactors. Catalyst between the outside surface and an inner shell.	+ lightweight: low installation costs + small pressure drops, low auxiliary costs + higher yields	- catalyst shrinks during start-up, which leads to irregular flows
Toyo Engineering Corporation reactor	Multi-stage radial flow reactor, cooling by vertical tubes	+ optimal reaction temperature + easy catalyst replacement + small pressure drops	
		Isothermal	
Lurgi converter	Shell and tube configuration. Cooling water in the shell, catalysts and gases in the tubes	+ easy design + easy loading of catalysts + most common adopted reactor concept	
MGC/MHI super-converter	Double walled tubes in a shell. The catalyst is loaded between the outer and inner tube	+ high reaction rates + high mechanical stability	
Casale isothermal methanol converter	Heat exchange surface is made of plates surrounded by the catalyst. Cooling fluid flows inside the plates	+ good temperature control + easy loading of catalyst + long catalyst life due to constant temperature + small pressure drops for axial radial concept	

The main difference between isothermal and adiabatic reactors is their performance in selectivity and the rate of reaction. The reaction to synthesize methanol from CO_2 and H_2 is exothermic, so the rate of reaction increases with increasing temperature. Therefore, since the process is able to increase in temperature in adiabatic processes, the rate of reaction increases. Given a certain amount of product required, less catalyst can be used in the process. Isothermal reactors operate at a constant temperature. At higher temperatures, a higher share of byproducts is formed. Therefore, isothermal reactors have a higher selectivity than adiabatic reactors.

Wet synthesis

The second option is wet synthesis. Again, gaseous feed stream reacts over a solid catalyst. The formed methanol is absorbed by the liquid state. The main advantage of this strategy is the reduced recycle ratio. Because methanol is removed from the reactants, higher conversions are possible due to Le Chatelier's principle. The greatest disadvantage of this type of reactor is the issues with modelling and scale-up, which is the reason this type of reactors is not yet used in practice. Another big disadvantage of liquid phase technologies for application in the container-sized design is the higher catalyst deactivation rates compared to gas phase technologies. Catalyst leaching was found to be increased in the presence of water and methanol (Lee, 1990).There are two technologies, Trickle Bed Reactors (TBR) and slurry reactors (SR) within wet synthesis. In TBR, the liquid state and the gaseous feed stream both flow through a catalyst bed and the formed methanol dissolves in the liquid. In the slurry reactor, the catalyst in suspended in an inert mineral oil.

One of the main problems, the higher catalyst deactivation, was studied by (Wang, Tan, Han, & Tsubaki, 2008). They compared the catalyst deactivation in a Fixed Bed Reactor (FBR) to the deactivation in a SR and found a significant drop in performance in the SR, whereas the catalyst in the FBR was relatively stable. According to the paper, the deactivation was caused by the increased amount of H_2O present. Other possible deactivation mechanisms such as poisoning or reaction heat were ruled out in this case but could of course play a role in other cases. Initial deactivation of catalyst is caused by a loss in surface area when some of the of the very finely dispersed copper crystallites agglomerate. The role of water in this is that the high partial pressures inhibit the reaction by competitive adsorption on the active sites. (Kung, 1992). Another deactivation mechanism that also happens in dry circumstances is copper particle sintering. The rate of sintering is temperature dependent. It occurs readily at temperatures from 500 K and at temperatures above 573 K, the growth of ZnO particles starts to contribute as well to the sintering and thus deactivation.

Membrane synthesis

The third option is membrane synthesis. In membrane synthesis, the reaction and the separation take place in the same process. For example, a shell shaped reactor is example filled with catalyst and tube-shaped membrane in which either the product or byproduct can permeate. A Membrane Reactor (MR) has many advantages. The conversion is much higher. In methanol synthesis, the water or the methanol permeates through the membrane, removing the product or byproduct from the reaction effectively increases the reaction rate. Another reported advantage is the milder operating conditions of MR, yielding higher energy efficiencies. The main disadvantage is that the technology is still in research phase. The zeolite membrane, which is the most promising option for methanol synthesis, still requires development. (Makertiharta, Dharmawijaya, & Wenten, 2017)

2.3.3 Methanol-water separation

As can be seen from equation 2.1, water is formed as a byproduct during methanol synthesis. The mixture that exits the reactor also contains unreacted carbon dioxide, carbon monoxide and hydrogen. Because of the elevated temperature and pressure, all the substances are in the gas phase. Most of the carbon dioxide, carbon monoxide and the hydrogen can be easily separated from the methanol and water using a flash drum. The separation of methanol and water is more challenging since their boiling points are close to each other. In researching the various options, the quality and the quantity are the two most important features of the technologies. The quality is measured in the outlet purity of the methanol and the water. The quantity is measured in the throughput of the equipment. A high throughput means larger equipment and higher cost and is therefore to be minimized.

There are several options for the separation process.

- The first option, which is used most in industry, is distillation. The most common form is conventional distillation using trays in a vertical column. Because of increasing energy efficiency requirements, various technologies are used to improve the concept. (Kiss, 2014) described various concepts such as thermal or mechanical vapor recompression (T/MVR), absorption heat

pump (AHP), or heat integrated distillation column (HIDIC). For methanol-water separation, the paper reports primary energy savings of 69% and a pay-back time of less than a year using MVR. The number of trays required for methanol/water distillation is 60, using an operating pressure of 3 bar and a reflux-to-minimum-reflux ratio of 1.31 (Seader, Henley, & Roper, 2011). The largest disadvantage to this type of separation is the height of the distillation. Even though the methanol/water mixture has a low tendency of foaming (Kister, 1992), a minimal tray spacing of 12 inches is reported (Kister, 1992). The total column height then becomes 18 meters, which is a problem for the container with its height of 2.4 meters. For this type of distillation, 8 columns are required, with an additional 7 compressors or fans to transport the vapor from the top of each column to the bottom of the next. The tray spacing found in literature is given for large scale distillation. The assumption can be made that for smaller scale, the tray spacing will also become smaller. However, the tray spacing is dependent on the behavior of the vapor/liquid mixture because the mixture will form a so-called froth on each tray. This effect is only dependent on gravity and is not influenced by the horizontal dimensions. Further lowering of the tray spacing will also result in a decreased operating vapor velocity (Kister, 1992)

- A possible solution of the height problem is the second option: the usage of packed beds instead of trays. Packed beds are vertically stacked corrugated sheets. The liquid flows down along the plates while to vapor flows upward through the intersecting channels. The main advantage of packed columns is the decreased height (Smith, 2012), which is especially relevant in this design. (Mori, Ibukia, Taguchia, Futamuraa, & Oluji, 2006) researched the performance of structured packed columns. They used a 2.16-meter-high column to separate methanol from water. The used reflux ratio was with 4.53 and the methanol and water compositions were not as pure compared to the 60-tray conventional distillation. The assumption is made that to compensate for these effects; the tower needs to be twice as high: 4.32 meters. This is still approximately 4 times smaller than with conventional distillation. With packed column distillation, two towers in series with only one additional pump are required. Another advantage is that the pressure drop in packed columns is lower, decreasing the amount of pump power required. (Kister, 1992)
- Another option within distillation is micro-distillation (Seok & Hwang, 1985). Micro distillation is carried out using a heat pipe. Vapor flows from the heated side to the cooled side and liquid flows along the tube walls in the opposite direction. Since the liquid is in constant contact with the vapor, there is a continuous exchange of mass between these two phases, giving a very effective separation. The more volatile component, methanol in this case, will accumulate at the cold side and the less volatile component, water in this case, will accumulate at the hot side. The equipment is shaped as a tube with a length of 50 cm and a diameter of 1 cm. For methanol/water separation, a product purity of 99% methanol and 100% water can be obtained at either ends of the tube. One micro-distiller produces 1.1 mol of methanol per hour (Seok & Hwang, 1985), so for this design. 762 of these distillers are required. This corresponds to a distillation process size of 0.16 m^3. Since the driving forces of this type of distillation are capillary forces and not gravity, micro-distillation can be carried out horizontally, which is beneficial for this design. The question is whether micro-distillation is possible in this design since the working principle is based on capillary action, which may not be strong enough for the scale of the design.
- The final option is using a sieve with molecular sized pores (molsieve). The pores of the sieve will have to be smaller than the size of the methanol molecule, but large enough for the water molecules to pass through. Despite what the name suggests, molecular sieves are not like macroscopic sieves, but exist in the form of spheres. The spheres absorb the smallest molecules in a mixture, separating them from the larger molecules. Zeolite molecular sieves are the only suitable molsieve for the methanol/water separation because of their pore size (Kister, 1992). Water molecules have a critical diameter of 2.75 Å whereas the critical diameter of methanol is 4.4 Å. A molsieve with a pore size between these two values will effectively separate the water and the methanol. An additional advantage of molsieves is that also trace amounts of hydrogen and carbon dioxide will be filtered, since their critical diameters are equal to that of water or smaller. A disadvantage of molsieves is the regeneration that is required for re-use. This regeneration is done by changing the pressure and increasing the temperature to 175 – 315 °C, depending on the type of molsieve (Sigma-Aldrich, 2017). The process is comparable to the carbon capture process. The adsorption is carried out easily, but the regeneration is an energy intensive process.

2.4 Heat integration

All the subprocess either require energy or produce energy. For an energy efficient process, it is imperative to reuse the heat that is produced in the various sub processes. A methodology to systematically connect the heating and cooling duties is the pinch technology (Mubarak Ebrahim, 2000). This technique identifies energy targets and defines the minimum driving force across the heat exchangers. Using this methodology, the smallest capacity of stand-alone heaters and coolers is obtained, by connecting the heat flows in the most efficient way.

2.5 Outlook and conclusions

After researching the various subsystems, several preliminary conclusions can be drawn to further narrow down the options to be reviewed in the BoD

Carbon capture

The DAC technology is far along in the developmental phase and is currently commercialized. A further optimization of the energy requirement is possible and will make the technology more competitive.

Electrolysis

With electrolysis, especially SOEC is very much in the developmental phase, mainly because of the issue of performance degradation. The SOEC technology is currently only viable using continuous operation and if the energy required for heating is recovered from the process.

There is another concept within electrolysis which is promising for future applications, which is called the battolyser (Mulder, Weninger, Middelkoop, Ooms, & Schreuders, 2017). This is a Ni-Fe battery and an alkaline electrolyser combined. This combination is very interesting for this design because energy storage is important, and a reduction in size means a possible increase in total production. The technology could also potentially increase the operating time and thus the profitability of the concept. Currently, the technology is still very much in the developmental phase and is therefore not considered as an option for this design, but it could be very relevant in the future.

Methanol synthesis

Three different parts of the methanol synthesis were researched. The RWGS route was found to be not worthy of the effort because no significant increase in production or efficiency was obtained, while a more extensive synthesis process was required.

For the reactor, dry synthesis was found to be preferred over wet and membrane synthesis mainly because of catalyst deactivation. A trade-off was found between the rate of reaction and product purity in the choice of reactor temperature.

In the methanol/water separation, the special constraint of the maximum height made for an interesting comparison between the various options, since gravity is usually the driving force of distillation processes. Molsieves were found to be uneconomical due to their capital cost. They could however play a role in a refinement step to clear the methanol from water, because the separation is very selective.

3 Basis of Design

3.1 Capacity

The capacity of the plant is limited by the size of the container. In the ideal case, the whole process from resources to product happens in one container. This is however not feasible since energy generation from renewables is generally not easily concentrated. The nature of renewable energy is that the source is widespread, but in low concentrations. For the same reason, the process of CO_2 capture is left out of the container since a huge volume of air is required to extract sufficient amounts CO_2. Back of the envelope calculations show that the size of the CO_2 capture is the same size as the rest of the synthesis combined. Therefore, the sub processes that remain inside the container are the desalination, the electrolysis and the methanol synthesis.

The volume of a standard 40 feet container is 67.7 m^3 (Maersk, 2014). To obtain the optimal size for the three subsystems present in the container, their size/capacity characteristic needs to be known. If this is compared with the stoichiometric ratios of the substances required, an optimal division in size of the three subsystems can be obtained.

3.1.1 Method

A methanol production of 100 kg/day is assumed for the first iteration and the process is assumed to be completely dynamically operated, for 6 hours per day. The methanol synthesis designed by (Kauw, 2012) is taken as a sample for the designed process. This process is used to obtain a first order estimate of the size of process. Using this information, the production capacity of the design is determined.

For the desalination and electrolysis, the estimation for the size/capacity characteristic is obtained by collecting size and capacity data from different manufacturers. The results are shown in table 6. The sizing of the methanol synthesis is more extensive. The synthesis shown in figure 1 is taken as benchmark for the determination of the required components (Mignard, Sahibzada, Duthie, & Whittington, 2003). The components of these systems are all estimated in a different way, depending for each component on the best way the estimation can best be made. In many cases, data used from equipment that can be bought online is used in this estimation. A part of the process that is recycled because the reactor efficiency is not 100%. A recycle ratio of 7.9 is used to calculate the mass flows for these components (Mignard, Sahibzada, Duthie, & Whittington, 2003). The recycle ratio is defined as the mass of the recycle flow over the mass of the fresh feed.

This example methanol synthesis is divided in different components:

- The size of the compressors is estimated using the power required, which is calculated using the enthalpy change in the process, multiplied by the reference mass flow. A compressor efficiency of 0.75 is assumed (Campbell, 2014).
- The size of the condensers is obtained by calculating the amount of heat that is exchanged. This characteristic is then used to estimate the capacity based on existing equipment.
- The size of the heat exchangers is calculated in the same fashion as the condensers. The amount of heat exchanged is used to estimate the capacity based on existing equipment.
- The separator size is estimated by using a residence time of the chemicals in the separator. The residence time used is 5 minutes (Hall, 2012)
- The distillation column size is estimated by comparing distillation installations that are used to brew alcoholic beverages, since these are of comparable size. This comparison is backed by data from a large-scale methanol distillation design (Hoogstraten & Dunn, 1998). Using a scaling factor of 0.6, the size calculated was in the same order of magnitude. The scaling factor of 0.6 is a rule of thumb that is used to estimate the cost of equipment when the cost of a piece of equipment is known in another size. The assumption is made here that costs and size scale linearly.
- The reactor size is calculated in the same fashion as the distillation column, by scaling down a large-scale methanol reactor (Almeland, Meland, & Edvardsen, 2009). Again, a scaling factor of 0.6 is used.
- The total size of the valves and pumps is assumed to be 10% of the size of the other equipment. This is because there is only one pipe segment per piece of equipment and the number of pumps and valves is very limited.

The size of the methanol storage tank is designed to contain 2 days of production. The size is estimated by multiplying the size of the methanol by 1.5. The mass of the container is comparable to the mass of an oil drum and is assumed to be 30 kg.

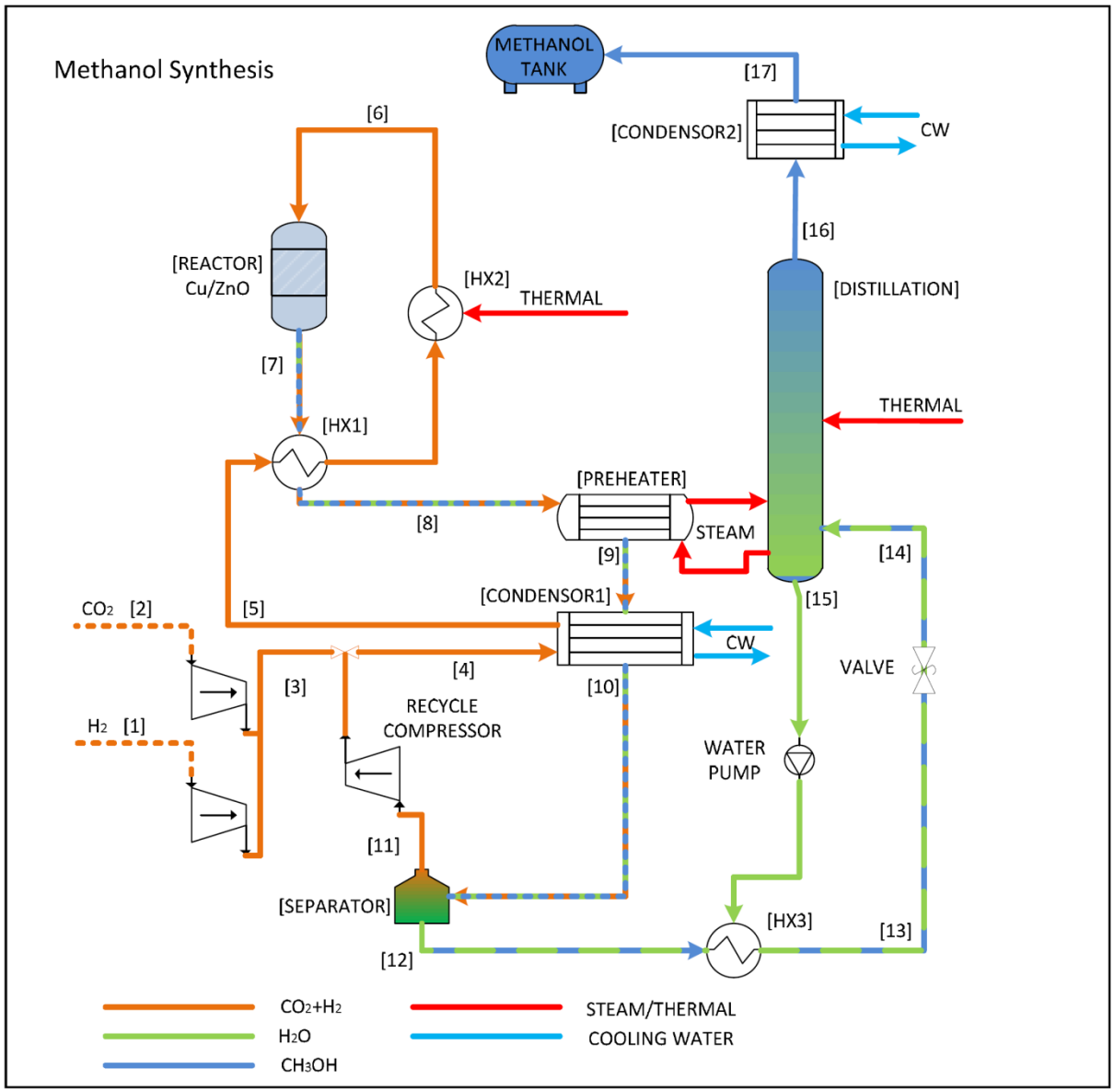

Figure 1 – Lurgi Methanol process parameters (Kauw, 2012)

Stream	Flow	Pressure [bar]	Pressure [Mpa]	Temperature [C]	Temperature [K]
1	H_2	1	0.1	20	293
2	CO_2	1	0.1	20	293
3	CO_2+H_2	55	5.5	60	333
4	CO_2+H_2	55	5.5	60	333
5	CO_2+H_2	53	5.3	120	393
6	CO_2+H_2	50	5.0	230	503
7	CH_3OH+H_2+CO_2+H_2O	49	4.9	285	558
8	CH_3OH+H_2+CO_2+H_2O	49	4.9	170	443
9	CH_3OH+H_2+CO_2+H_2O	48	4.8	130	403
10	CH_3OH+H_2+CO_2+H_2O	47	4.7	35	308
11	CO_2+H_2	45	4.5	35	308
12	CH_3OH+H_2O	45	4.5	35	308
13	CH_3OH+H_2O	45	4.5	60	333
14	CH_3OH+H_2O	1.1	0.11	60	333
15	H_2O	1.5	0.15	100	373
16	CH_3OH	1.1	0.11	65	338
17	CH_3OH	1	0.10	25	298

Figure 2 – Lurgi Methanol process schematic (Kauw, 2012)

3.1.2 Calculation & results

In the electrolysis and the methanol synthesis, the following chemical reactions are occurring:

Electrolysis $2H_2O \rightarrow 2H_2 + O_2$ (3.1)

Methanol Synthesis $CO_2 + 3H_2 \leftrightarrow CH_3OH + H_2O$ (2.1)

Complete reaction $2\,CO_2 + 6\,H_2O \rightarrow 2\,CH_3OH + 2\,H_2O + 3\,O_2$ (3.2)

Assuming a methanol production of 100 kg/day over the course of 6 hours, the production rates of the different components can be obtained from stoichiometry. The calculations of the mass flows from stoichiometry are shown in Appendix C. The mass flow and the characteristic property of each component are listed in table 6. The capacity and the characteristic property are used to obtain the size of the equipment, using data from manufacturers. From the obtained size and capacity, a size/capacity characteristic can be defined, which is used in rescaling the process to container dimensions.

Table 6 – Preliminary sizing of methanol synthesis components

Equipment	Capacity (kg/h)	Characteristic property	Size (m^3)	Size/capacity (kg/h/m^3_m)[1]	Mass (kg)	Source
Desalination	18.75	-	0.2	130	80	[1]
Electrolysis	14.5 m^3/h	-	19.08	2.4 m^3_p/h/m^3_m	3000	[2]
Compressor *CO_2 + H_2*	26.04	Power 0.9 kW	0.32	-	330	[3]
Compressor *Recycle stream*	205.7	Power 4.8 kW	0.32	-	330	[3]
Condenser *Product stream*	231.8	Heat exchanged 10 kW	0.067	150 kW/m^3_m	65	[4]
Condenser *Methanol*	16.67	Heat exchanged 0.5 kW	0.011	150 kW/m^3_m	11	[4]
Heat exchanger *Product to reactant*	231.8	Heat exchanged 20 kW	0.1	150 kW/m^3_m	97	[4]

[1] Unless otherwise specified, m^3_m is volume of machine, m^3_p is volume of product produced.

Heat exchanger *External to reactants*	231.8	Heat exchanged 3 kW	0.032	150 kW/m^3_m	31	[4]
Heat exchanger *Product to steam*	231.8	Heat exchanged 4.4 kW	0.041	150 kW/m^3_m	40	[4]
Heat exchanger *Water to product*	26.04	Heat exchanged 0.6 kW	0.012	150 kW/m^3_m	12	[4]
Separator	231.8	Residence time of 5 minutes	0.09	2700	-	-
Distillation	26.04	Capacity with scaling factor	0.5	50	-	-
Reactor	231.8	Capacity with scaling factor	0.83	30	-	-
Valves and pumps	-	Factor of other equipment	10% of synthesis	-	10% of synthesis	-
Methanol storage	-	Density 800 kg/m3	0.38	-	250	-
Total	**-**	**-**	**22.08**	**-**	**6040**	

[1] (Alibaba, 2017)
[2] (Hydrogenics, 2017)
[3] (Alibaba, 2017)
[4] (Alibaba, 2017)

A possible limitation from the use of containers is the maximum payload. For 40' standard containers, the maximum payload is approximately 28,800 kg. The components of which the masses are unknown are estimated to have the same average density as the components of the synthesis of which the mass is known. The total mass of the system is then 6,040 kg. For a 40' standard container, this is a factor of 4.8 below the maximum payload. Since 4.8 times the calculated volume (105 m^3) exceeds the container size, the maximum payload will not be a limitation.

To determine the design capacity, an assumption needs to be made about the space efficiency of the process in the container. The space efficiency is defined as the ratio between the volume of the equipment and the total volume. To be able to access the equipment, a path with a width of 75 cm in the container over the full length is cleared. Furthermore, the assumptions made that the equipment is closely packed and a packing efficiency of 75% is obtained. The total space efficiency is, using a container width of 2.350 m (Maersk, 2014)

$$\frac{2.35\ m - 0.75\ m}{2.35\ m} * 0.75 = 51\% \tag{3.3}$$

The total equipment volume then becomes $0.51 * 67 = 34.6$ m^3. This is 1.56 times the volume calculated for 100 kg per day. The capacity of the container sized methanol plant is therefore set at 150 kg/day.

3.2 In- and outputs

In this section, the quality and the quantity of the in- and outputs of the process are determined. As discussed in the first chapter, the inputs of the process have to be naturally abundantly available and the process must be circular. Reasoned from the intended product methanol, which has the chemical structure CH_3OH, a source for carbon, hydrogen and oxygen must be found. From the mentioned criteria, the elements CO_2, H_2O and O_2 remain as potential inputs to the process. Since little oxygen is required in the process, and carbon dioxide and water also contain oxygen, O_2 is also discarded as potential source.

The CO_2 is naturally available in equal concentrations in seawater and in the air. Both CO_2 concentrations are currently around 400 ppm. The concentration of CO_2 that is fed to the process should

have a concentration of more than 99.9%. A lower concentration will have as effect that more energy is wasted in compressing and transporting the gas and that the productivity of the reactor is lower. If it appears that in the technology selection that it is more expensive to obtain a high concentration of CO_2 than it is to deal with the impurities, an optimum will be found. The required mass flow of CO_2 is calculated from stoichiometry. The overall reaction of the process is

$$2\,CO_2 + 6\,H_2O \rightarrow 2\,CH_3OH + 2\,H_2O + 3\,O_2 \tag{3.2}$$

CO_2 reacts in equimolar amounts to methanol. With a molar mass of CO_2 of 44.01 g/mol and a molar mass of CH_3OH of 32.04 g/mol, 1.3736 kg of CO_2 is required for each kg of produced methanol.

H_2O is naturally available in many places such as seas, rivers and lakes. Since there is water in the air, it is also possible to extract water from the air. To produce methanol, the water needs to be converted to hydrogen first. This is done in an electrolyser. The purity requirements for the water are defined by the effect of salt accumulation in the electrolyte solution. If the water that is fed to the electrolyser contains salt, this salt will accumulate over time, since only pure hydrogen and oxygen exit the electrolyser. Therefore, the water purity must be higher than 99.99%. The required mass flow of water is calculated from stoichiometry. If the produced water is recycled, the overall reaction of the process is simplified to

$$2\,CO_2 + 4\,H_2O \rightarrow 2\,CH_3OH + 3\,O_2 \tag{3.3}$$

Two moles of water are produced for each mole of methanol. With a molar mass of H_2O of 18.015 g/mol, 1.1245 kg of water is required for each kg of produced methanol.

CH_3OH is the desired product in the process. The purity of the methanol required depends on the application. If methanol is required for fuel purposes, then small amounts of comparable hydrocarbons such as for example ethanol or acetone are harmless. The presence of water in the methanol is undesirable since it lowers the heat of combustion. For chemical purposes, the methanol should have a much higher purity since the chemical is used in further synthesis. Since the process is designed to both applications and the chemical requirements are much stricter, methanol with the highest purity is selected. The process will be designed to produce US federal grade AA methanol, as is shown in table 7

Table 7 – US Federal grade AA methanol (Seddon, 2006)

Methanol	>99.85%
Water (max. wt%)	0.1
Acetone+aldehydes (ppm)	<30
Acetone (ppm)	<20
Ethanol (ppm)	<10
Residue (mg/L)	<10

According to the reaction, O_2 is produced in the electrolysis. Oxygen is not a very valuable chemical, but the purity of the oxygen is very high and therefore has an increased value. The profitability of capturing and storing the oxygen will have to be considered for each specific case. In stationary applications close to other industries it can easily be profitable. In refugee camps, the oxygen could potentially be utilized for waste treatment with gasifiers. This might however not be the case for remote locations.

An alternative scenario is drafted in the context of the application in refugee camps. For fuel purposes, a lower grade of methanol is acceptable. The presence of ethanol is not undesirable in this case. Acetone is also not undesirable as byproduct for fuel purposes since acetone also combusts to form carbon dioxide and water. The presence of water in the methanol is still undesirable since the water lowers the heat of combustion of the product. The water concentration should be below 5%. Ethanol and acetone concentrations should be below 10% in order to still mainly produce methanol. This scenario is drafted in case the original scenario turns out to be not feasible in the early stages of development.

3.3 Sub processes

In this chapter, the process of producing methanol from CO_2 and H_2O is further specified. First, an overview is given of all the possible routes to produce methanol from these resources. Then, a multi criteria analysis is performed in order to select the best route. In the end of this chapter, the scope of the project is demarcated further.

3.3.1 Electricity generation

The process of converting carbon dioxide and water into methanol requires energy. From chapter 1.1, the following criteria for energy generation are defined: The source of this energy has to be renewable, the intermittency of the energy production, the degree of autonomy, the location flexibility and the costs. The complexity of the technology is also considered to be an important criterion. This is included in the autonomy criterion.

The possible technologies are thus confined to energy from solar (thermal or photovoltaic), wind, geothermal, hydro or biomass. Ideally, the source of the energy would be continuous since capital costs are an important factor. Intermittency of the source increases the capacity of the equipment for a given size and therefore also the capital costs. Geothermal, hydro and to a smaller extent biomass are the best options for a continuous energy source.

However, an even more important criterion is the autonomous operation of the process. Of the eligible candidates, solar PV is by far the best technology since the energy generation does not involve moving parts and does therefore require minimal maintenance. Biomass is discarded as option since autonomous harvesting of biomass for energy generation requires advanced robotics and even if the harvesting is not incorporated in the judgment, biomass still requires handling of solids that is generally executed by human labor. For autonomous operation a certain degree of robotics will either way be required.

Furthermore, the flexibility of location is important. The energy source should not be restricted to certain locations but should be possible anywhere. Energy from solar and wind are the only technologies that are possible everywhere. Geothermal is in theory also possible anywhere, but the flexibility is awful considering the drilling that is required for every location change. It is therefore discarded. Hydro is also discarded, since energy generation is only possible in a very limited number of places.

Finally, the cost is also an important factor. This criterion is measured by the levelized cost of electricity, in which all the costs for electricity production are expressed in a kWh-price. Between wind, solar thermal and solar PV, solar thermal is by far the most expensive one and is therefore discarded. According to (VGB Powertech, 2015) Solar PV is currently slightly more expensive than wind. However, the investment costs increase more for wind than it does for solar PV, so the costs are comparable.

In table 8, the different energy production technologies are listed. Their performance is rated for each criterion. A plus means that the technology scores well in a certain criterion and not a high value of that criterion.

Table 8 – Multi criteria evaluation of energy production technology

Technology	Intermittency	Autonomy	Location flexibility	Costs
Solar thermal	-	+/-	-	-
Solar PV	-	++	++	+
Wind	-	+/-	++	+
Geothermal	++	-	--	++
Hydro	++	+/-	--	++
Biomass	+	--	+	+/-

From table 8, it becomes clear that Solar PV is the best energy production technology for this application. The greatest advantage is the autonomous operation of solar panels. The costs are also reasonably low. The intermittent nature of the source poses a challenge since the capital costs will increase due to the intermittency. From a scientific perspective, however, it is interesting to research the dynamic operation of a container-sized production facility. Also, simplifications can be made easily in the case that another energy production technology is more feasible.

3.3.2 Carbon capture

Since the carbon capture is left out of the scope of this thesis in the demarcation, the selection of the CO_2 separation technology is based on the companies that are currently separating CO_2 from air. The carbon capture as a process is handled as a black box. The in- and outputs of this black box are determined for the rest of the process. A short review of the possibilities is given in the literature review in chapter 2.

Most of the companies currently producing processes that capture carbon directly from the air are employing the dry route. The main advantage of the dry route is the relatively low temperature. The temperature required for the desorption of the CO_2 can be mainly supplied by waste heat from the process, since temperatures of approximately 110 °C are sufficient. The absence of water from the process also strongly mitigates corrosion problems. The wet route has the advantage that less expensive materials are used in the process. The main disadvantage for the wet route however is the amount of water that evaporates in the process. This is especially relevant for locations with high solar irradiance because water is scarce in those locations.

Therefore, the dry route is selected as technology for the carbon capture in this design. To make an assumption about the purity and also the energy requirement of the carbon capture process, the patents of Climeworks and Antecy – companies that are employing the dry route – are consulted.

A purity of the carbon dioxide of >99% is assumed for the rest of the process. Even though a higher purity can be attained, it is interesting for research purposes to see the implications of a decreased purity. The remaining 1% is assumed to be air. The heat requirement is assumed to be 5000 KJ/kg CO_2, excluding pump and compressor work.

3.3.3 Desalination

As mentioned in chapter 2.3, the seawater needs to be completely desalinated before it can be fed to the electrolyser to prevent accumulation of salt and other minerals in the electrolyser. There are two options for removing salt from water. The first option is reverse osmosis. With reverse osmosis, salt water is pressurized and flows past a semipermeable membrane through which only water permeates. The seawater must be pressurized since without the extra pressure on the sea water side, the water will act according to the natural osmosis characteristic. It will flow from lower concentrations to higher concentrations. The second option is evaporation. The sea water is evaporated, and the generated steam is condensed to obtain pure water.

The reverse osmosis is the most economical option (Greenlee, 2009). The amount of energy required is an order of magnitude lower than the energy required for evaporation. Therefore, reverse osmosis is selected as technology for the desalination in this design. However, if there is an energy deficit in one of the other processes, it might be more economical to use the evaporation method since steam might be required either way. If in the design phase, it becomes apparent that there is an energy deficit which is larger than the amount of energy required for operation, this option is reconsidered.

3.3.4 Electrolysis

A multi criteria analysis is performed to determine the most suitable electrolyser. The first criterion is the size of the electrolyser because space is a limitation in this design. The second criterion is the dynamic operation performance of the electrolyser. The power source of the process is determined to be solar PV. This means that at least parts of the process will be operated dynamically. The start-up time of the equipment is therefore of major importance. The third criterion is the capital cost of the electrolyser. The process will run automatically and there will therefore not be any operational costs. The capital costs are together with the methanol price the only two factors that determine the feasibility and are therefore crucial. The fourth criterion is the lifetime of the electrolyser. The lifetime indirectly influences the costs but is of even bigger importance in this application since the process is to operate in remote locations where maintenance is difficult. The fifth criterion is the operating conditions. A low temperature and pressure are preferable since they require less energy and therefore decrease the number of solar panels required. The final criterion is the efficiency of the electrolyser.

Table 9 – Multi criteria evaluation of electrolysis

Technology	Size	Dynamic operation	Capital cost	Lifetime	Operating conditions	Efficiency
AEL	-	+/-	++	++	++	+
PEM	+/-	+	-	+	+	+
SOEC	?	--	--	-	-	++

From table 9, it becomes clear that AEL is the most suitable option for this design. SOEC is discarded because start-up time of SOEC is several hours, which would heavily decrease the profitability of the process. SOEC must also be kept at a very high temperature, making it incompatible with dynamic operation. No information was found on the size of SOEC because it has not been developed into a commercial product. The capital cost of AEL is about 10 times smaller than for PEM (Kjartansdóttir & Møller, 2014). Also, the lifetime of the alkaline electrolysis around twice as long compared to PEM. The operating conditions are similar but still slightly in favor of AEL. The only criterion on which AEL scores worse than PEM is on size. PEM cells are generally more compact than AEL. Both types of electrolyser can be operated dynamically. However, since a common problem with electrolysis is the degradation of the performance over time. Since the industry has more experience with alkaline electrolysis, AEL is preferred in this criterion. On efficiency, PEM scores a little bit better overall, but the advantage that AEL has is that the efficiency increases with smaller sizes. (Rand & Dell, 2007) This is favorable for the container sized process.

All in all, AEL scores the best on average on all criteria. The main disadvantage is the increased size, which decreases the total capacity of the container. Also, the slightly lower efficiency is a downside. The advantages of reduced cost and improved lifetime are however decisive. AEL is therefore selected as electrolyser technology in this design.

A problem with the dynamic operation of AEL is that if the electrolyser is turned off, the dissolved hydrogen and oxygen molecules present in the solution will tend to migrate through the membrane and undergo the reverse reaction, resulting in an increase in an undesired increase in pressure of the system. A possible solution is to keep the electrolyser running at a lower level during process downtime. However, since the electrolyser is by far the biggest component of the process, this will require a huge battery capacity. Another option is to short-circuit the system after turning it down, providing an energetically favorable route for the electrons through the electrodes. Since the solubility of oxygen in water is significantly higher than the solubility of hydrogen, there will be oxygen remaining in the liquid after all the hydrogen has reacted. For safety purposes, a pressure relieve valve should be present in the oxygen collector at the top, which can blow off the surplus oxygen. The amount of hydrogen and oxygen dissolved in the solution and the corresponding energy content is calculated in appendix D. If the dissolved hydrogen reacts with the oxygen through the short circuit, 64.6 Wh of energy needs to be dissipated. This amount of energy is not relevant to store, but the short circuit could be connected to the battery for safe dissipation of the energy. The dynamics of the electronics are not further studied in this report.

3.3.5 Methanol synthesis

Carbon dioxide pretreatment

In the literature study in chapter 2, the conclusion of the researchers was that the direct methanol synthesis was more efficient, economically. Considering the additional capital costs, which were identified as an important factor in this autonomous process, combined with the expensive heating with electricity of the RWGS reaction, the conclusion is drawn that the direct methanol synthesis, the CO_2 route, is the most economic for a container-sized plant. This route is therefore selected in this design.

Methanol synthesis reactor

The selection of the most optimal reactor for this design is performed by evaluating the options in three criteria.

- The first criterion is maintenance. Since the process will operate in remote locations, the level of maintenance should be minimized. Catalyst lifetime and reactor robustness are examples of maintenance and are therefore included in this criterion
- The second criterion is capital cost. Since capital cost was identified as important criterion in overall economic feasibility, it is also an important criterion in the reactor selection.

- The third criterion is the performance of the reactor. The performance is measured by performance indicators such as selectivity and the reaction rate. Also, pressure and temperature and type of catalyst are performance indicators because a low pressure and temperature and a cheap catalyst are

A multi criteria analysis is performed to determine the most suitable reactor. The results are shown in table 10. For overview purposes and because the properties are similar, the different types of reactors are grouped together.

Table 10 – Multi criteria evaluation of the reactor

Type of reactor	Maintenance	Capital cost	Reactor performance
Dry Adiabatic	+	+	+/-
Dry Isothermal	+	+	+/-
Wet	-	+	+
Membrane	(+)	+/-	++

- Maintenance and capital costs are good for the dry reactors, since the configuration of the reactors is simple and therefore the production costs low and maintenance is performed easily. Reactor performance is also good for both types. The isothermal reactor has a slight preference because due to the purity requirements, selectivity is preferred over rate of reaction.
- For the wet reactors, the maintenance is the biggest disadvantages. The increased catalyst deactivation rates are detrimental for the application in this design (Wang, Tan, Han, & Tsubaki, 2008), where the maintenance interval must be as long as possible. The capital costs are good because of the straightforward design. The reactor performance is also good. The conversion rate of wet reactors is better than the conversion rate of dry reactors due to Le Chatelier's principle
- No information was found with respect to the catalyst degradation, but the assumption is made that it is comparable to dry reactors, since the main reason for the decreased catalyst degradation is the H_2O that is present in wet reactors. The capital cost is assumed to be higher that other reactors, since the dry and wet reactors only use common materials in common geometries. Whereas the membranes inside the membrane reactors are costlier to manufacture. Finally, the reactor performance for membrane reactors is excellent due to the permeation of product through the membrane

Since the wet reactor scores bad on maintenance and the membrane reactor has an increased capital cost and is in developmental stage, the dry reactor type is selected for this design. Between adiabatic and isothermal, the latter is selected since the selectivity of this type of reactor is slightly better, and this is preferred over reaction rate.

In the category dry isothermal reactors, the basic Lurgi reactor is selected for this design. This was done for the pragmatic reason that there are kinetic models available in literature for this type of reactor because it is the most commonly adopted reactor type. By selecting this type of reactor, a more detailed kinetic study can be performed, which yields a higher quality of result and a deeper understanding of the process.

Methanol-water separation

The options for the separation process are conventional distillation, packed column distillation, micro-distillation and molsieve separation. In the literature review in chapter 2, the options are explained in more detail. The selection of the most optimal reactor for this design is performed by evaluating the options in six criteria.

- The first criterion is energy required for the process to operate. If for example the heat requirement is higher than the heat available, additional electrical energy is required which is costly. A low electrical energy requirement lowers the number of solar panels required and decreases the capital costs.
- The second criterion is the capital cost itself: the investment costs of the separation equipment. High capital costs have a negative effect on the economic feasibility of the design.
- The third criterion is the dimensions of the process. Since all the equipment should fit inside a standard 40 feet sea container, the width and height of the process can't exceed 2.5 meters. A negative score is rewarded if the dimensions of the optimal design of the equipment exceed the dimensional constraints and that as a result, the design has to be altered. A positive score logically is rewarded if the optimal design doesn't conflict with the constraints.

- The fourth criterion is the size of the equipment. The larger the size, the smaller the final production volume of methanol will be.
- The fifth criterion is the product purity.
- The sixth and final criterion is the facility of autonomous operation. The ability of the operation without on-site human interference.

A multi criteria analysis is performed to determine the most suitable reactor. The results are shown in table 11.

Table 11 – Multi criteria evaluation of the separation process

Type of separation	Energy requirement	Capital cost	Dimensions	Size	Product purity	Autonomous operation
Conventional distillation	+/-	+	-	-	+	+
Packed column distillation	+/-	+/-	-	+/-	+	+
Micro-distillation	+/-	+/-	+	+	+	+
Molsieve	+	+/-	+	+	++	-

From table 11, it becomes clear that all the options have a certain disadvantage.

- Conventional distillation has the disadvantage that in order to produce methanol of sufficient purity, a large number of stages are required which all have a fixed minimum height. For each additional vertical column, additional pumps and piping are required. The advantage is that the capital costs are low compared to the other options.
- The total height of the packed column is fourfold smaller than with the conventional column. The column still needs to be split in two in order to reach the desired purity, hence the negative score for dimensions. The capital cost of the packed columns is higher than the conventional columns since it is harder to produce the complex geometry of the packing.
- The advantage of micro-distillation is the compact size. The dimension of each single micro-distiller is a 10mm diameter tube with a length of 0.5 m. For this design, 762 of these tubes are required and they can be arranged as desired. This process can be designed to fit well together with the other process units in the container. As is mentioned in the literature review in chapter 2, this type of distillation is very suitable for methanol/water separation. The main disadvantage of micro-distillation is the increased capital cost. (Seok & Hwang, 1985) used glass fiber to retain the liquid and copper ends for increased heat transfer. Also, the tubes are not easily produced. Due to the high number of single tubes however, the costs might be reduced significantly through mass production, which is in line with the general idea of this design. Furthermore, research could be carried out to obtain similar results with cheaper materials.
- The advantages of molsieves are the compact size and the product purity. Since the water/methanol mixture is brought into contact with grains of molsieve, the equipment can simply be a compact vessel. The uniform size of the pores of the molsieve give a complete separation of water and methanol. The energy requirement for the molsieves is smaller, since no heat energy is put into heating of the methanol. In the regeneration step, the water is heated to be separated from the molsieve, so there is still some energy required, but is it less compared to the other possibilities. The main disadvantage is that the solid zeolites require handling. This is either a labor-intensive process or robotics are required. Moreover, it needs to be replaced after a certain time of production due to a decrease in performance. Hence the low score for autonomous operation.

Micro-distillation is selected as separation technology in this design. Is has the best score on average. The decisive factor was the simplicity of the design and the good geometric properties (freedom of design of fitting process units together). The increased capital costs are a relevant downside. The possible reduction of costs with mass production is in line with the container-sized design, which seeks to achieve economic gain from the economy of number instead of economy of scale.

3.4 Mode of operation

The selected type of electricity generation, solar PV, is an intermittent source. The logical solution is to design a process that also operates dynamically. However, the assumption is made that there is solar irradiance one fourth of the time. This effectively increases the capital costs of the design by four times for a certain capacity. As was determined earlier, the capital costs of the process are identified as a major share of the costs. It is therefore interesting to investigate the possibility of continuous operation of the process by adding an energy storage device and storage vessels between the sub processes as a buffer for when no electricity is generated. This chapter contains the determination of the mode of operation of the sub processes.

To compare dynamic and continuous operation, an overview of both the processes is given.
Figure 2 shows a schematic of the dynamic process. Since the process is operated dynamically, no buffer capacity is required.

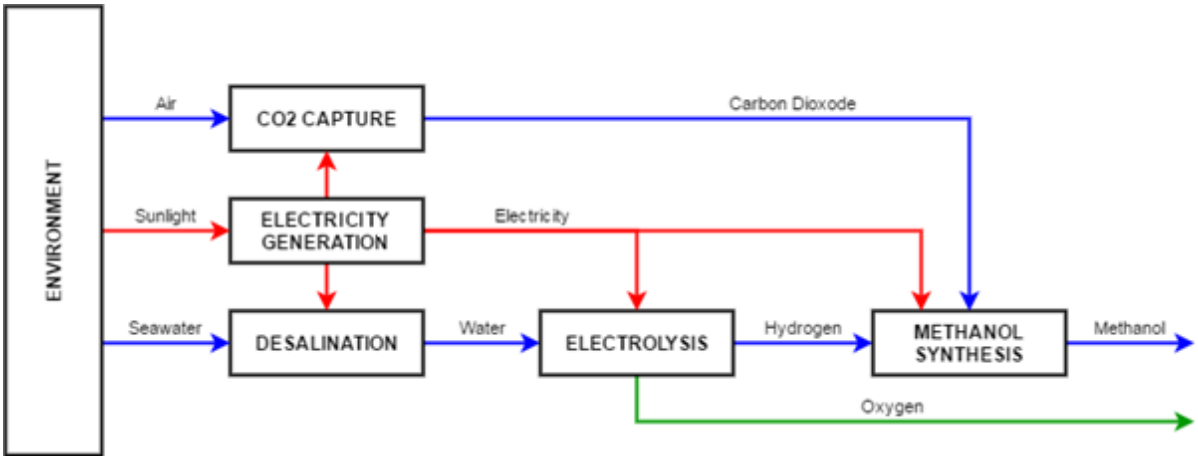

Figure 3 – Flowchart representation of the process in the DOS

In figures 2 and 3, the blue lines represent a mass flow, red lines represent an energy flow and green lines represent mass flows that are a considered to be a byproduct.

Figure 3 shows a schematic of the continuous process. Since the process is operated continuously, intermediate storage capacity of energy and mass is required. This increases the number of components but decreases the size of the sub processes.

As can be seen from this comparison, the continuously operated process has much more subsystems than the dynamically operated process. In practice, the dynamically operated system will also have a small energy storage device which will provide the process with a continuous flow of electricity by leveling the high frequent oscillations of the energy supply (e.g. if a cloud were to block the sun for a couple of minutes)

The starting point of the consideration is that the process is dynamically operated. For each sub process, the specific implications of continuous operation are determined. The size of the storage tank and the increased required energy storage capacity is calculated. The advantages and disadvantages are listed. A final consideration is done of the result, to check whether the total design is coherent and optimal. All the calculations to obtain the numerical values are presented in appendix B.

The size of the storage tank is calculated using a storage factor. This storage factor accounts for the effective space occupation of the storage tank. The total volume required for the storage of a certain substance is equal to the volume produced in one full day of operation, multiplied by the storage factor. This storage factor is estimated to be 1.5. The required battery capacity is calculated by multiplying the power required for each process by the amount of time the process operates without generation of energy. To increase system resilience, the capacity of the battery is increased to the capacity required for a full day of operation without energy generation. The advantages are that the process can also operate continuously on days with less solar resistance and that the lifetime of the battery increases due to fewer deep discharge cycles.

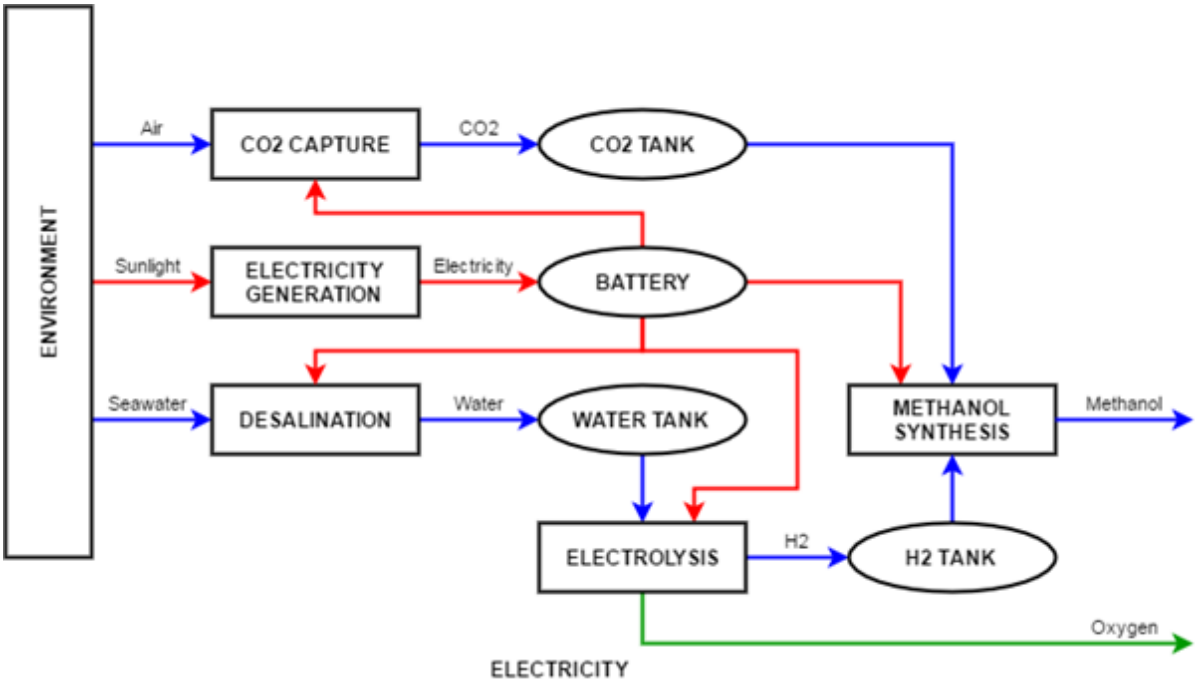

Figure 4 – Flowchart representation of the process in the COS

3.4.1 Energy production

The energy generation is a process that is dynamic by definition because of the intermittent nature of solar irradiance. The intermittency in energy supply could be solved by adding a battery which is large enough to supply the process with electricity when there is no solar irradiance. If the intermittency of energy supply is solved, the entirety of the process can run continuously. However, the required capacity of the battery is too big. For the methanol production calculated in chapter 3.1, a 1.77 MWh battery is required, as calculated in appendix B. The advantage of a process that is four times smaller is outweighed by the disadvantage of the extra costs for a larger battery. For all the sub-processes, this trade-off between an increase in storage capacity and energy storage requirement and the decrease of equipment size is investigated. A fully continuously operated scenario (COS) is therefore discarded.

3.4.2 CO_2 capture

The CO_2 capture is a process that is performed in batch mode. So even in the dynamically operated scenario (DOS), there must be a storage tank. The size of this tank is of course much smaller than in the COS. The required size of the CO_2 storage tank for the COS is 0.41 m^3. This is at an operating pressure of 80 bar and a temperature of 25 °C where the carbon dioxide is a liquid. Since the surroundings can be hotter than 25 °C, the temperature of the CO_2 will increase and since the volume is fixed, the pressure will also increase. To mitigate this effect, the storage tank should be isolated well. The feedstock of the process – which is air – is always available no air storage tank has to be present. The amount of additional energy storage capacity required for the COS is equal to 61.8 kWh. This size is acceptable, but the remark must be made that this only includes electrical energy. There is also low-grade heat required for this process, which originating from the methanol synthesis. Therefore, if the carbon capture process is operated continuously, the methanol synthesis must also be operated continuously.

3.4.3 Desalination

For the desalination, only a water tank needs to be available in the COS. The size of the water storage tank is 0.38 m^3. The amount of additional energy storage capacity required for the COS is equal to 4.8 kWh. This is tiny compared to the 251 kW of installed power required for dynamic operation as calculated in Appendix B. Since a battery will be present anyway for system resilience, it is little extra effort to increase the capacity. The desalination will therefore be carried out continuously, reducing the size of the equipment four-fold, while adding a small water storage tank and adding some battery capacity.

3.4.4 Electrolysis

The electrolysis is the process with the highest electricity requirement. In the COS, a battery capacity of 1.36 MWh is required. This corresponds to a state of the art lithium ion battery of 5.6 tons. The increase in capital cost of this battery, combined with the required presence of a hydrogen and water storage tank easily outweighs the advantage of a smaller electrolysis process. Therefore, continuous operation of the electrolysis is discarded.

3.4.5 Methanol synthesis

The COS for the methanol synthesis requires a hydrogen and carbon dioxide storage tank and additional battery capacity. Assuming a pressure of 300 bar currently used in practice, the size of the hydrogen tank is 2.12 m^3. There are reports of hydrogen storage at a pressure of 700 bar – which will decrease the storage size by a factor of 2 – but there are still a lot of problems to be solved. Leaking of gas (Song, 2012), hydrogen embrittlement (Chen, 2008), safety (Ren, Liao, & Liu, 2006). The size of the CO_2 storage tank is 0.41 m^3. The amount of additional battery capacity equals 303 kWh. The advantages of the COS for the methanol synthesis are again the reduced capital investment and the easier operation. However, except for the catalyst, the synthesis mainly consists of steel parts. Therefore, the reduced capital cost of the smaller size of the process is does not outweigh the increased capital cost of the battery and the storage tanks. The COS for methanol synthesis is therefore discarded.

3.4.6 Determined scenario

All the design choices are combined in the DS. A schematic representation of this scenario is shown in figure 4. Of all the intermediate storage tanks present in the COS shown in figure 3 only the water tank turned out to be feasible. The battery also remained in the determined scenario, but is two orders of magnitude smaller in than in the COS. In this design, the part of the process that operates continuously works well with the dynamically operated parts. Since the feedstock of seawater and air can be considered as continuous sources with a virtually infinite buffer, the source has only shifted one process further downstream. The buffer is now desalinated water instead of seawater. The desalination also doesn't require waste heat from the process and is truly capable of running on the power of a relatively small battery.

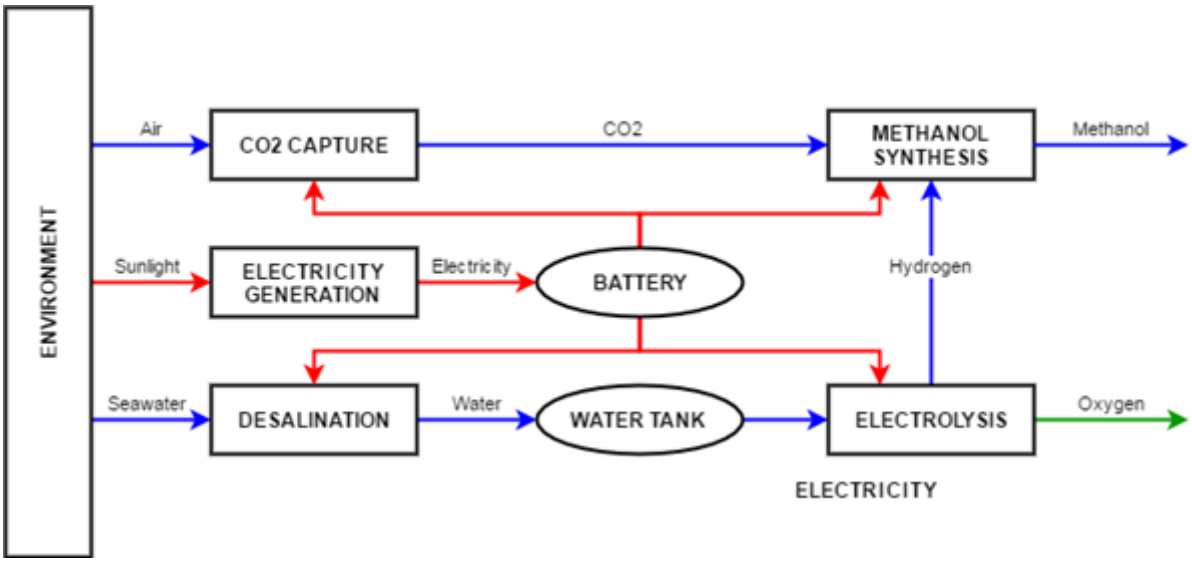

Figure 5 – Flowchart representation of the process of the DS

3.5 Scope of the project

To model the entire process described in the introduction surpasses the scope of the master thesis. Therefore, either a simplification of the process or a demarcation of the process is required. Considering the level of detail required for a master thesis, the best option is to demarcate the process. In this way, the focus of the thesis can be on the part of the process that is unknown, which is relevant for answering the main question. Since the selection of too many processes can lead to a decrease in quality of the work, the number of processes that is studied more extensively is confined to one or two processes. A division will be made between processes that will be subjected to a more thorough study and processes that will be regarded as a black box. The in- and outputs of processes will be specified: The electrical energy required in kilowatts, the heat energy required in pressure, temperature and mass flow, the output mass flows and their composition and input mass flows.

The selection of the processes that are investigated further are based on the special features of this design. The special features of this design compared to other methanol synthesis processes are the size of the process, the dynamic operation and the autonomous operation. The effects of these three features are the most interesting to research. Table 12 lists all the sub processes and ranks them on scientific relevance for research. A process that is well known on small scale and dynamic and autonomous operation is of low relevance whereas a process that is generally operated on a large scale and is operated continuously in the presence of operators is of high relevance.

Table 12 – Scientific research relevance of the sub processes

Sub process	Small scale	Dynamic operation	Autonomous operation
Desalination	--	-	-
Energy generation	--	--	--
Carbon capture	+/-	+/-	+/-
Electrolysis	+/-	+	+/-
Methanol synthesis	++	+	++

- The desalination is not operated dynamically, and the smaller size is also not new to this type of technology. The membrane technology that is used is very developed so scientifically it poses little challenge. The process is therefore not studied more extensively and is regarded as a black box in the design.
- The electricity generation is performed by solar PV panels. This technology is subject to ongoing research to improve the efficiency. While it is scientifically an interesting subject, it poses no challenge in this design. The technology is built for the small scale and by no means would it make sense to operate the panels dynamically.
- The carbon capture process is performed by means of a direct air capture (DAC). DAC is a new technology and it is a batch process and thus inherently dynamic. The companies developing this technology are working on a large scale as well as smaller scale. Both dynamic operation and the small scale are moderately relevant to research since these companies are also working on it.
- The electrolysis is performed by alkaline electrolyser cells. This technology is already applied on a larger as well as a smaller scale. It is therefore only moderately interesting to research. Dynamic operation for electrolysis is interesting to research since electrolysis generally happened continuously, using a steady power source.
- The methanol synthesis process is interesting in all the categories. Traditionally, methanol synthesis always happens on a large scale, in continuous operation mode and under supervision of plant operators. Some dynamic characteristics are known since there are is always downtime due to maintenance, but continuous operation is the standard.

The methanol synthesis is selected as sub process that is investigated in further detail. The carbon capture, electrolysis, energy generation and desalination are considered as black boxes in the design.

Included in the scope of the project is the heat integration between the different sub processes. Some processes have a positive energy balance, while others have a negative energy balance. Heat is hard to obtain in remote locations, it is important to efficiently reuse the heat as much as possible, otherwise the heat needs to be generated by the available electricity.

4 Modelling

The process is modeled using the flowsheeting software Aspen except for the distillation. The type of distillation selected in the basis of design is micro-distillation. This relatively unknown technology is not present in the Aspen built-in distillation equipment process units. It is therefore not possible to incorporate the distillation into the Aspen model in a straightforward way. An alternative approach is required. Matlab is selected as software for the micro-distillation. Matlab models however, cannot be implemented directly into Aspen. There is an alternative route available using flowsheeting software Coco (Baten, 2018). This open source software package can incorporate Matlab models, and the resulting process units can be implemented into Aspen (Raquel De María, 2013). However, since the reactor and distillation units are sequential in the model, it is not imperative for the optimization that the two processes are simulated in the same program. The optimization step is more time-consuming in this scenario, but the implementation of processes from one software to the other is more complicated.

4.1 Aspen Plus

The process is mainly modeled in Aspen. This paragraph elaborates on each process unit that was designed in Aspen. The desalination, the carbon capture and the electrolysis are processes which are regarded as a black box. Therefore, this paragraph will not elaborate on these processes since Aspen is not performing calculations. For these components, the mass and energy balances of the components are composed, and this information is used in the design. The inlet conditions of all the substances in the process are assumed to be a temperature of 25 °C and a pressure of 1 bar.

4.1.1 General model description

Figure 6 shows a schematic of the whole process as designed in Aspen. In the red, top-left block, carbon dioxide enters the process from the carbon capture. It enters the system at a pressure of 0.1 bar and needs to be pressurized to the 30 bar pressure level of the mixer in the orange block in the center. In the blue, bottom-left block the water from the desalination enters the process. This water is pressurized to 30 bar when it enters the alkaline electrolyser where the water is split into hydrogen and oxygen. The hydrogen proceeds to the mixer in the orange block in the center where it is mixed with the carbon dioxide. The mixture is then pressurized to 55 bar and heated to 250 to meet the reactor condition in the purple top-right block. Because not all the carbon dioxide and hydrogen react to form methanol in one pass, the reactor exit stream is recycled and fed back into the reactor. After every pass the produced methanol and water is separated from the hydrogen and carbon dioxide and other gases. To prevent accumulation of nitrogen and oxygen in the system which entered the system with the carbon dioxide, a small fraction of the gas recycle flow is purged. The methanol and water that is separated is depressurized to atmospheric pressure and flashed for a second time to remove more gaseous components. The methanol-water solution is then fed to the distillation column where the methanol is separated from the water.

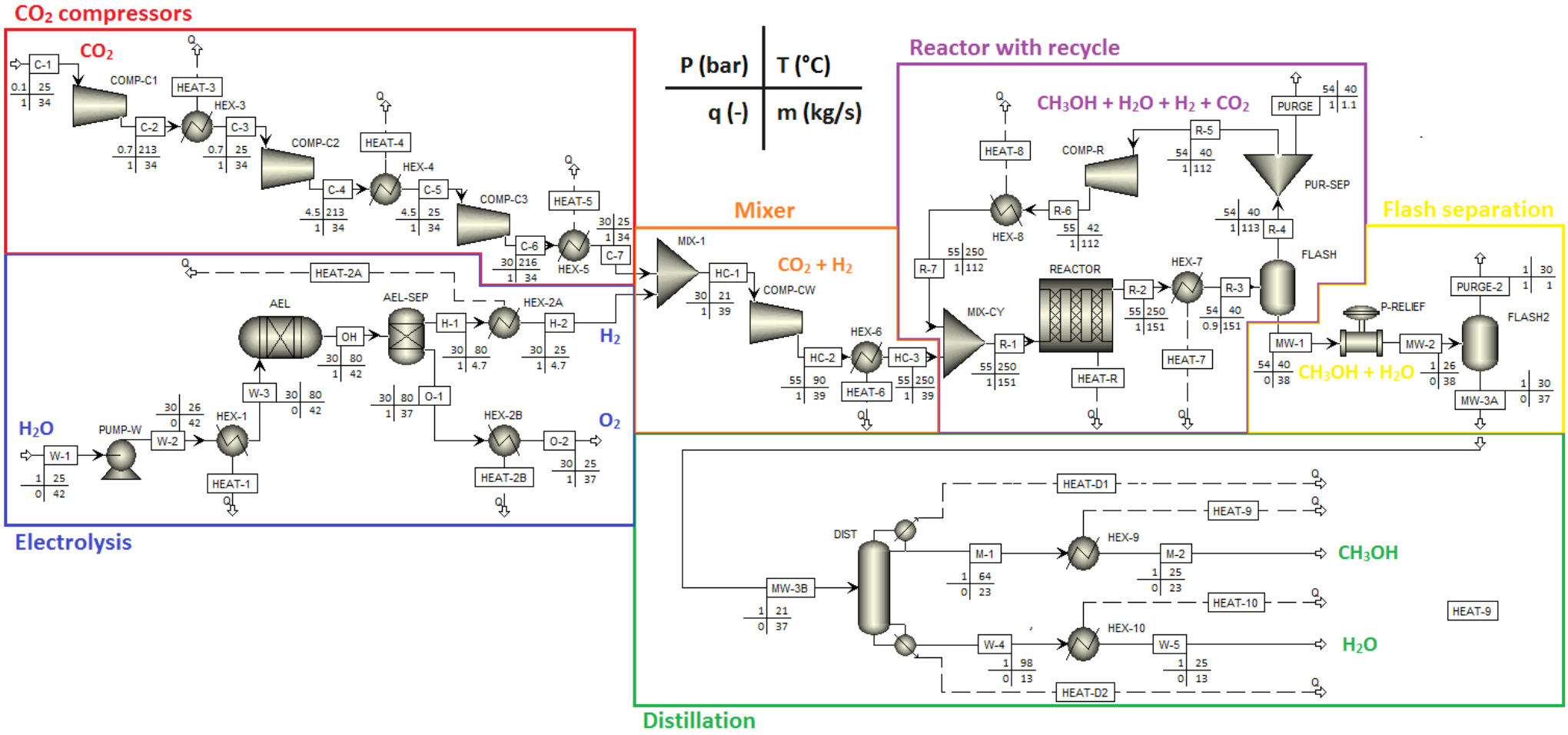

Figure 6 – Aspen process overview

4.1.2 Detailed modeling

Reactor

Property method selection

The most straightforward model is the ideal gas law. This model assumes no intra molecular interactions. For a gas at atmospheric pressure, this model is quite accurate. At elevated pressures, close to the critical region and for liquids in general however, the interactions between the molecules will become significant for the overall behavior and a more complex model is required. Examples of these kinds of models are the Soave-Redlich-Kwong (SRK) and the Peng-Robinson (PR) models. For substances with a high polarity, an activity coefficient model gives a more accurate representation of the reality. For water and methanol, a model such as UNIFAC or NRTL gives better results. For carbon dioxide and hydrogen, SRK and PR give sufficient results since these molecules are not polar. (María, Díaz, Rodríguez, & Sáiz, 2013) used the RK-ASPEN model for the whole process, except for the distillation, where NRTL-RK property method was used. (Van-Dal & Bouallou, 2013) used Redlich-Kwong-Soave equation of state with modified Huron-Vidal mixing rules (RKSMHV2) for the processes above 10 bar and also used the NRTL-RK method for processes below 10 bar. In this design, the same approach that (Van-Dal & Bouallou, 2013) use is applied. Most of the equipment is therefore modelled using the RKSMHV2 property method, while the remaining equipment uses RK-ASPEN.

Operating conditions

In line with (Kauw, 2012) and (Lee, 1990), an operating temperature and pressure for the reactor of 250 °C and 55 bar are selected. These operating conditions are varied when the model is finished for further optimization.

Reactor model

The plug flow reactor module is selected in Aspen as the type of reactor unit because the reactor geometry is similar to a plug flow reactor. The reactor consists of multiple tubes with a high length to diameter ratio in which the catalyst particles are situated. The flow in these tubes resembles plug flow. A kinetic model that is found in literature can be implemented in this type of reactor unit. The reactor is isothermal and operates at a temperature of 250 °C. For the reaction kinetics, the Langmuir-Hinshelwood-Hougen-Watson (LHHW) model is used. The reactions that are modelled in the reactor are the formation of methanol from CO_2 and the RWGS reaction that also occurs in the reactor. These two reactions are shown in equation 2.1 and 2.2

$$CO_2 + 3H_2 \leftrightarrow CH_3OH + H_2O \tag{2.1}$$

$$CO_2 + H_2 \leftrightarrow CO + H_2O \tag{2.2}$$

The reaction rates of the reactions are obtained using the kinetic model proposed by (Bussche & Froment, 1996). The estimation of the values kinetic model was based on experimental data obtained in a bench scale setup. The temperature range was 180 – 280 °C and the pressure 51 bar. The reaction rate for the methanol reaction is shown in equation 4.1. The reaction rate of the RWGS reaction is shown in equation 4.2

$$r_{MeOH} = k_{MeOH} \cdot \frac{(p_{co_2} p_{H_2}) - \left(\frac{1}{K_{p1}}\right)\left(\frac{p_{CH_3OH} p_{H_2O}}{p_{H_2}^2}\right)}{\left(1 + K_a\left(\frac{p_{H_2O}}{p_{H_2}}\right) + K_b\sqrt{p_{H_2}} + K_c p_{H_2O}\right)^3} \tag{4.1}$$

$$r_{RWGS} = k_{RWGS} \cdot \frac{p_{co_2} - \left(\frac{1}{K_{p2}}\right)\left(\frac{p_{CO} p_{H_2O}}{p_{H_2}}\right)}{1 + K_a\left(\frac{p_{H_2O}}{p_{H_2}}\right) + K_b\sqrt{p_{H_2}} + K_c p_{H_2O}} \tag{4.2}$$

Where

$$k_i = A_i exp\left(\frac{B_i}{RT}\right) \tag{4.3}$$

$$\log_{10} K_{p1} = \frac{3066}{T} - 10.592 \tag{4.4}$$

$$\log_{10} K_{p2} = -\frac{2073}{T} + 2.029 \quad (4.5)$$

Equation 4.3 is used to determine the values of $k_{MeOH}, k_{RWGS}, k_a, k_b$ and k_c.

The model described by equation 4.1 – 4.5 cannot directly be implemented into Aspen, since the software requires certain types of kinetic models. To make the model compatible with Aspen, the equations of thermodynamic equilibrium were incorporated in the kinetic constants and the equation was modified to suit Aspen requirements. The modified model is captured in equations 4.6 – 4.8. The pressures are in Pa and the temperature in K.

$$r_{CH_3OH} = \frac{k_1 P_{CO_2} P_{H_2} - k_6 P_{H_2O} P_{CH_3OH} P_{H_2}^{-2}}{\left(1 + k_2 P_{H_2O} P_{H_2}^{-1} + k_3 P_{H_2}^{0.5} + k_4 P_{H_2O}\right)^3} \quad (4.6)$$

$$r_{RWGS} = \frac{k_5 P_{CO_2} - k_7 P_{H_2O} P_{CO} P_{H_2}^{-1}}{1 + k_2 P_{H_2O} P_{H_2}^{-1} + k_3 P_{H_2}^{0.5} + k_4 P_{H_2O}} \quad (4.7)$$

The k-values in equations 4.6 and 4.7 are calculated using equation 4.8 and table 13 (Van-Dal & Bouallou, 2013)

$$\ln k_i = A_i + \frac{B_i}{T} \quad (4.8)$$

Table 13 – K-values for the kinetic reaction models (Van-Dal & Bouallou, 2013)

Parameter	A_i	B_i
k_1	-29.87	4811.2
k_2	8.147	0
k_3	-6.452	2068.4
k_4	-34.95	14928.9
k_5	4.804	-11797.5
k_6	17.55	-2249.8
k_7	0.131	-7023.5

Catalyst loading

The mass of catalyst present in the reactor is calculated by comparing the reactor size from (Van-Dal & Bouallou, 2013) to the reactor in this design. The density and particle size are equal to (Van-Dal & Bouallou, 2013). Since the dimensions of the tubes in which the catalyst is loaded is similar, the same catalyst type and dimensions are used. Table 14 lists the catalyst properties of this design. The shape factor of 1 equals spherical catalyst particles. The assumption is made that the catalyst particles are spherical since it will yield the lowest pressure drop. The tube roughness is predefined by Aspen and is in line with data from (Pipe Flow Software, 2017).

Table 14 – Characteristics of the catalyst (Van-Dal & Bouallou, 2013)

Catalyst density (kg_{cat}/m^3_{cat})	1775
Particle diameter (mm)	0.5
Catalyst mass (kg)	70.7
Shape factor (-)	1
Tube roughness (µm)	45,72

Pressure drop

The Ergun equation presented in equation 4.9 is used to calculate the pressure drop in the reactor. This equation is a standard function in Aspen which requires the tube roughness, particle diameter and the shape factor shown in table 14. The resulting pressure drop over the reactor is validated in appendix H.

$$-\frac{dP}{dz} = \frac{150(1-\epsilon)^2}{\epsilon^3}\frac{\mu U}{\phi_s^2 D_p^2} + 1.75\frac{(1-\epsilon)}{\epsilon^3}\frac{\rho U^2}{\phi_s D_p} \quad (4.9)$$

Where U is the superficial velocity, ϵ is the bed voidage, μ the fluid viscosity, D_p the particle diameter, ϕ_s the particle shape factor and ρ the fluid density. All these parameters are either from table 14 or calculated by Aspen.

Reactor recycle loop

The outgoing stream from the reactor is cooled down to a temperature of 40 °C before it is fed to the flash drum. The division of the substances in the flow is dependent on the temperature and the pressure of the flash. The vapor part of the flash is recycled to the entrance of the reactor, while the liquid part of the flash is fed to the micro-distiller to separate the remaining components from the methanol.

Since the reactor does not have a conversion rate of 100%, a recycle loop is required to obtain full conversion. The risk of instability of an Aspen model increases significantly when a recycle loop is added. Therefore, the tear stream must be chosen with caution. The initial value of this tear stream was estimated at a logical value to reduce the number of iterations required and increase the models solving speed.

Electrolysis modelling

(Balabel, Zaky, & Sakr, 2014) investigated the performance of AEL coupled to solar PV. An operating temperature and pressure of 25 °C and 1 bar was used in the process. Additionally, in another study performed by (Santos, Sequeira, & Figueiredo, 2013), it was reported that the efficiency was not significantly higher at higher operating pressures. According to (Allebrod, Mogensen, Hjelm, & Ebbesen, 2013), higher temperatures and pressures lead to increased performance, but that the degradation mechanisms were stronger at these elevated pressures and temperatures. (Yde, 2013) agree on the degradation of material and have done research to more stable materials. A common temperature of 80 °C is mentioned, which is selected as the operating temperature in this design. The elevated temperature electrolysis is still in development phase and is therefore discarded but might be interesting in the future. The pressure is set at 30 bar because of increased performance and because pressurizing a liquid using a pump is cheaper than pressurizing a gas using a compressor.

Distillation modelling

The determined distillation method is micro distillation. In chapter 4.2, an extensive description of the modelling in Matlab is given. However, since it was not possible to obtain valid results using this model, the distillation is also modelled in Aspen. Conventional distillation was modeled to obtain the required heat inputs and outputs used in heat integration in chapter 6.3. Furthermore, modelling the conventional distillation gives more insight into the effects of the design choices such as length, reflux ratio and feed location. The main goal of modelling the distillation in Aspen, is to obtain information about the heat requirement. The performance of the conventional distillation will be different from the micro-distillation. Therefore, the feed flow is assumed to only contain methanol and water, instead of also containing traces of other substances and a small percentage of CO2. This makes the design of the distillation column easier.

Carbon capture

A purity of CO2 of 99.9% is assumed, based on a product sheet of Climeworks. The remaining 0.1% is assumed to be 79 vol. % nitrogen and 21 vol. % oxygen. The presence of argon, other noble gases and trace elements is dealt with by assuming that these substances are nitrogen. This is justified since – them being inert gases – they show similar behavior to nitrogen. Using the molar masses of nitrogen and oxygen, the mass percentages are 76.7% and 23.3%, respectively. The outlet mass flow in kg/day then becomes 34.37

Desalination

Since the desalination is a known and proven concept, it is not included in the model.

Compressors

The compressors are modelled by defining the pressure ratio. The inlet pressures are defined for all the ingoing flows and the pressures are calculated using the pressure ratios. With nearly isentropic compression, the temperature increases along with the pressure. There are multiple compressors in the system: a CO_2 compressor, a syngas compressor, and a recycle loop compressor. Because of the high pressure difference between the absorbed CO_2 and the syngas mixer, a cascade of compressors is required to pressurize the CO_2 in order to control the temperature. A carbon capture outlet pressure as low as 0.1 bar is required to obtain CO_2 of high purity. The pressure of the syngas mixer is 30 bar. This results in a pressure ratio of 300. For compressing CO_2, this would result in a temperature of 954 °C, using equation 4.10 for polytropic compression (Don W. Green, 2008).

$$T_{2_{co_2}} = T_{1_{co_2}} \cdot \left(1 + \frac{\left(\frac{p_{2_{co_2}}}{p_{1_{co_2}}}\right)^{\frac{\kappa_{co_2}-1}{\kappa_{co_2}}} - 1}{\eta_{isen_{co_2}}} \right) \quad (4.10)$$

Where η_{isen} denotes the isentropic efficiency of the compressor, assumed at 0.75, indices 1 and 2 denote the stage before and after compression, respectively and κ denotes the isentropic exponent. To reduce the presence of high temperatures which are harmful for the compressors, the pressure is increased in steps. Using 3 compressors with equal pressure ratio's, a pressure ratio of 6.7 is selected. As can be seen from figure 6, the maximum temperature that is obtained after each stage is equal to 216 °C, which is an acceptable design criterion for a compressor.

4.2 Matlab

The objective of this part of the thesis is to design the micro-distillation unit in Matlab. To implement this part into the total design and connect the heat and cooling duties for an optimal and energy efficient system. This paragraph describes the methodology of designing the model of the distillation column.

4.2.1 Theoretical basis

The micro-distillation tube is similar to a packed distillation column. for both columns, the vapor and liquid are in constant contact with each other. This makes it hard to perform equilibrium calculations, since the location of the system boundaries are arbitrary. In conventional distillation, each stage is in equilibrium and mass is transferred to the stages above and below. To deal with this problem, the concept of HETP is introduced. HETP stands for height equivalent to a theoretical plate and is defined as the total height (or length in case of micro-distillation) divided by the number of theoretical stages. A piece of column with the length of one HETP is equal to one stage of a conventional distillation column. In the model, the column is divided into cells with the length of one HETP. The assumption is made that equilibrium is reached in each of these cells. The separation process is calculated using an isothermal flash calculation. The micro-distillation column is modelled as a cascade of isothermal flash drums.

The methodology for calculating an isothermal flash is called the mass, equilibrium, summation and heat (MESH) method. In this method, all the equations necessary to calculate the resulting flow are present. The method consists of four steps. The first step is the Material balance. The equations in this step are listed below and are derived from the law of conservation of mass.

$$F = L + V \quad (4.11)$$

$$Fz_i = Lx_i + Vy_i \quad (4.12)$$

Where F, L and V are the feed, liquid and vapor flow, respectively. The unit is moles. z_i, x_i and y_i are the compositions of their respective flows. The subscript i varies from 1 to n, the number of substances in the system. The second step is the Equilibrium relation. The compositions of the liquid and vapor fractions are calculated using the equations in this step. The equilibrium relation is

$$y_i = K_i x_i \quad (4.13)$$

Where K_i is the equilibrium constant. K is dependent on pressure and temperature, and since the temperature varies over the length of the column, K is calculated for each temperature. For obtaining the values of parameters, the equation of state program REFPROP™ (further referred to as REFPROP) is selected, since the model already works with a REFPROP plugin. The data REFPROP provides uses an equation of state to estimate the K-values. REFPROP has implemented three models for the thermodynamic properties of pure fluids: equations of state explicit in Helmholtz energy, the modified Benedict-Webb-Rubin equation of state, and an extended corresponding states (ECS) model (Eric Lemmon, 2007).

On comparing the K-values obtained from REFPROP with experimental data (Kiyofumi Kurihara, 1993), it was found that the two differ significantly from one another. Additional experimental data (J. Soujanya,

2010) at a comparable pressure matches more closely with the experimental data from (Kiyofumi Kurihara, 1993) than with the values found in REFPROP. In appendix I, the data is compared, and the differences are elaborated. In the model, the REFPROP data is used since the enthalpies are obtained using a REFPROP-plug-in. This plug-in is not compatible with experimental data because the model is instable when using the experimental data. Also, with the experimental data, an interpolation function is required, which further reduces the model accuracy.
The third step is the Summation of moles. This step states that the sum of the mass fractions in liquid and vapor phase should always be equal to one, as described in equations 4.14 and 4.15

$$\sum_i x_i = 1 \tag{4.14}$$

$$\sum_i y_i = 1 \tag{4.15}$$

The fourth and final step of this methodology is the Heat balance. The heat balance states that the energy in- and output must be equal. The heat balance is derived from the first law of thermodynamics.

$$\Delta U = Q - W \tag{4.16}$$

$$\dot{m}\left(H_{in} + \frac{u_{in}^2}{2} + gz_{in}\right) - \dot{m}\left(H_{out} + \frac{u_{out}^2}{2} + gz_{out}\right) = W - Q \tag{4.17}$$

Since the system is not doing any work or work is exerted on the system, the work is equal to zero. The difference in height is also zero because the distillation column is placed horizontally, the gravity terms can therefore also be omitted. The velocity of the fluids is not equal to zero, but they are negligible however. The velocities in the column are in the order of centimeters per second. Using SI units, the kinetic energy term is in the order of 1E-4 m^2/s^2. The enthalpies are in the order of 1000 KJ/kg, which is 1E6 J/kg in SI units (J/kg is equal to m^2/s^2). Therefore, it is concluded that the influence of the velocity on the energy balance is negligible. The heat transfer from and/or to the system has a nonzero value at the condenser and evaporator sections. Equation 4.18 is the energy balance after these simplifications.

$$\dot{m}H_{in} - \dot{m}H_{out} = -Q_{ex} \tag{4.18}$$

The first term is the energy of the incoming flow and is defined as the mass flow times the enthalpy. The second term is the energy of the outgoing flows. Since the outgoing flows are in liquid and vapor phase, a distinction is made between these two phases. Q_{ex}, finally, is the heat transfer from the system to the surroundings. Because the parameters L, V and F are in moles, and the energy balance uses kg as a unit for the material, each term in the equation needs to be multiplied by the corresponding molar mass. The energy balance is shown in equation 4.19.

$$Q_{ex} + FH_F M_F - LH_L M_L - VH_V M_V = 0 \tag{4.19}$$

Where H is the enthalpy of the flow and the superscripts indicate the type of stream: liquid, vapor or feed flow. M is the molar mass of the flow. Q_{ex} is zero in each cell because the column is assumed to be perfectly isolated.

4.2.2 Model elaboration

The MESH method as a set of equations is the basis for the whole model. All the equations used in the model are derived from these equations. This section elaborates on how these equations are inserted into the model and on the coding approach in general.

As mentioned before, the column is divided into cells. In each cell of the column, the composition, the temperature and the number of moles in the vapor and liquid fraction of the flow is calculated. This is shown schematically in Figure 1. The incoming vapor and liquid flows have different compositions and temperatures. Together compose the feed flow, which is flashed and results in the outgoing vapor and liquid flows. The sum of the enthalpies of the ingoing flows are equal to the sum of the enthalpies of the outgoing flows.

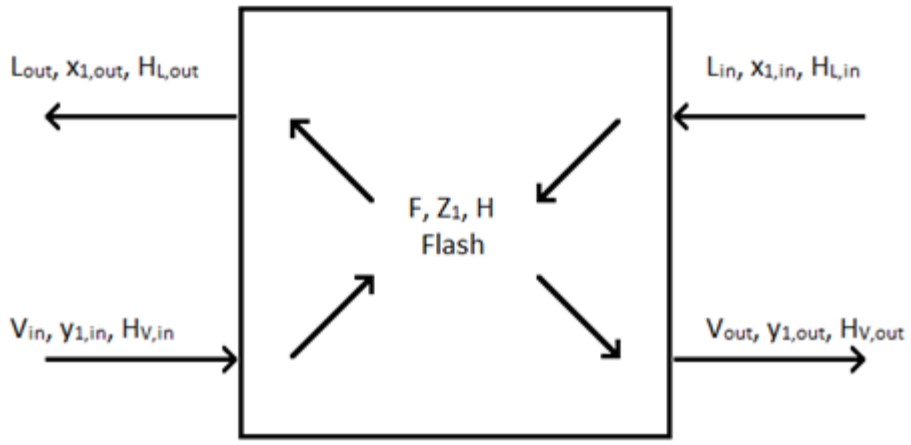

Figure 7 – Single cell material and energy balance

In each cell, the values of the parameters from the previous iterative step are used unless the required parameters are already calculated. The feed flow for a certain cell is calculated combining the vapor and liquid flows from the neighboring cells. Figure 2 shows a schematic of the column. The vapor flows from the evaporator (red) on the left side to the condenser (blue) on the right side while the liquid flows through the wick along the columns edges (green) in the opposite direction. The location of the feed input is a design parameter and the location in the schematic is not representative.

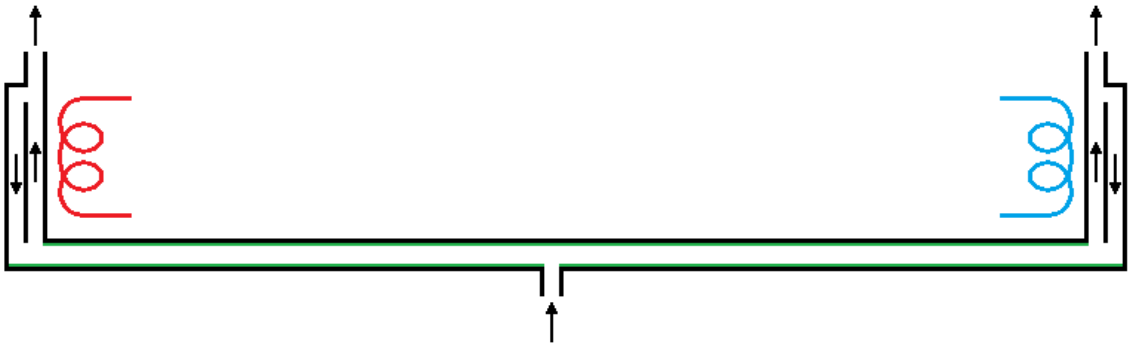

Figure 8 – Micro-distillation column schematic

The model simulates a steady state operation of the column. The final steady state is initially unknown and is obtained by iteration. An initial state is selected, and this state is used to predict the subsequent iteration. Figure 9 shows the matrix that is being produced for each state parameter. Each column of the matrix represents one cell of the column, where adjacent columns represent adjacent cells; column 1 represents the evaporator cell and column n the condenser cell (where n is the number of cells and columns). The rows represent the iterations that the model undergoes. The final row is the solution to the model and the solution can be checked by comparing the final row with the penultimate row. If the sum of the differences is smaller than a certain preset value, the model has reached a stable solution. The reason that the model builds such an extensive matrix is that in this way, the stabilizing process of the model can also be monitored.

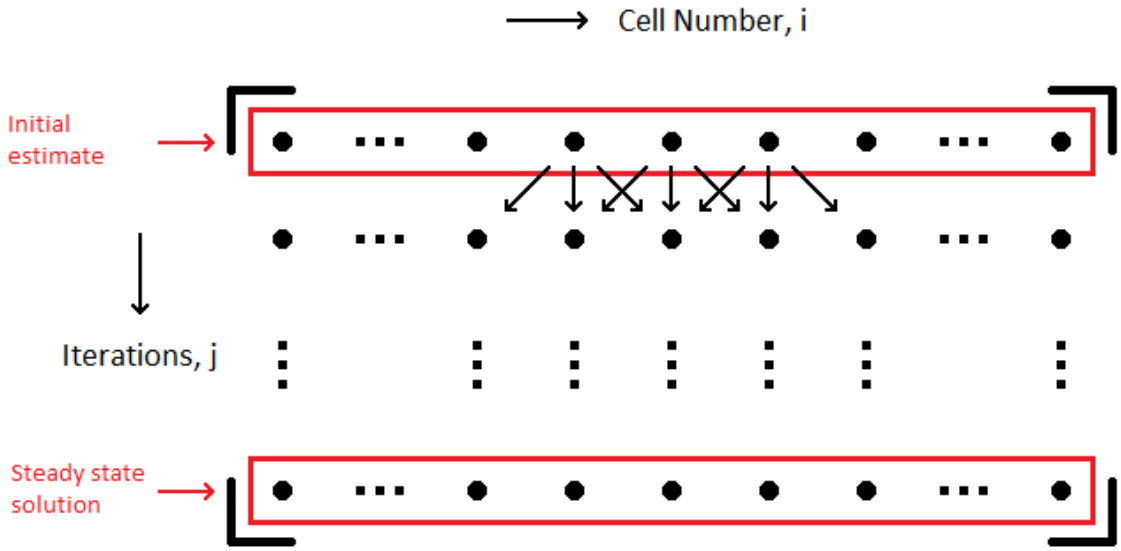

Figure 9 – Coding methodology

The equations of the MESH method are used to calculate the state parameters in each cell. First, the material balance is considered. For each cell, the feed flow is composed of the vapor fraction of the flow from the left cell together with the liquid fraction of the flow from the right cell. The composition of the feed flow is calculated the same way, the liquid fraction composition of the right cell and the vapor fraction composition of the left cell is used for the calculation.

Since the molar vapor flow and the molar liquid flow are not equal, an additional functionality is built into the model. This is called the mass transfer factor (mtf). This mass transfer factor determines the amount of substance that migrates to the adjacent cell. If mtf is equal to one, all the resulting product from the flash is transported to the adjacent cell, while if mtf is equal to one, all the product remains in the cell.

If i is taken as the number the cells in the column and j as the number of iterations, the material balance as it can be found in the code in appendix E is derived from equations 4.11 and 4.12.

$$F(i,j) \;=\; V(i-1,j-1) \;+\; L(i+1,j-1) \tag{4.20}$$

$$z_1(i,j) = \frac{V(i-1,j-1)y_1(i-1,j-1) + L(i+1,j-1)x_1(i+1,j-1)}{F(i,j)} \tag{4.21}$$

Including the mass transfer factor into the equation for the feed results in equation 4.22

$$\begin{aligned} F(i,j) \;=\; & V(i-1,j-1)mtf_V + V(i,j-1)(1-mtf_V) \\ & + L(i+1,j-1)mtf_L + \; L(i,j-1)(1-mtf_L) \end{aligned} \tag{4.22}$$

The implementation of the mtf results in an extended equation for the calculation of the feed since a part of the feed is not determined by the vapor or liquid moles that are already present in the cell. From here on, the equations are presented as if the mtf is equal to one. For the complete equations used, the reader is referred to appendix E. The mtf's are omitted from here on for readability purposes.

As can be seen from equations 4.20 – 4.22, is that all the information from the previous iteration is used to calculate the current solution. The second step is the equilibrium relation, which relates the compositions in the vapor and liquid states. The K-values required are dependent on pressure and temperature. The pressure is assumed constant, but the temperature is unknown. The heat balance is introduced to calculate the enthalpy, from which the temperature can be obtained. The heat balance is derived from equation 4.19 and is shown in equation 4.23.

$$H_L L + H_V V = H_F F \tag{4.23}$$

The unit of enthalpy in REFPROP is kJ/kg, therefore the mole fractions are converted to mass fractions using equation 4.24.

$$w_i = x_i \cdot \frac{M_i}{\sum_i (x_i M_i)} \tag{4.24}$$

Where w_i is the mass fraction, for substance i. A subscript L or V is added to denote the corresponding phase. The calculations of the mass fractions for both phases and substances are shown in equations 4.25 – 4.28.

$$w_{1,L}(i,j) = x_1(i,j-1) \cdot \frac{M_1}{x_1(i,j-1)M_1 + x_2(i,j-1)M_2} \tag{4.25}$$

$$w_{2,L}(i,j) = 1 - w_{1,L}(i,j) \tag{4.26}$$

$$w_{1,V}(i,j) = y_1(i,j-1) \cdot \frac{M_1}{y_1 M(i,j-1)_1 + y_2(i,j-1)M_2} \tag{4.27}$$

$$w_{2,V}(i,j) = 1 - w_{1,V}(i,j) \tag{4.28}$$

The mass fractions and the temperatures together are used to retrieve the enthalpy of the incoming liquid and vapor flows using the REFPROP plug-in. The mass fractions for the feed flow are also calculated which is required for calculating the temperature in the cell after the enthalpy is calculated. This is shown in equation 4.29. The equation including the mtf can be found in appendix E.

$$w_{1_{F(i,j)}} = \frac{w_{1_L}(i,j)\, L(i+1,j-1) + w_{1_V}(i,j)\, V(i-1,j-1)}{F(i,j)} \tag{4.29}$$

All the unknowns in equation 4.23 except for H_F are known. H_F is calculated differently in various cells. For regular cells, the heat balance is solved for H_F, and is shown in equation 4.30. The equation including the mtf can be found in appendix E

$$H_F(i,j) = \frac{H_L(i,j)L(i,j-1) + H_V(i,j)V(i,j-1)}{F(i,j-1)} \tag{4.30}$$

To conclude the heat balance, the temperature is obtained from REFPROP, using the enthalpy, pressure and the mass fractions.

Special cells

At the condenser and evaporator end, and at the feed inlet, the material and heat balance are altered. As can be seen from figure 2, at both ends of the column a part of the fluid is recycled back into the column. In distillation literature, this is called the reflux ratio. In this section, only the evaporator side is discussed. At the condenser, the same methodology is applied, but the vapor is converted to liquid there instead of the other way around. The altered mass and heat equations for the feed inlet cell are discussed.

The reflux ratio is incorporated in the model using equations 4.31 to 4.33, which are based on equations (Mat. Balance MESH)

$$V_{rflx}(j) = rflx_{evap} \cdot L(i,j-1) \tag{4.31}$$

$$F(i,j) = V_{rflx}(j) + L(i+1,j-1) \tag{4.32}$$

$$z_1(i,j) = \frac{V_{rflx}(j) y_1(i,j-1) + L(i+1,j-1) * x_1(i+1,j-1)}{F(i,j)} \tag{4.33}$$

$rflx_{evap}$ is the reflux ratio at the evaporator. In equation 4.32, the terms containing $V(i-1,j-1)$ and $L(i,j-1)$ are replaced by $V_{rflx}(j)$ because there is no vapor inflow from the left side, and all the liquid in the leftmost cell is transferred into the evaporator and returned to the cell as a vapor.

For the feed cell, the mass balance equations are also based on equations 4.11 and 4.12, but an extra term is added. F_{ex} is the number of moles entering the feed cell and $z_{1_{ex}}$ is the composition of the feed.

$$F(i,j) = V(i-1,j-1) + L(i+1,j-1) + F_{ex} \tag{4.34}$$

$$z_1(i,j) = \frac{V(i-1,j-1)y_1(i-1,j-1) + L(i+1,j-1)x_1(i+1,j-1) + F_{ex}z_{1_{ex}}}{F(i,j)} \tag{4.35}$$

The mass fractions are calculated in the same fashion as in equations 4.25 – 4.28, except that the same terms are omitted and added as in the mass balance equation above. For the exact equations used, the reader is referred to the Matlab code in appendix E.

The heat balance for the evaporator end cell is based on equation 4.30 and is shown in equation below. The enthalpies of the liquid and vapor phase are calculated in the same fashion as the normal cells

$$H\_F(i,j) = \frac{H_L(i,j)L(i+1,j-1) + H_V(i,j)V_{rflx}(j)}{F(i,j)} \tag{4.36}$$

For the system feed inlet cell, the heat balance equation is also based on equation 4.30 for the normal cells.

$$H_F(i,j) = \frac{\left(H_L(i,j) * L(i+1,j-1) + H_V(i,j) * V(i-1,j-1) + H_{F_{ex}} * F_{ex}\right)}{F(i,j)} \tag{4.37}$$

When the enthalpies and the masses of the liquid and vapor fractions are determined, the remaining flash calculations are the same for all cells.

Flash calculation

With the temperatures known, the K-values can be obtained. As mentioned before, the REFPROP plugin for Matlab cannot retrieve the K-values directly. Using the plugin, it is possible to obtain the mass fractions of the liquid and vapor phase of both substances for a given composition and temperature. Using equations 4.35 – 4.28, equation 4.38 and 4.39 can be obtained to calculate x_1 and y_1.

$$\mathrm{x1(i,j)} = \frac{\frac{w_{1\mathrm{L(i,j)}}}{\mathrm{M_1}}}{\frac{w_{1\mathrm{L(i,j)}}}{\mathrm{M_1}} + \frac{w_{2\mathrm{L(i,j)}}}{\mathrm{M_2}}} \tag{4.38}$$

$$\mathrm{y1(i,j)} = \frac{\frac{w_{1\mathrm{V(i,j)}}}{\mathrm{M_1}}}{\frac{w_{1\mathrm{V(i,j)}}}{\mathrm{M_1}} + \frac{w_{2\mathrm{V(i,j)}}}{\mathrm{M_2}}} \tag{4.39}$$

From the summation of moles, in the case of a methanol/water mixture:

$$x_2 = 1 - x_1 \tag{4.40}$$

$$y_2 = 1 - y_1 \tag{4.41}$$

With all the compositions known, the K-values can be calculated.

$$K_1 = \frac{y_1}{x_1} \tag{4.42}$$

$$K_2 = \frac{y_2}{x_2} \tag{4.43}$$

Finally, the vapor to feed ratio α can be calculated. a is calculated using the Rice-Rachford equation, stated in equation 4.44.

$$\sum_i \frac{z_i(K_i-1)}{1+a(K_i-1)} = 0 \tag{4.44}$$

$$\frac{z_1(K_1-1)}{1+a(K_1-1)} + \frac{z_2(K_2-1)}{1+a(K_2-1)} = 0 \quad (4.45)$$

Using a, the vapor flow can be calculated and from the vapor flow, the liquid flow is calculated using the Material balance, concluding the iteration loop.

$$V = aF \quad (4.46)$$

$$L = F - V \quad (4.47)$$

Heat transfer

The heat transfer Q_{ex} from the condenser and to the evaporator are calculated using the heat op vaporization of water and the heat of vaporization of methanol. The value that is calculated acts as a first order estimate. This value is an initial value and is later varied for optimization. From (Seok & Hwang, 1985), it is known that the column contains 20 cm^3 of liquid initially. The assumption is made that the same amount of liquid is present in the column during steady state operation. It is further assumed for the enthalpies that the mixture is pure water at the evaporator end and pure methanol at the condenser end. The heat duty of the condenser and evaporator is calculated by the multiplying the amount of liquid in the condenser and evaporator, respectively, by the change in enthalpy of the liquid. The amount of liquid is calculated by calculating the fraction of the available space that the condenser and evaporator take up, respectively. The enthalpy change in the evaporator is calculated by multiplying the mass of the liquid by the change in enthalpy from water of 95°C to saturated vapor. The enthalpy change in the condenser is calculated by multiplying the mass of the liquid by the change in enthalpy from methanol vapor of 70°C to saturated liquid. These values are again estimations of the temperature at the evaporator and condenser inlets.

Initial values

Because the model works iteratively, a set of initial values of certain parameters is required. When the code in appendix E is considered, it can be deduced that an initial value is required for V, L, x_1, y_1, x_2 and y_2. V and L are both estimated rather arbitrarily since their ratio is not considered once they compose the feed. The only important condition is that the summation of the two is equal to F, the total mass of the feed flow. For one cell, this is equal to the total mass in the system, divided by the number of cells in the column. In the model, both V and L are set at half the feed flow. In order to calculate x_1 and y_1, the temperature is estimated over the length. A temperature gradient from 95 °C to 70 °C is assumed in the column to decrease the time to converge. The K-values at the assumed temperatures are calculated and x_1 and y_1 are calculated using the same method as described above.

5 Design

This section elaborates on the implication of the smaller scale of this design compared to the large scale and size of traditional process plants.

- The piping of the process plant does not scale proportionally to the other equipment. This is because of reasons of structural integrity and robustness of the tubes. The disadvantage that this entails is the relative increase of materials used. There is however also a beneficial effect. The wall thicknesses of the piping are much smaller, and the amount of material used scales quadratically with diameter. The distances between equipment are also kept to a minimum due to the confined space available. The advantage of the relatively larger tubes is the fact that the flow in the tubes will be laminar whereas the flow in large power plants is always well within the turbulent region; with a Reynolds number in the order of 1E5. Since pressure drop scales proportionally to the Reynolds number, the pressure drops in the piping will be negligible, which in turn reduces the amount of pumping and compressor power required.
- Because the flows in this design are much smaller compared to large scale process plants, the ratio of pipe surface to displaced volume is much larger. The heat transfer is therefore much higher. The advantage is that for the heat exchangers in the process the design will be much easier. The disadvantage is that the heat is much harder to retain when it is desired. It is therefore imperative for an energy efficient system to reduce the distance between the outlet of hot streams and the entrance of the subsequent heat exchangers as much as possible. In the design of the heat integration, it is important to also reduce the distance between connected heat exchangers. In general, the layout of the process plant must be designed in such a way that the length of the hot streams is as short as possible. In the light of increased energy efficiency, the potential additional length of the colder streams is justified. All the hot streams in the design are provided with isolating material.

Inherent to the small scale of the design is the large numbers in which this design is intended to be produced. This also has implications for the design.

- For mass production, the fabrication method of the components must be straightforward and as standardized as possible. For large scale process plants, the complexity of components is of minor importance, since it only has to be produced one time. For this small-scale design, the fabrication process must be automatic in order for it to become economically viable.
- The cost of the raw materials used in mass production is of importance because there is a strong correlation between the material cost and the cost of the finalized product in mass production. The higher the number of identical products fabricated, the closer the cost can be estimated by the material cost multiplied by a certain constant.

6 Results and Discussion

In this chapter, the results of the fulfillment of the basis of design in the steady state model is discussed. The chapter is divided into

6.1 Aspen Plus

This paragraph is divided into a section concerning the optimization of the model and a section in which the results are presented in the form of a mass and energy balance.

6.1.1 Optimization

Reactor

The configuration of the reactor is based on the capacity calculations in chapter 3. This section aims to increase the reactor efficiency by optimizing certain parameters. The variables in this optimization are the length of the reactor tubes, the number of tubes, the tube diameter and the catalyst loading. To assess the effect of the variables on the performance, the change in recycle stream mass flow is considered. The goal of the optimization is to obtain a high methanol yield, as pure as possible while decreasing the capital costs and keeping in mind the other design criteria. Table 17 shows the configurations that are simulated. The varied parameter is highlighted in each configuration.

In table 18, the results of the various configurations are shown. The recycle stream mass flow is given, along with the compositions. Also, the composition of the flow after the final flash separation is given, to assess the influence on the final product stream. The base case is based on data from (Van-Dal & Bouallou, 2013) and all the variations of the variables are compared to these results.
Looking back at the design criteria, the capital costs and low maintenance (autonomous operation) are the criteria that are most important in this consideration. The effect on the purity and quantity of methanol is negligible since all the results are within a 0.5% range.

Looking at table 18, the following effects of the variables are identified:

- An increase in the length of the tubes of 33% results in a decrease of the recycle stream of 1%. Alternately, a decrease of the length of the tubes of 33% results in an increase of the recycle stream with 4%. This significantly reduces the size of the reactor while the recycle stream increases only slightly. The length of the tubes is therefore reduced to 0.2 meter.
- An increase of the number of reactor tubes with 150 (23 %) decreases the recycle stream by less than 1%. Alternately, a decrease of the number of tubes with 150 (23 %) results in an increase of the recycle stream with 2,3%. Since the capital costs are an important factor in the design, the number of tubes is decreased to 500 in the design. The number of tubes is inversely proportional to the Reynolds number, which will increase with 23 %. This results in a flow that is still well within the laminar region.
- An increase of the diameter by 25% to 2.5 mm results in a decrease of the recycle stream of less than 1%. An increase in diameter of the tubes increases the total tube area by more than 50%. Alternately, a decrease of the diameter by 25% to 1.5 mm results in an increase of the recycle stream of 6.3%. Since this is a considerable increase and 2 mm is sufficient for a uniform temperature profile, this option is also discarded. Also, with 1.5 mm diameter tubes, the reactor will be more prone to clogging since the catalyst particles are 0.5 mm in size.
- The normal catalyst loading is at 65% of the maximal loading, which is based on the available reactor volume and the bulk density. An increase of the catalyst loading of 27% results in a decrease of the recycle stream of 1 %. Alternately, a decrease of the catalyst loading of 22% results in an increase of the recycle stream of 2%. Using less catalyst will result in the remaining catalyst being used more intensively and thus degrading faster. Since low maintenance cost is an important design criterion, the amount of catalyst is not decreased. It is also not increased since the gain is only small.

Overall, reducing the size of the reactor is beneficial for the final design. It can therefore be concluded that the base case reactor was oversized. Table 15 shows the optimized configuration and the results of the final reactor.

Table 15 – Reactor configuration in the optimized case

	Optimized case
Length (m)	0.2
Number of tubes	500
Tube diameter (m)	0.02
Catalyst loading (kg)	36.26

Table 16 shows the result of the optimization. In this table, the flash optimization that is discussed below is included in the results.

Table 16 – Results of the optimized case

	Optimized case
Recycle stream mass flow	151.393
Reactor outlet mass flows	
WATER	13.472
CO2	73.243
HYDROGEN	26.294
METHANOL	25.68
CO	9.855
OXYGEN	0.636
NITROGEN	2.215
Product stream flows	
WATER	13.165
CO2	0.682
HYDROGEN	trace
METHANOL	23.121
CO	0.002
OXYGEN	< 0,001
NITROGEN	< 0,001

A table with more extensive data of the reactor optimization as shown in tables 17 and 18 can be found in Appendix G

Table 17 – Reactor optimization configurations

	Base case	Longer tubes (eq. Loading)	Shorter tubes (eq. Loading)	More tubes (eq. Loading)	Fewer tubes (eq. Loading)	Larger diameter (eq. Loading)	Smaller diameter (eq. Loading)	Higher catalyst loading	Lower catalyst loading
Length (m)	0.3	**0.4**	**0.2**	0.3	0.3	0.3	0.3	0.3	0.3
Number of tubes	650	650	650	**800**	**500**	650	650	650	650
Tube diameter (m)	0.02	0.02	0.02	0.02	0.02	**0.025**	**0.015**	0.02	0.02
Catalyst loading (kg)	70.70	94.27	47.13	87.02	54.38	110.47	39.77	**90.00**	**55.00**

Table 18 – Reactor optimization results

	Base case	Long tubes (eq. Loading)	Short tubes (eq. Loading)	More tubes (eq. Loading)	Fewer tubes (eq. Loading)	Larger diameter (eq. Loading)	Smaller diameter (eq. Loading)	Higher catalyst loading	Lower catalyst loading
Recycle stream mass flow	144.67	142.98	150.35	143.61	148.07	142.59	153.84	143.53	147.45
Reactor outlet mass flows									
WATER	13.59	13.592	13.576	13.588	13.579	13.592	13.57	13.588	13.587
CO2	69.106	67.938	73.122	68.526	71.607	67.745	75.502	68.443	70.891
HYDROGEN	24.631	24.344	25.323	24.329	24.968	24.235	25.815	24.34	25.088
METHANOL	26.214	26.194	26.252	26.188	26.229	26.184	26.284	26.188	26.246
CO	8.361	8.083	9.238	8.159	8.86	8.015	9.825	8.149	8.807
OXYGEN	0.629	0.627	0.63	0.626	0.629	0.626	0.634	0.626	0.629
NITROGEN	2.202	2.198	2.206	2.196	2.203	2.194	2.214	2.195	2.202
Product stream flows									
WATER	13.22	13.227	13.194	13.224	13.204	13.229	13.181	13.224	13.211
CO2	0.65	0.649	0.662	0.652	0.658	0.648	0.665	0.651	0.652
HYDROGEN	trace	trace	trace	trace	trace	trace	trace	trace	trace
METHANOL	23.243	23.258	23.183	23.252	23.207	23.263	23.151	23.251	23.219
CO	0.002	0.002	0.002	0.002	0.002	0.002	0.002	0.002	0.002
OXYGEN	< 0,001	< 0,001	< 0,001	< 0,001	< 0,001	< 0,001	< 0,001	< 0,001	< 0,001
NITROGEN	< 0,001	< 0,001	< 0,001	< 0,001	< 0,001	< 0,001	< 0,001	< 0,001	< 0,001

Flash optimization

Using the Aspen model, the most efficient separation conditions are investigated. In a p-T flash, the pressure and temperature are variables. Altering the pressure from the reactor outlet pressure will result in additional capital costs. The greater the pressure difference, the higher the costs for the recycle compressor. The beneficial effect of altering the pressure must therefore be greater than the negative effect of increased capital costs. As can be seen from table 19, an increase in temperature results in an improved separation of the liquids from the gases. Furthermore, the amount of dissolved CO2 decreases which is desirable and the recycle mass flow increases which is undesirable. Comparing the influence of the flash conditions to the reactor configurations, it can be concluded that the influence of the flash on the recycle stream is much stronger. Therefore, a temperature of 40 °C is selected to reduce the recycle loop size as much as possible. A lower temperature might increase the effectiveness of the separation in the way that more CO_2 would be recycled, and more methanol would end up in the product stream. However, the atmospheric temperature in the designated area's suitable for this design will come close to 40 °C. Therefore, 40 °C is taken as the lowest value that can be achieved in this design without active cooling. A decrease in pressure results also in an improved separation of the liquids from the gases. The effect is however outweighed by the increase in the total mass flow in the recycle loop, which increases the size of the equipment in the recycle loop. The pressure is therefore kept at 54 bar, which is the approximately the pressure after the pressure drop of the reactor and the heat exchanger.

Table 19 – Recycle stream flash separation optimization

Pressure (bar)	**54**	**54**	**54**	**30**	**30**	**30**
Temperature (°C)	**40**	**50**	**60**	**40**	**50**	**60**
Reactor mass flow (kg/h)	140,988	149,598	161,584	156,543	170,63	190,317
Product mass flow (kg/h)	38,065	37,976	37,851	37,906	37,77	37,558
Water	13,227	13,245	13,24	13,318	13,316	13,286
CO2	1,375	1,257	1,17	1,009	0,903	0,826
Hydrogen	0,044	0,042	0,041	0,023	0,022	0,021
Methanol	23,395	23,409	23,376	23,541	23,51	23,41
CO	0,019	0,018	0,019	0,012	0,012	0,012
O2	0,002	0,002	0,002	0,001	0,001	0,001
N2	0,004	0,004	0,004	0,003	0,002	0,002

It becomes clear from table 19 that a flash separation at a lower pressure is more effective in separating the liquids from the gases. To remove the negative consequences of the increased mass flow in the recycle loop, the additional flash separation is added between the first flash separation and the distillation, because the distillation is operated at 1 bar. In table 20, the effect of the second flash separator is shown. After the final stage, only a small fraction of CO_2 is present in the solution as undesired product.

Table 20 – Second flash separation results

	Feed	**Bottom**	**Top**
Water	13,235	13,216	0,019
CO2	1,318	0,655	0,663
Hydrogen	0,043	trace	0,043
Methanol	23,401	23,234	0,167
CO	0,018	0,002	0,017
O2	0,002	< 0,001	0,001
N2	0,004	< 0,001	0,004

The results in table 19 and 20 are based on the reactor configurations of the base case scenario and are not updated to the optimized case scenario. The assumption is that the parameters will change in the same way for both scenario's and that it is therefore not necessary to perform this optimization twice.

6.1.2 Results

This paragraph contains the findings of the Aspen model. The heat streams obtained from Aspen Plus are used as input for pinch analysis to further optimize the energy efficiency of the process. The results from the simulation of the optimized model are used in the mass balances in this section. The mass balances of the components in which no change occurs are omitted. The names of the streams as shown in figure 6 are used in the mass balances. The full results of all the streams in the model can be found in appendix A.

First, the input streams of the process are listed in table 21. The inlet stream from the carbon capture contains 0.1% air, which is modelled as 21% oxygen and 79% nitrogen. The inlet stream from the water desalination is assumed to be 100% water.

Table 21 – CO_2 and H_2O Input streams mass flows in kg/h

Stream	**C-1**	**W-1**
WATER		42.167
CO2	34.34	
HYDROGEN		
METHANOL		
CO		
OXYGEN	0.008	
NITROGEN	0.026	
TOTAL	34.374	42.167

The desalinated water is fed to the electrolyser which separates the water completely into oxygen and hydrogen. A small amount of hydrogen remains in the oxygen stream, but this is negligible. The mass balance is shown in table 22

Table 22 – Electrolyser mass balance in kg/h

Stream	**In**	**Out**	
	W-3	**H-1**	**O-1**
WATER	42.167		
CO2			
HYDROGEN		4.718	< 0.001
METHANOL			
CO			
OXYGEN			37.449
NITROGEN			
TOTAL	42.167	4.718	37.449

The carbon dioxide is merged with the hydrogen from the electrolyser in the mixer as shown in table 23.

Table 23 – CO_2 and H2 mixer mass balance in kg/h

Stream	**In**		**Out**
	C-7	**H-2**	**HC-1**
WATER			
CO2	34.34		34.34
HYDROGEN		4.718	4.718
METHANOL			
CO			
OXYGEN	0.008		0.008
NITROGEN	0.026		0.026
TOTAL	34.374	4.718	39.092

In the recycle stream mixer, the carbon dioxide and hydrogen stream is mixed with the recycle stream from the recycle stream purge. The mass balance is shown in table 24.

Table 24 – Recycle stream mixer mass balance in kg/h

Stream	In		Out
	HC-3	R-7	R-1
WATER		0.285	0.285
CO2	34.34	70.525	104.865
HYDROGEN	4.718	26.15	30.868
METHANOL		2.368	2.368
CO		9.713	9.713
OXYGEN	0.008	0.63	0.638
NITROGEN	0.026	2.192	2.218
TOTAL	39.092	111.863	150.955

Table 25 shows the reactor mass balance. As can be seen from the table, hydrogen and carbon dioxide are converted to methanol and water. The side product carbon monoxide and impurities nitrogen and oxygen are pumped around in the recycle loop.

Table 25 – Reactor mass balance in kg/h

Stream	In	Out
	R-1	R-2
WATER	0.285	13.479
CO2	104.865	72.633
HYDROGEN	30.868	26.456
METHANOL	2.368	25.699
CO	9.713	9.832
OXYGEN	0.638	0.638
NITROGEN	2.218	2.218
TOTAL	150.955	150.955

The gas mixture exiting the reactor is cooled down and then fed to flash separator, where the feed is separated into a gas and a liquid fraction. Stream R-4 is the gas fraction and remains in the recycle loop while the stream MW-1 is the product stream obtained from the recycle. Table 26 shows the mass balance of the recycle stream flash separator.

Table 26 – Recycle stream flash separator mass balance in kg/h

Stream	In	Out	
	R-3	R-4	MW-1
WATER	13.479	0.287	13.191
CO2	72.633	71.242	1.391
HYDROGEN	26.456	26.412	0.043
METHANOL	25.699	2.392	23.308
CO	9.832	9.811	0.021
OXYGEN	0.638	0.636	0.002
NITROGEN	2.218	2.214	0.004
TOTAL	150.955	112.995	37.96

Approximately a one percent fraction of the gases that exit the flash separator are separated from the recycle stream in the purge. This purge step is necessary to remove nitrogen and oxygen from the system which would otherwise accumulate in the recycle stream. Table 27 shows the mass balance of the recycle stream purge.

Table 27 – Recycle stream purge mass balance in kg/h

Stream	In	Out	
	R-4	R-5	PURGE
WATER	0.287	0.285	0.003
CO2	71.242	70.53	0.712
HYDROGEN	26.412	26.148	0.264
METHANOL	2.392	2.368	0.024
CO	9.811	9.713	0.098
OXYGEN	0.636	0.63	0.006
NITROGEN	2.214	2.192	0.022
TOTAL	112.995	111.865	1.13

The liquid stream from the recycle stream flash separator is expanded to atmospheric pressure and flashed again to further purify the product stream. Table 28 shows the mass balance of the product stream flash separator mass balance.

Table 28 – Product stream flash separator mass balance in kg/h

Stream	In	Out	
	MW-2	MW-3A	PURGE-2
WATER	13.191	13.171	0.02
CO2	1.391	0.675	0.716
HYDROGEN	0.043		0.043
METHANOL	23.308	23.133	0.175
CO	0.021	0.002	0.019
OXYGEN	0.002		0.001
NITROGEN	0.004		0.004
TOTAL	37.96	36.982	0.978

The liquid stream from the product stream flash separator is stripped of the CO_2 and other impurities and is fed to the distillation column as shown in table 29. The outgoing flows are the product streams of the process.

Table 29 – Distillation mass balance in kg/h

Stream	In	Out	
	MW-3B	METHANOL	WATER
WATER	13.171	0.14	13.099
CO2			
HYDROGEN			
METHANOL	23.133	23.231	0.191
CO			
OXYGEN			
NITROGEN			
TOTAL	36.982	23.371	13.29

Combining all the inputs and outputs of the whole process gives an insight in the efficiency of the process. Table 30 shows the mass balance of the in- and outgoing streams of the process.

Table 30 – Total mass balance of the system in kg/h

Stream	In		Out				
	C-1	W-1	METHANOL	WATER	O-2	PURGE-1	PURGE-2
WATER		42.167	0.14	13.099		0.003	0.02
CO2	34.34					0.712	0.716
HYDROGEN						0.264	0.043
METHANOL			23.231	0.191		0.024	0.175
CO						0.098	0.019
OXYGEN	0.008				37.449	0.006	0.001
NITROGEN	0.026					0.022	0.004
TOTAL	34.374	42.167	23.371	13.29	37.449	1.13	0.978

6.1.3 Discussion

The obtained results are considered in the light of the design criteria set in chapter 3. Table 7 specifies the desired purity of the methanol. The methanol stream from the distillation has a purity of 99.4 %. This is however excluding the dissolved carbon dioxide, which is not included in this figure because the distillation was carried out using a simplified mixture of methanol and water. The purity of the methanol water mixture can be obtained from table 28. 1.8 % of the mixture is not water or methanol. Assuming the most likely and worst-case scenario that all the dissolved gases will cling to the lighter fraction, which is methanol, and assuming a 99% separation of methanol from water (Seok & Hwang, 1985), a purity of the methanol of 96.6 % is obtained. This is not the required 99.85% mentioned in table 7. Additional purifying steps and optimization of the distillation are required to reach this value. They are not described in this report because of the uncertainties with the purity of the methanol from the distillation.

Another interesting parameter to consider is the material efficiency. i.e. the amount of mass lost to by-products. Two types of waste are identified. Table 31 specifies the values per component in kg/h.

- Produced methanol that is lost in side streams. In the recycle purge, in the product stream flash separator and in the distillation, methanol is dissolved in the side stream. This adds up to 0.39 kg/h of methanol lost on a production of 23.231 kg/h or a 1.65% loss.
- Captured CO2 and produced H2 that is not converted to methanol. In the recycle purge and in the product stream flash separator. For the CO_2, this adds up to 1.428 kg/h of lost CO_2 on a production of 34.34 kg/h from table 21 or a 4.2% loss. For the H_2, this adds up to 0.307 kg/h on a production of 4.718 kg/h from table 22 or a 6.5% loss.

Table 31 – Material efficiencies of the process

	Methanol	CO_2	H_2
Recycle purge	0.024	0.712	0.264
Product stream flash separator	0.175	0.716	0.043
Distillation	0.191		
Total	0.39	1.428	0.307

The loss of intermediate product is a potentially much greater problem. As can be seen from tables 24 to 27, the recycle loop mass flows of CO_2 and H_2 are multiple times their production rates and the intermediate product CO is also present in considerable quantities. Considering the intermittent nature of this process plant, it is important that the intermediate products are retained from shut-down to start-up.

The optimization of the reactor and the flash separator was not extensive. The goal of the optimization of the reactor was to optimize for costs. However, the implication for the costs of changing the variables are not known. The basic optimization has served its purpose in identifying the extent of the effect that changing a certain parameter has on the process. It gives a general idea of what to investigate further and it is more optimal than the base case scenario, but it is not the most optimal solution.

6.2 Matlab

The Matlab model of the micro-distillation could not be validated. The obtained results from the simulation are therefore not reported. This section elaborates on the assumptions made in programming the model and gives an explanation why the obtained data is invalid. The results obtained showed expected behavior to a certain degree but due to the persistent issues, no logical data was obtained or can be obtained with the starting points and assumptions used.

In designing the micro-distillation model, the following assumptions were made.

- The column is divided into cells. Each cell is equal to a tray in conventional distillation in the sense that the steady state is obtained.
- There is no pressure difference over the column, and the column operates at ambient pressure.
- The capillary forces that are the driving force of the separation are not modelled (because the pressure is assumed constant).
- In reality, the mass transfer between the cells is powered by the pressure difference. Since the pressure is assumed constant, the assumption is made that a varying fraction of mass is transferred to the adjacent cells in each iteration. The exact fraction of mass that is transferred is user specified and is optimized for optimal results.
- In each iteration, the cells reach the vapor liquid equilibrium before the mass is transferred to the adjacent cells.
- REFPROP data is used to calculate the enthalpies, temperatures, compositions and other parameters of the substances.
- The condenser and reboiler heat duty is defined by setting the reflux flows as saturated vapor at the reboiler and saturated liquid at the condenser. The energy in- and output are calculated by comparing the enthalpy of the saturated liquid and vapor with the outgoing flows at the condenser and reboiler.
- The vapor-liquid equilibrium data used is obtained from REFPROP. Although the values from REFPROP do not match experimental data, it is compatible with the enthalpy and temperature data that is also obtained from REFPROP. Using the experimental data yields an instable model.

The problem is that the REFPROP data underestimates the methanol concentration slightly, given a certain temperature and pressure. Therefore, the mass balance is incorrect, and methanol disappears from the system with each iteration until there is almost no methanol left. To address this problem, a mass correction factor is introduced.

The correction factor m_{corr} corrects the methanol deficit for each iteration. It is calculated using equation 6.1.

$$m_{corr} = \frac{\sum_i^n \left(L(i,j-1)x_1(i,j-1) + V(i,j-1)y_1(i,j-1) \right)}{\sum_i^n \left(L(i,j)x_1(i,j) + V(i,j)y_1(i,j) \right)} \tag{6.1}$$

The sum of the newly calculated moles of liquid and vapor are multiplied respectively by the liquid and vapor fractions to calculate the total amount of moles of methanol in the system. This is compared to the total number of moles of methanol in the system in the previous iteration. The vapor and liquid concentrations x_1 and y_1 are multiplied by m_{corr} to retain the same amount of methanol in the system.

There is however a negative side effect to m_{corr}. If m_{corr} is for example lower than 1, this means that x_1 and y_1 are corrected to a lower value for the next iteration, while the rest of the parameters keep their original value. A decrease in x_1 and y_1 logically results in a decrease of the mass fractions $w_{1,L}$ and $w_{1,v}$. This in turn results in an increase of the enthalpy because water has a higher enthalpy than methanol for the same pressure and temperature. It can be concluded that if m_{corr} is not equal to 1, there is no energy balance in the model.

The extent of this effect is quantified by considering the number of liquid moles in the system. Because an increase in temperature increases the fraction of moles in the vapor phase. In figure 10, m_{corr} and the sum of liquid moles are plotted versus the number of iterations. In order to consider the effect that m_{corr} has on the energy balance, 2 cases are plotted. For the first case, m_{corr} is defined as in equation 6.1 while in the second case, m_{corr} is set at 1, as if it were not implemented. In the second case where m_{corr} is not included in the model, the energy balance is correct. This is checked by setting the mtf's for liquid and vapor to zero. In that scenario, the temperature for the whole column remains at the same temperature, indicating a correct energy balance.

The model was simulated using an mtf_L of 1 and an mtf_V of 0.1. The number of cells was set at 20. Simulations with other values (n=40 and mtf_V = 1) for the mtf's and the number of cells gave similar results for the energy balance.

As can be seen from figure 10, the steady state solution converges to lower number of liquid moles in the system, which is caused by an incorrect energy balance. The exact mechanics of the imbalance are not studied. A value of m_{corr} higher than 1 should logically result in lower temperatures and thus a higher liquid content. There are however other factors at play. As can be seen from figure 10, the amount of liquid in the system drops drastically in the first iterations. This is not only due to the implementation of m_{corr} since the liquid also drops without it. A possible explanation for this drop is the lack of physical boundaries that are modelled. In reality, if the volume available for both phases are in the same order, the number of moles of liquid must be much higher than the number of moles of vapor because of their difference in density.

Mixing rules

The reason for the deficit in the mass balance is unclear. A possible explanation can be found in the mixing model that REFPROP uses. To test this hypothesis, the model is simulated with a mixture of benzene and toluene. This nearly ideal mixture is used to determine whether the mass deficit is due to an inaccurate mixing model. In figure 11, the mass correction factor is plotted versus the number of iterations. Apart from the initial divergence in the first ca. 20 iterations, it can be seen that m_{corr} diverges less with the benzene-toluene mixture, but it is still not equal to one. Therefore, it cannot be concluded that an incorrect model for mixing rules by REFPROP is the main cause of this deficit. It can be one of the effects in play, but the underestimation of the fractions by almost 1% during the first iterations indicate that there is another reason for the deficit. A deeper and more thorough research of a possible explanation for this behavior is outside the scope of this study.

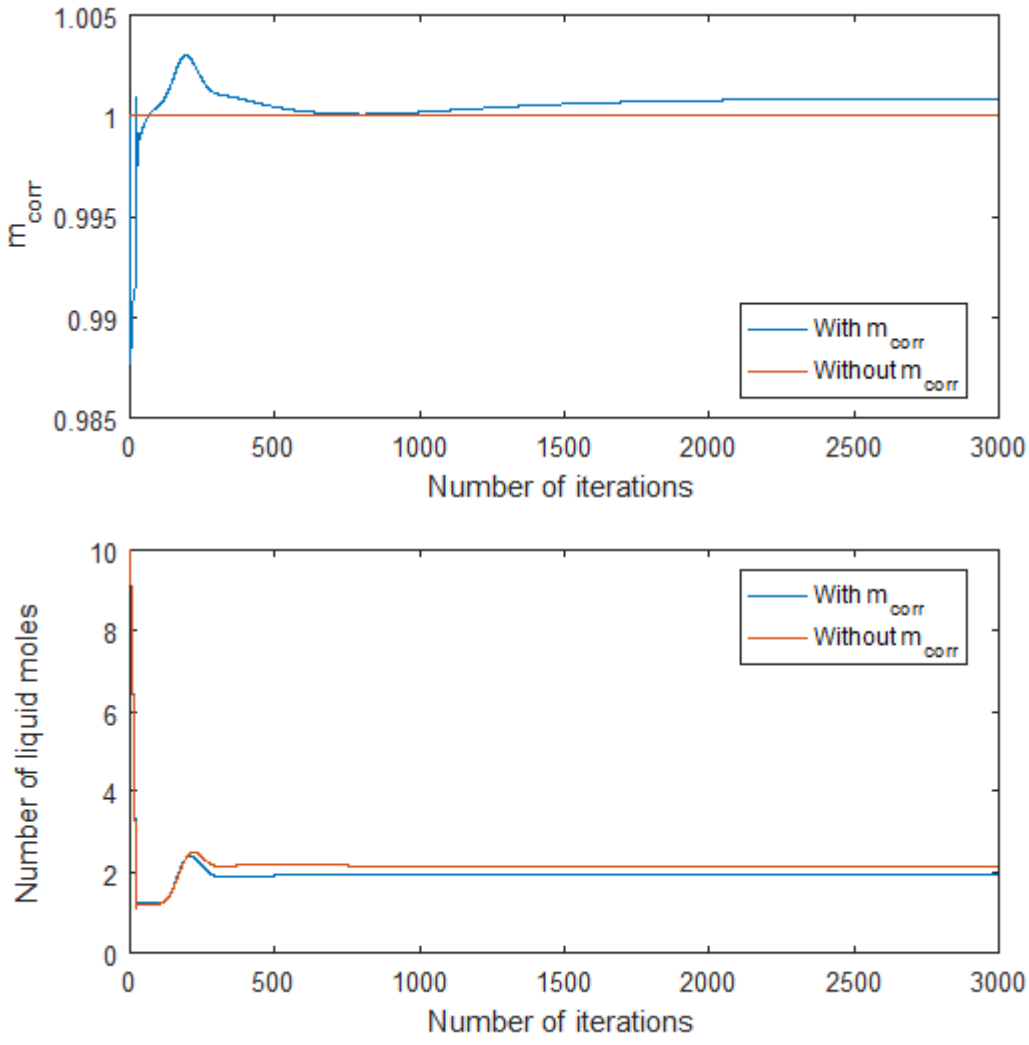

Figure 10 – Mass correction factor and number of liquid moles

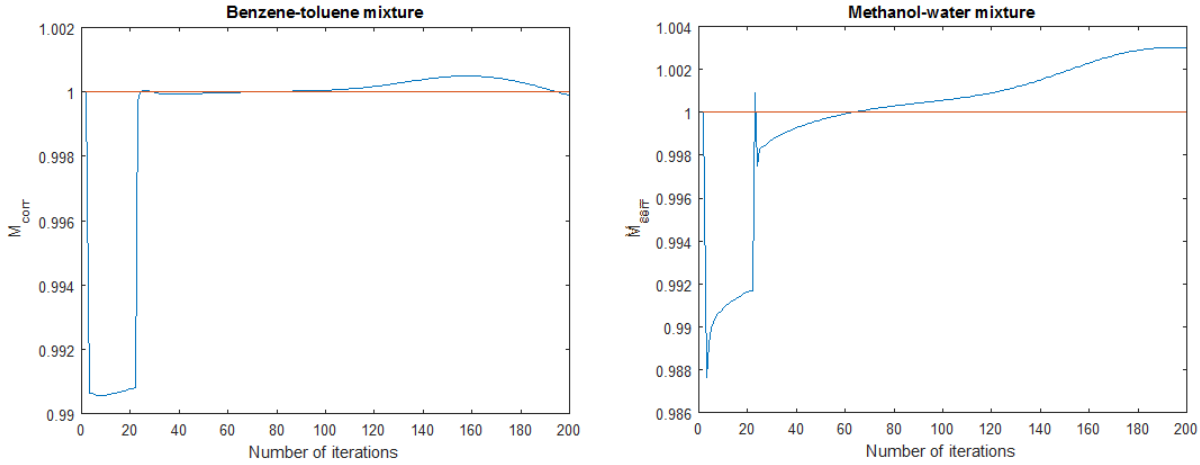

Figure 11 – Mass correction factors for different mixtures

It is concluded that the energy balance is incorrect if the mass correction factor is used and that the mass balance is incorrect if the mass correction factor is not used. Returning to the assumptions on which this model is based, it can be concluded that REFPROP data is not suitable for the iterative calculations used in the simulation of micro-distillation columns.

6.3 Heat integration

The heating and cooling duties of the process are identified. In figure 6, the heat streams listed in table 32 can be found. The stream *HEAT-CO2* is not present on the process overview. This is the heat requirement of the carbon capture process as described in the basis of design chapter. The assumed 5000 kJ/kg CO_2 required is multiplied by the production of CO_2 to obtain the heat duty. For condensing or evaporating flows, the temperature range was taken as 1 °C above and below the operating temperature. The type of heat flow is denoted by a C or an H, standing for cold and hot streams, respectively.

Table 32 – Input data of the components for the pinch analysis

Stream name	Location	Type	Q (kJ/h)	T_{begin} (°C)	T_{end} (°C)	$T_{begin,int}$ (°C)	$T_{end,int}$ (°C)	CP (W/°C)
HEAT-1	AEL water	C	9926	26	80	29	83	51
HEAT-2A	AEL hydrogen	H	3744	80	25	77	22	19
HEAT-2B	AEL oxygen	H	2002	80	25	77	22	10
HEAT-3	CO2 - 1	H	6060	213	25	210	22	9
HEAT-4	CO2 - 2	H	6151	213	25	210	22	9
HEAT-5	CO2 - 3	H	6885	216	25	213	22	10
HEAT-6	CO2 + H2	C	16900	90	250	93	253	29
HEAT-7	Reactor exit	H	174183	250	40	247	37	230
HEAT-8	Recycle compressor	C	98660	42	250	45	253	132
HEAT-9	Distillation methanol	H	2837	64	25	61	22	20
HEAT-10	Distillation water	H	4132	98	25	95	22	16
HEAT-D1	Condenser	H	46674	65	64	62	61	12965
HEAT-D2	Reboiler	C	55041	93	98	96	101	3058
HEAT-R	Reactor	H	43858	251	249	248	246	6091
HEAT-CO2	Carbon capture	C	171870	99	101	102	104	23871

Pinch analysis is applied on these heat flows to determine the most efficient connection between these flows. The problem table method as described in (Sinott & Towler, 2009) is used to determine the minimum utility requirements. A minimum temperature difference between heat exchanging flows of 6°C is selected. This is a relatively low temperature difference. This is justified because the flows are small and therefore have a high surface to volume ratio.

First, the interval temperatures are calculated. The interval temperature is calculated by subtracting half the minimum temperature difference from the hot streams as shown in equation 6.2 and adding half the minimum temperature difference to the cold streams as shown in equation 6.3.

$$T_{int} = T_{act} - \frac{\Delta T_{min}}{2} \tag{6.2}$$

$$T_{int} = T_{act} + \frac{\Delta T_{min}}{2} \tag{6.3}$$

The interval temperatures are listed in table 32 along the actual temperatures. In table 33, the interval temperatures are sorted from highest to lowest. The second column shows the range of the interval. For each interval, the streams are listed which coincides with that interval is listed. Heating duties are denoted by a plus while cooling duties are denoted with a minus.

Table 33 – Ranked order of interval temperatures

Upper temperature °C	Interval Delta T °C	Streams in interval
253		
248	5	6 + 8
247	1	(6 + 8) – R
246	1	(6 + 8) – (7 + R)
213	33	(6 + 8) – 7
210	3	(6 + 8) – (5 + 7)
104	106	(6 + 8) – (3 + 4 + 5 + 7)
102	2	(6 + 8 + CO_2) – (3 + 4 + 5 + 7)
101	1	(6 + 8) – (3 + 4 + 5 + 7)
96	5	(6 + 8 + D2) – (3 + 4 + 5 + 7)
95	1	(6 + 8) – (3 + 4 + 5 + 7)
93	2	(6 + 8) – (3 + 4 + 5 + 7 + 10)
83	10	8 – (3 + 4 + 5 + 7 + 10)
77	6	(1 + 8) – (3 + 4 + 5 + 7 + 10)
62	15	(1 + 8) – (2A + 2B + 3 + 4 + 5 + 7 + 10)
61	1	(1 + 8) – (2A + 2B + 3 + 4 + 5 + 7 + 10 + D1)
45	16	(1 + 8) – (2A + 2B + 3 + 4 + 5 + 7 + 9 + 10)
37	8	1 – (2A + 2B + 3 + 4 + 5 + 7 + 9 + 10)
29	8	1 – (2A + 2B + 3 + 4 + 5 + 9 + 10)
22	7	– (2A + 2B + 3 + 4 + 5 + 9 + 10)

The heat balance is carried out for the intervals to determine whether there is an energy surplus or deficit in that interval. Equation 6.4 shows the formula for calculating the net heat for the n^{th} interval.

$$\Delta H_n = (\Sigma CP_c - \Sigma CP_h) * \Delta T_n \tag{6.4}$$

Where the CP's are obtained from table 32. The result of the calculations is shown in the third column of table 34. The next step is to accumulate the heat surplus or deficit from the higher temperature intervals down to the lower temperature intervals. This is shown in table 34 Accumulating the heat from the higher interval to the lower implies that the temperature difference is such that the heat can be transferred between the hot and cold streams. The presence of a negative value in the fourth column indicates that the temperature gradient is in the wrong direction and that the exchange is not thermodynamically possible. This can be overcome by adding a hot utility at the top with the power of the highest negative value. The interval temperature with the highest negative value is defined as the pinch. 104 °C is determined as the pinch temperature, corresponding to a cold stream temperature of 101 °C and a hot stream temperature of 107 °C.

From the last column of table 34, the cold and hot utilities required can be deduced. The hot utility is the amount of power added at the top and is equal to the highest negative value which is 24.13 kW. The cooling duty is equal to the remaining power after all the heat is added and is equal to 39.65 kW.

Table 34 – Pinch analysis calculation results

Interval temperature (°C)	Interval Delta T (°C)	Delta H (kW)	Cumulative H (kW)	Added hot utility H (kW)
253				
248	5	0.81	0.81	24.94
247	1	-5.93	-5.12	19.01
246	1	-6.16	-11.29	12.85
213	33	-2.29	-13.57	10.56
210	3	-0.24	-13.81	10.32
104	106	-10.32	-24.13	0.00
102	2	47.55	23.42	47.55
101	1	-0.10	23.32	47.45
96	5	14.80	38.12	62.25
95	1	-0.10	38.02	62.15
93	2	-0.23	37.80	61.93
83	10	-1.42	36.37	60.50
77	6	-0.55	35.83	59.96
62	15	-1.81	34.02	58.15
61	1	-13.09	20.93	45.06
45	16	-2.25	18.69	42.82
37	8	-2.18	16.51	40.64
29	8	-0.34	16.17	40.30
22	7	-0.65	15.52	39.65

To assess the added value of this heat exchanger network, the cooling and heating duties found are compared to the duties required if the streams were not connected. Table 35 shows the savings realized due to the implementation of a heat exchanger network. A 75% saving for the heating duties and a 52% savings for the cooling duties was obtained. Since all the heats needs to be generated from solar power, heat savings are very important. The exact implication for the costs need to be researched further, but the increased capital costs of integrating heat exchange in the system likely outweighs the decrease in solar panels required.

Table 35 – Total heating and cooling duties

Duties	#	Heating (kW)	#	Cooling (kW)
			2A	1.04
			2B	0.56
			3	1.68
			4	1.71
			5	1.91
	1	2.76	7	48.38
	6	4.69	9	0.79
	8	27.41	10	1.15
	D2	15.29	D1	12.97
	CO_2	47.74	R	12.18
Total		97.89		82.37
Total connected		24.13		39.65
Savings		75%		52%

6.4 System efficiency

An interesting performance indicator of the process is the system efficiency. This efficiency is defined as the energy content of the methanol produced divided by the amount of energy the system consumes. One hour operation time is taken as reference time.

The total energy consumed by the process is a summation of three energy flows. The electricity required for operating the process as calculated in appendix B, the heat required for processes and the power of the fans for the required cooling, both calculated in the heat integration in chapter 6.3.
The power required for the fans is calculated with the assumption that a coefficient of performance (COP) of 3 can be attained since the fans will use the surrounding air to cool the processes.

$$P = \frac{Cooling\ duty}{COP} = \frac{39.65}{3} = 13.22\ kW \tag{6.5}$$

Table 36 – Energy requirements of the process by type

Energy type	Power (kW)
Process Electricity	251
Process heat	24.1
Fan power for cooling	13.22
Total	288,2

From table 36 it can be concluded that one hour of operation of the process consumes 288.2 kWh.

The total energy produced in the process is defined by the energy content of the methanol. The lower heating value (LHV) of the methanol is used to calculate the energy content of the produced methanol. The LHV is defined as the energy that is released upon complete burning of the fuel. The difference with the higher heating value (HHV) is that with the HHV, the formed water is condensed, and the energy obtained from condensing the water is included in the figure, while this is excluded with the LHV. The LHV of methanol is 20.1 MJ/kg. The mass of methanol produced in one hour is obtained from table 29 and is equal to 23.231 kg/h. The water in the methanol is subtracted from the mass of the mixture for the calculation of the gained energy shown in equation 6.6.

$$23.231 * 20.1 = 466{,}9\ MJ \tag{6.6}$$

One kWh is equal to 3.6 MJ. The total required energy for one hour of production is calculated in equation 6.7.

$$288.2 * 3.6 = 1038\ MJ \tag{6.7}$$

The total efficiency of the process then becomes

$$\frac{466{,}9}{1038} = 45\% \tag{6.8}$$

This result is quite high. The real efficiency of the plant will be lower. No heat losses are included in this calculation. The minimum interval temperature in the pinch analysis accounts for some inefficiencies, but not all. Dynamic operation will furthermore decrease the efficiency due to start-up and shut down inefficiencies.

7 Conclusions and Recommendations

7.1 Conclusions

The objective of this thesis was to design an autonomously operating, container-sized methanol production process making use of only naturally abundantly available resources. A comprehensive literature review was carried out to determine the realization of the functions of the sub processes in the basis of design. The identified processes were simulated using Aspen and Matlab software. The results of this simulation are interpreted to answer the main question posed at the beginning:

To what extent is it possible to operate an autonomous container sized methanol production plant with significant production volume, using only naturally abundantly available resources?

From the simulation of the model in Aspen, it became clear that the concept of this methanol production plant is technically feasible. The extent to which it is possible to operate this process with respect to the requirements stated in the main question was researched using the model.

Autonomous operation of the process plant is possible due to the reduced size of the plant. The presence of operators is not required because for a small mass-produced plant, the engineering costs of autonomous actuation per product can become very small. The safety of small plants is also higher because of the reduced quantities of poisonous or flammable substances. The components in the design were selected on their ability to operate autonomously. Components that possibly require human intervention like activated carbon or other zeolites were avoided for this reason. Biomass was also discarded as an option for energy generation due to the incompatibility with autonomous operation.

The main necessity of the container sized approach is the possibility for distributed mass production which is the novelty in this design. The container size and the physical constraints of the container has implications for the design. The dimensions of the container are a restriction for the size of the equipment. This is most visible for the distillation sub process, where micro distillation was selected in favor of conventional distillation due to the confined height. The downscale of equipment yielded two identified implications besides the selected distillation technology. The reactor was initially scaled down proportionally. After optimization, the reactor was reduced in size by 49 %. It is however possible that the compared reactor was optimized for another purpose and that the comparison is therefore not fully appropriate. The difference is still significant though. The final identified implication is the heat exchange in the system. Heat exchange occurs much faster in the smaller sized equipment. This has an advantage and a disadvantage for the system efficiency. the advantage is that heat is easily exchanged between flows, but the disadvantage is that heat is harder to contain when it is desirable at a certain location. Extensive isolation is required.

Considering the significant production volume requirement, the results of the simulation in Aspen showed that 140 kg of methanol can be produced daily under the following conditions:

- 3 standard sized 40 feet sea containers are required for the entire process. 2 of them are dedicated to capture CO_2 from the air. The electrolysis, the water desalination and the methanol synthesis are situated in the other container.
- A purity of the methanol of at least 96.6 % is obtained, with water and CO_2 as impurities. The CO_2 entering the process has a purity of 99,9 %. The other 0,1 % is air. The seawater is assumed to be completely desalinated.
- The use of naturally abundantly available materials is realized using solar PV. 288 kW of solar electricity and 24 kW of heat energy is required for full operation. This is equal to a solar park with an area of 1663 m^2 assuming that there is an average solar irradiation of 6 hours per day.
- A total efficiency of the process of 45 %, with the solar electricity and heat as input and the lower heating value of methanol as output.

The purity requirements set in the basis of design could not be verified because the distillation simulation in Matlab is erroneous. From designing the model, it is concluded that either the energy balance is incorrect with a correct mass balance or that the mass balance is incorrect with a correct energy balance. It can be concluded that REFPROP data is not suitable for the iterative calculations used in the simulation of micro-distillation columns.

7.2 Recommendations

This master thesis answers the main question posed in the introduction. There is more to say on the subject than is mentioned in this report. The scope of the master thesis is however not sufficient. This section recommends subjects for further study that will add to the answering of the main question.

The most important aspect of the design that has been omitted in this study is the dynamic operation of the process plant. With Solar PV as energy source for the process with its intermittent nature, the operation is inherently dynamic. Dynamic operation is rare in chemical processes. Start up and shut down are of course known procedures, but a process that runs on an intermittent energy source is novelty in the field. It is therefore interesting to study the implications for the economic- and process efficiency of the plant during part-load operation. Possible interesting phenomena to study are start-up time and response time of components, efficiency of production at part-load, preservation of intermediate products, heating and cooling of equipment and the solar irradiance over time for specific locations.

Another very important aspect of the process for the viability is the costs of the process. To answer the main question from an economic perspective, a techno-economic evaluation of the process is necessary to assess the effectiveness of the economy of numbers approach (compared to the traditional economy of scale approach). In this report, the design was optimized with respect to capital costs, but these costs were not quantified. A more extensive study is required to assess whether a significant cost reduction can be obtained.

The reason that the Matlab model is not functioning properly is because REFPROP underestimates the methanol fraction in flash calculations. Although this error is very small, it adds up with each iteration until finally all the methanol has disappeared. The correction of this error with a correction factor led to an invalid energy balance. A possible solution could be to implement an alternative equation of state or research multiple equation of state and assess their performance in iterative calculations. Another possible solution is to use the Aspen custom modeler to model a micro-distillation unit.

Further study into cost reduction is recommended. Capital cost and the cost of energy generation are identified as the main cost drivers. One possible cost reducing measure could be to make use of internet of things (IoT) technology. Using multiple types of sensors to monitor the process real-time helps to improve the efficiency of the system, the degree of autonomous operation. It can also be used to predict failure of components so that maintenance can be carried out preventive and more regulated to further cut costs.

Some sub processes require energy in the form of heat instead of electricity. The carbon capture is an example of such a process. The implementation of solar thermal energy into the process is interesting to investigate because the efficiency of solar PV to turn sunlight into heat is much lower than solar thermal tubes. The material cost is also lower. Research should be carried out to determine the most fruitful combination between solar thermal and solar PV.

For further optimization of the process, it is important to understand what parts of the process consume the most electricity or energy and are the cost drivers of the plant. It is in these parts where the highest gain is to be obtained and further optimization is recommended. The carbon capture is a process that requires a lot of heat compared to the rest of the process. Since this is a relatively new technology, it is expected that higher efficiencies are possible here which will have a significant impact. Large scale carbon capture processes are using much less energy so there is potential. The compression of the captured CO_2 is also identified as an issue. A pressure ratio of 550 must be delivered by the compressors to pressurize the CO_2 from the carbon capture outlet to the reactor inlet. The electrolysis is a process that requires by far the greatest share of the electric power required. A small increase in efficiency here will drastically reduce the total plants power requirement.

References

Alibaba. (2017). Retrieved May 22, 2017, from Alibaba.com: https://www.alibaba.com/product-detail/YOUBER-Seawater-desalination-for-boat-ship_60541692146.html?s=p

Alibaba. (2017). Retrieved May 22, 2017, from Alibaba.com: https://www.alibaba.com/product-detail/Air-Compressor-50-Bar-Compressors-Pump_60593260967.html?s=p

Alibaba. (2017). Retrieved May 22, 2017, from Alibaba.com: https://www.alibaba.com/product-detail/High-Quality-Shell-and-Tube-Type_60609718045.html

Alibaba. (2017). Retrieved June 12, 2017, from Alibaba.com: https://www.alibaba.com/product-detail/Factory-sales-ro-water-desalination-for_60642380874.html

Allebrod, F., Mogensen, M. B., Hjelm, J., & Ebbesen, S. D. (2013). *High Temperature and Pressure Alkaline Electrolysis.* Department of Energy Conversion and Storage, Technical University of Denmark.

Almeland, S., Meland, K., & Edvardsen, D. (2009). *Process design and economical assessment of a methanol plant.* Trondheim: Norwegian University of Science and Technology.

B. Anicic, P. T. (2014). Comparison between two methods of methanol production from carbon dioxide. *Energy 77*, 279-289.

Balabel, A., Zaky, M. S., & Sakr, I. (2014). Optimum Operating Conditions for Alkaline Water Electrolysis Coupled with Solar PV Energy System. *ARABIAN JOURNAL FOR SCIENCE AND ENGINEERING*, 4211–4220.

Baranenko, V., & Kirov, V. (1989). Solubility of hydrogen in water in a broad temperature and pressure range. *Soviet Atomic Energy 66(1)*, 30-34.

Baten, J. v. (2018, 3 14). Retrieved from COCO - the CAPE-OPEN to CAPE-OPEN simulator: https://www.cocosimulator.org/

Bozzano, G., & Manenti, F. (2016). Efficient methanol synthesis: Perspectives, technologies and optimization strategies. *Progress in Energy and Combustion Science 56*, 71 - 105.

Bussche, K. M., & Froment, G. F. (1996). A Steady-State Kinetic Model for Methanol Synthesis and the Water Gas Shift Reaction on a Commercial Cu/ZnO/Al2O3 Catalyst. *Journal of catalysis 161*, 1-10.

Campbell, J. (2014). *Gas Conditioning and Processing, Volume 2: The Equipment Modules, 9th Edition, 2nd Printing.* Norman, Oklahoma: Editors Hubbard, R. and Snow–McGregor, K., Campbell Petroleum Series.

Carmo, M., Fritz, D. L., Mergel, J., & Stolten, D. (2013). A comprehensive review on PEM water electrolysis. *International Journal Of Hydrogen Energy 38*, 4901 - 4934.

Chen, R. Z. (2008). Hydrogen embrittlement of metallic materials in high-pressure hydrogen at normal temperature. *Taiyangneng Xuebao/Acta Energiae Solaris Sinica*, 502-508.

Don W. Green, R. H. (2008). *Perry's Chemical Engineer's Handbook 8th edition.* New York: McGraw-Hill.

Edwards, J. (2008, August 29). *Design and rating shell and tube heat exchangers.* Retrieved June 30, 2017, from Chemcad: http://www.chemstations.com/content/documents/Technical_Articles/shell.pdf

EPA. (1982). *Preliminary perspective on pure methanol fuel for transportation.* Ann Arbor: United States Environmental Protection Agency.

Eric Lemmon, M. H. (2007, april). *Microsoft Word - REFPROP8.doc.* Retrieved from National Institute of Standards and Technology | NIST: https://www.nist.gov/sites/default/files/documents/srd/REFPROP8.PDF

Gandia, L., Arzamedi, G., & Dieguez, P. (2013). *Renewable Hydrogen Technologies: Production, Purification, Storage, Applications and Safety.* Elsevier.

Graves, C., Ebbesen, S., Mogensen, M., & Lacknera, K. (2011). Sustainable hydrocarbon fuels by recycling CO2 and H2O with renewable or nuclear energy. *Renewable and Sustainable Energy Reviews 15(1)*, 1-23.

Greenlee, L. L. (2009). Reverse osmosis desalination: Water sources, technology, and today's challenges. *Water Research*, 2317-2348.

Hall, S. (2012). *Rules of Thumb for Chemical Engineers, Fifth Edition.* Oxford: Butterworth-Heinemann.

Hoogstraten, C. v., & Dunn, K. (1998). *The Design of a distillation column.* Cape Town: University of Cape Town.

Hydrogenics. (2017). *Hydrogen Generators.* Retrieved June 28, 2017, from Hydrogenics: http://www.hydrogenics.com/wp-content/uploads/2-1-1-industrial-brochure_english.pdf

Hydrogenics. (2017). *Hydrogen Production.* Retrieved May 23, 2017, from Hydrogenics: http://www.hydrogenics.com/wp-content/uploads/2-1-1-1-hylyzer-1-223F620871645.pdf

IGP Energy. (n.d.). *Methanol Data | IGP Energy*. Retrieved May 12, 2017, from IGP Energy: http://igpenergy.com/methanol-overview/methanol/

J. Soujanya, B. S. (2010). Experimental (vapour + liquid) equilibrium data of (methanol + water), (water + glycerol) and (methanol + glycerol) systems at atmospheric and sub-atmospheric pressures. *The Journal of Chemical Thermodynamics 42 (5)*, 621–624.

Jain, R. (2010). *United States Patent No. 12/419,513.*

Jefferson, M. (2008). Accelerating the transition to sustainable energy systems. *Energy Policy 36(11)*, 4116-4125.

Johnson, B. (2018, March 12). *Most affordable Solar Panels | Letsgosolar.com*. Retrieved from Consumer Guide to Home Solar Panels | Letsgosolar.com: https://www.letsgosolar.com/solar-panels/rankings/affordable/

Jones, R. L. (2016). *United States Patent No. 14/697,466.*

Kauw, M. (2012). *Recycling of CO2, the perfect biofuel. Master Report.* Groningen: University of Groningen.

Kiss, A. (2014). Distillation technology - still young and full of breakthrough opportunities. *Chemical Technology and Biotechnology 89*, 479-498.

Kister, H. Z. (1992). *Distillation design.* New York: McGraw Hill-Education.

Kiyofumi Kurihara, M. N. (1993). Isobaric vapor-liquid equilibria for methanol + ethanol + water and the three constituent binary systems. *Journal of Chemical Engineering Data 38 (3)*, 446–449.

Kjartansdóttir, C., & Møller, P. (2014). *Development of Hydrogen Electrodes for Alkaline Water Electrolysis.* DTU Mechanical Engineering.

König, D., Baucks, N., Dietrich, R.-U., & Wörner, A. (2015). Simulation and evaluation of a process concept for the generation of synthetic fuel from CO2 and H2. *Energy 91*, 833-841.

Kung, H. H. (1992). Deactivation of methanol synthesis catalysts - A review. *Catalysis Today 11*, 443 - 453.

Lee, S. (1990). *Methanol Synthesis Technology.* Boca Raton: CRC Press, Inc.

Lehne, J., Blyth, W., Lahn, G., Bazilian, M., & Grafham, O. (2016). Energy services for refugees and displaced people. *Energy Strategy Reviews 13-14*, 134-146.

Maersk. (2014, July 29). *www.maerskline.com.* Retrieved May 10, 2017, from Maersk Line: http://www.maerskline.com/~/media/maersk-line/Countries/int/Files/used-container-sales/maersk-line-equipment-guide.pdf

Mahmoudkhani, M., & Keith, D. (2009). Low-energy sodium hydroxide recovery for CO2 capture from atmospheric air - Thermodynamic analysis. *International Journal of Greenhouse Gas Control 3(4)*, 376-384.

Makertiharta, I., Dharmawijaya, P., & Wenten, I. (2017). Current Progress on zeolite membrane reactor for CO2 hydrogenation. *AIP Conference Proceedings*, (pp. 040001-1 - 040001-6).

María, R. D., Díaz, I., Rodríguez, M., & Sáiz, A. (2013). Industrial Methanol from Syngas: Kinetic Study and Process Simulation. *International Journal of Chemical Reactor Engineering*, 469–477.

Mignard, D., Sahibzada, M., Duthie, J., & Whittington, H. (2003). Methanol synthesis from flue-gas CO2 and renewable electricity: a feasibility study. *International Journal of Hydrogen Energy 28*, 455-464.

Mori, H., Ibukia, R., Taguchia, K., Futamuraa, K., & Oluji, Ž. (2006). Three-component distillation using structured packings: Performance evaluation and model validation. *Chemical Engineering Science 61(6)*, 1760-1766.

Mubarak Ebrahim, A. K. (2000). Pinch technology: ancient tool for chemical-plant energy and capital-cost saving. *Applied Energy 65*, 45-49.

Mulder, F., Weninger, B., Middelkoop, J., Ooms, F., & Schreuders, H. (2017). Efficient electricity storage with a battolyser, an integrated Ni–Fe battery and electrolyser. *Energy & Environmental Science 10(3)*, 756-764.

O'Connor, P. (2016). *United States Patent No. 15/036,473.*

Pipe Flow Software. (2017). *Pipe Roughness*. Retrieved July 6, 2017, from Pipe Flow Software ® Official: http://www.pipeflow.com/pipe-pressure-drop-calculations/pipe-roughness

Pray, H. A., Schweickert, C. E., & Minnich, B. H. (1952). Solubility of Hydrogen, Oxygen, Nitrogen, and Helium in Water at Elevated Temperatures. *Industrial and Engineering Chemistry 44(5)*, 1146-1151.

Rand, D., & Dell, R. (2007). *Hydrogen Energy: Challenges and Prospects.* RSC Energy Series v. 1. Royal Society Of Chemistry.

Raquel De María, I. D. (2013). Industrial Methanol from Syngas: Kientic Study and Process Siumlation. *International Journal of Chemical reactor Engineering 11(1)*, 469-477.

Ren, J., Liao, S., & Liu, J. (2006). Progress in large-scale hydrogen storage technology. *Xiandai Huagong/Modern Chemical Industry 26(3)*, 15-18.

Santos, D. M., Sequeira, C. A., & Figueiredo, J. L. (2013). Hydrogen production by alkaline water electrolysis. *Quimica Nova*, 1176-1193.

Seader, J., Henley, E., & Roper, D. (2011). *Separation Process Principles.* Hoboken, NJ: John Wiley & Sons, Inc.

Seddon, D. (2006). *Gas Usage & Value: The Technology and Economics of Natural Gas Use in the Process Industries.* Tulsa, OK: PennWell Corporation.

Seok, D., & Hwang, S.-T. (1985). Zero-Gravity Distillation Utilizing the Heat Pipe Principle (Micro-Distillation). *AIChE 31(12)*, 2059-2065.

Sigma-Aldrich. (2017). *Nederland | Sigma-Aldrich*. Retrieved June 19, 2017, from Molecular Sieves - Technology Information Bulletin | Sigma-Aldrich: http://www.sigmaaldrich.com/chemistry/chemical-synthesis/learning-center/technical-bulletins/al-1430/molecular-sieves.html

Sinott, R., & Towler, G. (2009). *Chemical Engineering Design, fifth edition.* Oxford: Elsevier Science & Technology.

Smith, C. L. (2012). *Distillation - An engineering perspective.* John Wiley & Sons.

Smolinka, T. (2014, April 3). Retrieved May 23, 2017, from www.fch.europa.eu: http://www.fch.europa.eu/sites/default/files/2%20Water%20Electrolysis%20Status%20and%20Potential%20for%20Development.pdf

Song, P. G. (2012). Prospects analysis of integrated-wrapped multi-layer vessels used as high pressure gaseous hydrogen storage vessels. *Advanced Materials Research*, 1755-1759.

Swagelok. (2017). *Swagelok.* Retrieved June 30, 2017, from MS-01-107.PDF: https://www.swagelok.com/downloads/webcatalogs/EN/MS-01-107.PDF

Tromans, D. (1998). Temperature and pressure dependent solubility of oxygen in water: a thermodynamic analysis. *Hydrometallurgy 48*, 327-342.

Van-Dal, É. S., & Bouallou, C. (2013). Design and simulation of a methanol production plant from CO2 hydrogenation. *Journal of Cleaner Production*, 38-45.

VGB Powertech. (2015). *Levelised Cost of Electricity.* Essen, Germany: VGB PowerTech e.V.

Wang, D.-s., Tan, Y.-s., Han, Y.-z., & Tsubaki, N. (2008). Study on deactivation of hybrid catalyst for dimethyl ether synthesis in slurry reactor. *Journal of Fuel chemistry and Technology 36(2)*, 171-175.

Wurzbacher, J. A. (2015). *Development of a temperature-vacuum swing process for CO2 capture from ambient air.* Zurich: ETH Zurich.

Yang, H., Xu, Z., Fan, M., Gupta, R., Slimane, R. B., Bland, A. E., & Wright, I. (2008). Progress in carbon dioxide separation and capture: A review. *Journal of Environmental Sciences 20(1)*, 14-27.

Yde, L. K. (2013). *2nd Generation Alkaline Electrolysis: Final report.* Århus: Århus University Business and Social Science – Centre for Energy Technologies.

Appendix A – Aspen results

Table 37 – Results from the optimized Aspen model

	C-1	C-2	C-3	C-4	C-5	C-6	C-7
Temperature C	25	213.1	25	213.4	25	215.9	25
Pressure bar	0.1	0.67	0.67	4.489	4.489	30	30
Vapor Frac	1	1	1	1	1	1	1
Mole Flow kmol/hr	0.781	0.781	0.781	0.781	0.781	0.781	0.781
Mass Flow kg/hr	34.374	34.374	34.374	34.374	34.374	34.374	34.374
Volume Flow cum/hr	193.623	47.121	28.818	7.009	4.218	1.046	0.538
Enthalpy Gcal/hr	-0.073	-0.072	-0.073	-0.072	-0.073	-0.072	-0.074
Mass Flow kg/hr							
WATER							
CO2	34.34	34.34	34.34	34.34	34.34	34.34	34.34
HYDROGEN							
METHANOL							
CO							
OXYGEN	0.008	0.008	0.008	0.008	0.008	0.008	0.008
NITROGEN	0.026	0.026	0.026	0.026	0.026	0.026	0.026
Mole Flow kmol/hr							
WATER							
CO2	0.78	0.78	0.78	0.78	0.78	0.78	0.78
HYDROGEN							
METHANOL							
CO							
OXYGEN	< 0,001	< 0,001	< 0,001	< 0,001	< 0,001	< 0,001	< 0,001
NITROGEN	0.001	0.001	0.001	0.001	0.001	0.001	0.001

	H-1	H-2	HC-1	HC-2	HC-3	M-1	M-2
Temperature C	80	25	21.1	90	250	64.4	25
Pressure bar	30	30	30	55	55	1	1
Vapor Frac	1	1	1	1	1	0	0
Mole Flow kmol/hr	2.34	2.34	3.122	3.122	3.122	0.733	0.733
Mass Flow kg/hr	4.718	4.718	39.092	39.092	39.092	23.371	23.371
Volume Flow cum/hr	2.329	1.97	2.513	1.717	2.508	0.031	0.029
Enthalpy Gcal/hr	0.001	< 0,001	-0.074	-0.072	-0.068	-0.041	-0.042
Mass Flow kg/hr							
WATER						0.14	0.14
CO2			34.34	34.34	34.34		
HYDROGEN	4.718	4.718	4.718	4.718	4.718		
METHANOL						23.231	23.231
CO							
OXYGEN			0.008	0.008	0.008		
NITROGEN			0.026	0.026	0.026		
Mole Flow kmol/hr							
WATER						0.008	0.008
CO2			0.78	0.78	0.78		
HYDROGEN	2.34	2.34	2.34	2.34	2.34		
METHANOL						0.725	0.725
CO							
OXYGEN			< 0,001	< 0,001	< 0,001		
NITROGEN			0.001	0.001	0.001		

	MW-1	MW-2	MW-3A	MW-3B	O-1	O-2	OH
Temperature C	40	25.7	30	21.2	80	25	80
Pressure bar	54	1	1	1	30	30	30
Vapor Frac	0	0.028	0	0	1	1	1
Mole Flow kmol/hr	1.514	1.514	1.469	1.466	1.171	1.171	3.511
Mass Flow kg/hr	37.96	37.96	36.982	36.661	37.449	37.449	42.167
Volume Flow cum/hr	0.059	1.112	0.044	0.043	1.148	0.958	3.477
Enthalpy Gcal/hr	-0.095	-0.095	-0.093	-0.092	< 0,001	> -0,001	0.001
Mass Flow kg/hr							
WATER	13.191	13.191	13.171	13.239			
CO2	1.391	1.391	0.675				
HYDROGEN	0.043	0.043	trace		< 0,001	< 0,001	4.718
METHANOL	23.308	23.308	23.133	23.422			
CO	0.021	0.021	0.002				
OXYGEN	0.002	0.002	< 0,001		37.449	37.449	37.449
NITROGEN	0.004	0.004	< 0,001				
Mole Flow kmol/hr							
WATER	0.732	0.732	0.731	0.735			
CO2	0.032	0.032	0.015				
HYDROGEN	0.022	0.022	trace		< 0,001	< 0,001	2.341
METHANOL	0.727	0.727	0.722	0.731			
CO	0.001	0.001	< 0,001				
OXYGEN	< 0,001	< 0,001	trace		1.17	1.17	1.17
NITROGEN	< 0,001	< 0,001	trace				

	R-1	R-2	R-3	R-4	R-5	R-6	R-7
Temperature C	250	250	40	40	40	42.1	250
Pressure bar	55	54.995	54	54	54	55	55
Vapor Frac	1	1	0.91	1	1	1	1
Mole Flow kmol/hr	18.231	16.774	16.774	15.261	15.108	15.108	15.109
Mass Flow kg/hr	150.955	150.955	150.955	112.995	111.865	111.865	111.863
Volume Flow cum/hr	14.69	13.467	7.515	7.456	7.382	7.301	12.181
Enthalpy Gcal/hr	-0.207	-0.218	-0.259	-0.165	-0.163	-0.163	-0.139
Mass Flow kg/hr							
WATER	0.285	13.479	13.479	0.287	0.285	0.285	0.285
CO2	104.865	72.633	72.633	71.242	70.53	70.53	70.525
HYDROGEN	30.868	26.456	26.456	26.412	26.148	26.148	26.15
METHANOL	2.368	25.699	25.699	2.392	2.368	2.368	2.368
CO	9.713	9.832	9.832	9.811	9.713	9.713	9.713
OXYGEN	0.638	0.638	0.638	0.636	0.63	0.63	0.63
NITROGEN	2.218	2.218	2.218	2.214	2.192	2.192	2.192
Mole Flow kmol/hr							
WATER	0.016	0.748	0.748	0.016	0.016	0.016	0.016
CO2	2.383	1.65	1.65	1.619	1.603	1.603	1.602
HYDROGEN	15.312	13.124	13.124	13.102	12.971	12.971	12.972
METHANOL	0.074	0.802	0.802	0.075	0.074	0.074	0.074
CO	0.347	0.351	0.351	0.35	0.347	0.347	0.347
OXYGEN	0.02	0.02	0.02	0.02	0.02	0.02	0.02
NITROGEN	0.079	0.079	0.079	0.079	0.078	0.078	0.078

	W-1	W-2	W-3	W-4	W-5	PURGE	PURGE-2
Temperature C	25	25.8	80	98.2	25	40	30
Pressure bar	1	30	30	1	1	54	1
Vapor Frac	0	0	0	0	0	1	1
Mole Flow kmol/hr	2.341	2.341	2.341	0.733	0.733	0.153	0.045
Mass Flow kg/hr	42.167	42.167	42.167	13.29	13.29	1.13	0.978
Volume Flow cum/hr	0.056	0.056	0.045	0.015	0.013	0.075	1.138
Enthalpy Gcal/hr	-0.16	-0.16	-0.157	-0.049	-0.05	-0.002	-0.002
Mass Flow kg/hr							
WATER	42.167	42.167	42.167	13.099	13.099	0.003	0.02
CO2						0.712	0.716
HYDROGEN						0.264	0.043
METHANOL				0.191	0.191	0.024	0.175
CO						0.098	0.019
OXYGEN						0.006	0.001
NITROGEN						0.022	0.004
Mole Flow kmol/hr							
WATER	2.341	2.341	2.341	0.727	0.727	< 0,001	0.001
CO2						0.016	0.016
HYDROGEN						0.131	0.022
METHANOL				0.006	0.006	0.001	0.005
CO						0.004	0.001
OXYGEN						< 0,001	< 0,001
NITROGEN						0.001	< 0,001

Appendix B – Energy and storage capacity

Electrolysis

The energy requirement for the electrolysis sub process is calculated using data from manufacturers. Hydrogen Technologies, a division of Statoil uses an alkaline electrolyser to produce in the range of 0.85 – 42.5 kg/h with an efficiency of 82.3 % (Kjartansdóttir & Møller, 2014). The required hydrogen production for the continuously operated scenario (COS) is 1.18 kg/h, which is well in the given range. The theoretical required energy to produce one kilogram of hydrogen is 39.4 kWh/kg. The power requirement for the electrolysis then becomes

$$\frac{39.4\frac{kWh}{kg}}{82.3\%} * 1.18\frac{kg}{h} = 56.5\ kW \quad \text{(B.1)}$$

For the dynamically operated scenario (DOS), the production of hydrogen is four times greater since the same amount of hydrogen needs to be produced in 6 hours instead of 24 hours.

$$\frac{39.4\frac{kWh}{kg}}{82.3\%} * 4.72\frac{kg}{h} = 226\ kW \quad \text{(B.2)}$$

The required battery capacity is the total amount of energy required for one full day of operation. The required battery capacity for the electrolysis in the COS then becomes:

$$24\ h * 56.5\ kW = 1.36\ MWh \quad \text{(B.3)}$$

Desalination

The energy requirement for the desalination sub process is also calculated using data from manufacturers (Alibaba, 2017). A desalination facility with a capacity of 100 L/h requires 0.2 kW of power. The required battery capacity is the total amount of energy required for one full day of operation. The required battery capacity for the desalination in the COS then becomes

$$24\ h * 0.2\ kW = 4.8\ kWh \quad \text{(B.4)}$$

The DOS is not calculated since the desalination is determined to be operated continuously in the selected scenario

Carbon capture

The energy requirement for the carbon capture process is calculated by calculating fan power. The greatest share of the energy is required in the form of low grade heat energy. This energy will be supplied by the remaining heat energy from the methanol synthesis. The fan power is solely dependent on the pressure drop over the adsorbent. An electrical energy requirement of 300 kWh per ton of adsorbed CO_2 is reported (Wurzbacher, 2015). The daily production of carbon dioxide is 206 kg. The required battery capacity for the carbon capture in the COS then becomes:

$$\frac{206\ kg}{1000\ kg} * 300\ kWh = 61.8\ kWh \quad \text{(B.5)}$$

Methanol synthesis

The electrical energy requirement of the methanol synthesis is calculated by adding the power of all the pumps and compressors present in the system. The power of the pumps and the compressors are calculated using equation B.6

$$P = \frac{\Delta H \cdot \dot{m}}{\eta} \quad \text{(B.6)}$$

Where ΔH is the enthalpy difference between the inlet and outlet in kJ/kg, $\dot{m}$ is the mass flow in kg/s and η is the efficiency. The enthalpy difference is obtained from REFPROP using the process conditions obtained from Aspen. The mass flows are also obtained from Aspen. The total efficiency is assumed to be 50% on average for the pumps and compressors. Table B.1 lists all the values used for the calculation of the power requirement of each compressor and pump.

Table 38 – Compressor and pump power requirement

Equipment	Inlet enthalpy (kJ/kg)	Outlet enthalpy (kJ/kg)	Enthalpy difference (kJ/kg)	Mass flow (kg/h)	Power (kW)
Water pump	104,92	110,94	6,02	42.167	0.14
CO_2 comp. 1	506,69	681,46	174,77	34.374	3.34
CO_2 comp. 2	506,16	680,48	174,32	34.374	3.33
CO_2 comp. 3	502,56	674,48	171,92	34.374	3.32
Mixer comp.	902,34	1074,8	172,46	39.092	3.74
Recycle comp.	1373,0	1381,8	8,8	111.863	0.55

The total power requirement for the methanol synthesis is obtained by adding the power requirements of the single components

$$0.14 + 3.34 + 3.33 + 3.32 + 3.74 + 0.55 = 14.42\ kW \quad \text{(B.9)}$$

The required battery capacity for the carbon capture in the COS then becomes:

$$24\ h * 14.4\ kW = 346\ kWh \quad \text{(B.8)}$$

Energy generation

The battery size required to obtain the COS, is the required battery capacity of all the other processes combined and is therefore easily calculated:

$$1.36\ MWh + 4.8\ kWh + 61.8\ kWh + 346\ kWh = 1.77\ MWh \quad \text{(B.10)}$$

Storage tanks

Additionally, storage tanks are required to sustain a continuous flow of feedstock and product. A storage tank is required between two processes whose mode of operation is different. For all the storage tanks, the same methodology is applied. The water production is multiplied by the storage factor and is divided by the density to obtain the effective space occupation of the storage tank. The densities at a temperature of 25 °C are obtained from REFPROP. The selected pressures are obtained from standards from the industry. Table B.2 lists all the storage tanks, the daily production volume, the density of the substance and the calculated size. The equation used to calculate the size is

$$f_s * \dot{m} * \rho \quad \text{(B.11)}$$

Where f_s is the storage factor, $\dot{m}$ is the production volume in kg/day and ρ is the density of the substance in kg/m^3.

Table 39 – Process parameters of the storage tanks

Storage tank contents	**Production volume (kg/day)**	**Density (kg/m3)**	**Size (m3)**
Water	253	997	0.38
Carbon dioxide	206	750	0.41
Hydrogen	28.3	20	2.12
Oxygen	224.7	192	1.76
Methanol	150	786	0.29

Power requirement

The total electricity requirement of the process is obtained by adding the requirements of all the sub processes. The power requirements are listed above and are added up in equation B.12.

$$226 + 0.2 + \frac{61.8}{6} + 14.4 = 251\ kW \quad \text{(B.12)}$$

The power output per solar panel is assumed to be 255 W, the output of the most cost efficient solar panel according to (Johnson, 2018). Assuming a standard sized solar panel of 65 by 39 inch, the surface area per solar panel and the total solar panel area can be calculated.

$$65 * 0.0254 * \ 39 * 0.0254 = 1.64\ m \quad \text{(B.13)}$$

$$\frac{1.64 * 251}{0.255} = 1614\ m^2 \quad \text{(B.14)}$$

The pinch analysis carried out in chapter 6 resulted in an additional heating requirement of 24.13 kW. Evacuated tube solar collectors can be used to heat liquids for process heat. These collectors are assumed to have an efficiency of 50% and are assumed to generate 500 W/m^2. The total solar thermal area is calculated in Equation B.15

$$\frac{24.13}{0.5} = 48.3\ m^2 \quad \text{(B.15)}$$

The total area required for electricity generation is 1663 m^2.

Appendix C – Stoichiometric mass flow

Using the molar masses shown in Table C.1 and equations 2.1 and 3.1, the stoichiometric ratios of the reactions shown in equation C.1 and C.2 are calculated for 1 mol of methanol.

Table 40 – Molar masses of substances

Substance	Molar mass (g/mol)
CO_2	44
H_2O	18
CH_3OH	32
O_2	32
H_2	2

Electrolysis	$2H_2O \rightarrow 2H_2 + O_2$	(3.1)
Methanol Synthesis	$CO_2 + 3H_2 \rightarrow CH_3OH + H_2O$	(2.1)
Electrolysis	$36g\ H_2O \rightarrow 4g\ H_2 + 32g\ O_2$	(C.1)
Methanol synthesis	$44g\ CO_2 + 6g\ H_2 \rightarrow 32g\ CH_3OH + 18g\ H_2O$	(C.2)

For a production of 100 kg of methanol per day, the daily mass flows of all the substances can be calculated from equation C.1 and C.2. They are shown in table C.2

Table 41 – Daily mass flows of all the substances

Substance	Daily production (kg/day)
CO_2	137.35
H_2O	168.67
CH_3OH	100
O_2	149.8
H_2	18.87

If the water that is produced in the methanol synthesis is recovered in pure form, the water requirement can be reduced by 56.22 kg/day. This is assumed in the size estimation in chapter 3.

The size of the electrolyser is calculated using the normal volume of the gases that exit the electrolyser, because comparative data was available in this form. The volume is calculated using the density at standard temperature and pressure (STP).

Appendix D – Electrolyser energy content

When the electrolyser is switched off, the solution in the electrolyser is still saturated with oxygen and hydrogen. The amount of oxygen dissolved in the solution is calculated using equation D.1 (Tromans, 1998)

$$C_{aq} = p_{O_2}\left(\frac{0.046T^2+203.357Tln\left(\frac{T}{298}\right)-(299.378+0.092T)(T-298)-20591}{8.3144T}\right) \quad (D.1)$$

Where C_{aq} is the molal concentration of dissolved O_2 in mol O_2/kg H_2O), p_{O2} is the partial pressure of oxygen in atm and T is the temperature in K. The equation is valid for values of K between 273 and 616 K and pressures up to 60 atm. The pressure and temperature of the electrolyser are set at 1 bar and 298 K, the molal concentration of dissolved oxygen then becomes:

$$C_{aq} = 1\left(\frac{0.046*298^2+203.357\cdot 298\cdot ln(1)-(299.378+0.092\cdot 298)(0)-20591}{8.3144\cdot 298}\right) \quad (D.2)$$

$$C_{aq} = 0.00128\ \frac{mol\ O_2}{kg\ H_2O} = 0.0409\ \frac{g\ O_2}{kg\ H_2O} \quad (D.3)$$

The amount of hydrogen dissolved in the solution is calculated using the table with theoretical data in figure D.1 (Baranenko & Kirov, 1989) and checked with the graph with experimental data in figure D.2 (Pray, Schweickert, & Minnich, 1952). Using the electrolyser temperature and pressure, the concentration of hydrogen in the water is calculated using interpolation

$$0.0212 - \frac{0.0212-0.0127}{2} = 0.017\frac{Ncm_3}{g} \quad (D.4)$$

The concentration in the table and graph are given in Ncm_3/g, which is equal to the amount of ml of hydrogen at STP per gram of water. Using the density of hydrogen at STP, which is 0.08988 g/L, the mass of hydrogen dissolved in the solution can be calculated.

$$0.017\ \frac{L\ H_2}{kg\ H_2O} * 0.08988\frac{g}{L}H_2 = 0.00153\ \frac{g\ H_2}{kg\ H_2O} = 0.000764\ \frac{mol\ H_2}{kg\ H_2O} \quad (D.5)$$

The amount of electrolyte in the electrolyser is calculated using the current density, required power and the voltage of the electrolyser. The current density of the electrolyser is assumed to be 3 A/m^2 (Carmo, Fritz, Mergel, & Stolten, 2013). The voltage and power are obtained from an industrial example from (Hydrogenics, 2017), who operate on 400 V and use 4.9 kWh/Nm^3. The production of hydrogen is 3.145 kg/h, which is equal to 35 Nm3/h. The required power then becomes.

$$4.9\frac{kWh}{Nm^3} * 52.5\frac{Nm^3}{h} = 257\ kW \quad (D.6)$$

The electrolyte volume then becomes

$$\frac{257\ kW}{\frac{400\ V}{3\frac{A}{m^2}}} * 0.01\ m = 2.143\ m^3 = 2143\ L \quad (D.7)$$

This is the total volume. Half of the volume is saturated with dissolved oxygen and the other half is saturated with hydrogen. The total mass of oxygen and hydrogen in the system is, assuming a density of water of 1 kg/L

$$m_{H_2} = 0.00153\ \frac{g\ H_2}{kg\ H_2O} * \frac{1}{2} * 2143\ kg = 1.64\ g \quad (D.8)$$

$$m_{O_2} = 0.0409\ \frac{g\ O_2}{kg\ H_2O} * \frac{1}{2} * 2143\ kg = 43.9\ g \quad (D.9)$$

The energy content of the dissolved hydrogen can be calculated using the specific energy of hydrogen, which is 142 MJ/kg.

$$1.46 * 10^{-3}\ kg * 142\frac{MJ}{kg} = 0.233\ MJ = 0.0646\ kWh \quad (D.10)$$

P_{vg}, MPa	T, °C								
	0	50	100	150	200	250	300	350	370
0,1	0,0212	0,0127							
0,5	0,106	0,0789	0,0645						
1,0	0,213	0,156	0,148	0,104					
2,5	0,537	0,408	0,393	0,421	0,270				
5,0	1,069	0,814	0,810	0,942	0,982	0,401			
10	2,136	1,629	1,638	1,993	2,414	2,594	1,090		
15	3,171	2,417	2,441	3,042	3,825	4,735	4,805		
20	4,190	3,209	3,247	4,074	5,247	6,850	8,413	5,721	
30	6,172	4,726	4,826	6,145	8,235	11,097	15,426	19,231	18,157
40	8,055	6,214	6,367	8,232	10,993	15,398	22,255	33,383	36,744
50	9,839	7,640	7,857	10,313	13,826	19,877	30,565	50,218	62,031

Figure 12 – Theoretical concentration of hydrogen in water at varying p and T.

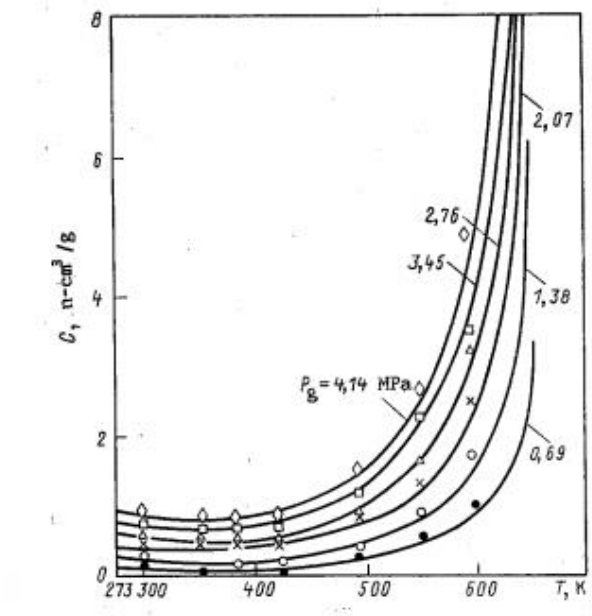

Figure 13 – Experimental concentration of hydrogen in water at varying p and T.

Appendix E – Distillation Matlab code

The Matlab code for the micro-distillation is presented here. The lay-out of the code is not altered for increased readability. The reader is advised to copy the text of the code and paste it in a text editing program with unlimited page width. A digital copy of this report can be found at https://repository.tudelft.nl/islandora/search/?collection=education.

```
% Model for a single heat pipe of a micro-distillation unit
% model by Marnix de Jong - dejong.marnix@gmail.com
tic

close all
clear all
clc

%% Boundary conditions
% Constants
p    = 101.325;              % [kPa] pressure
M1   = 32.042e-3;            % [kg/mol] molar mass methanol
M2   = 18.015e-3;            % [kg/mol] molar mass water
n    = 20;                   % number of cells
jmax = 200;                  % maximum number of iterations
F_ex    = 0;                % [mol/h] system feed flow %2.2 according to seok
z1_ex   = 0.5;               % [mol/mol] composition system feed flow
T_ex    = 75;                % [°C] Temperature of the system feed flow
w1_ex    = z1_ex*M1 / (z1_ex*M1 + (1-z1_ex)*M2);           % mass fraction
methanol in feed mixture
w2_ex   = 1 - w1_ex;
H_Fex     = refpropm('H','T',T_ex + 273.15,'P',p,'methanol','water',[w1_ex
w2_ex]);
rflx_evap = 1;                                             % [-] reflux ratio
evaporator
rflx_cond = 1;                                             % [-] reflux ratio
condenser
feed     = round(n/2);                                    % cell number where
the feed enters the column
T_evap   = refpropm('T','P',p,'Q',0,'water') - 273.15;
T_cond   = refpropm('T','P',p,'Q',0,'methanol') - 273.15;

gmax = 0;       % g and h can be used to run multiple settings for the mass
transfer factor subsequently
hmax = 1;

Temperature_profile = NaN(n,(gmax+1)*(hmax+1));
Concentration_profile = NaN(n,(gmax+1)*(hmax+1));

for g = 0:gmax
    for h = 0:hmax
        mtf_L    = 1;                  % mole transfer factor liquid phase,
fraction of moles that is transported to the adjacent cell
        mtf_V    = 0.1;              % mole transfer factor vapor phase


        % preallocating matrices for speed
        F       = NaN(n,jmax); z1     = NaN(n,jmax); z2    = NaN(n,jmax);
        L       = NaN(n,jmax); x1     = NaN(n,jmax); x2    = NaN(n,jmax);
        V       = NaN(n,jmax); y1     = NaN(n,jmax); y2    = NaN(n,jmax);
        w1_L    = NaN(n,jmax); w1_V   = NaN(n,jmax); w1_F = NaN(n,jmax);
        w2_L    = NaN(n,jmax); w2_V   = NaN(n,jmax); w2_F = NaN(n,jmax);
        M_L     = NaN(n,jmax); M_V    = NaN(n,jmax); M_F   = NaN(n,jmax);
```

```
        H_Lo    = NaN(n,jmax); H_Li    = NaN(n,jmax); H_F   = NaN(n,jmax);
        H_Vo    = NaN(n,jmax); H_Vi    = NaN(n,jmax);
        K1      = NaN(n,jmax); K2      = NaN(n,jmax);
        L_rflx  = NaN(1,jmax); V_rflx = NaN(1,jmax);
        alpha   = NaN(n,jmax);
        T       = NaN(n,jmax);
        m_corr  = NaN(1,jmax);

        %% initial values
        for j = 1
            for i = 1:n
                F(i,j)  = 1;
                V(i,j) = 0.5*F(i,j);
                L(i,j) = 0.5*F(i,j);
                T(i,j)  = 80;                                    % auxiliary -
small negative temperature gradient as an initial condition
                w1_F(i,j)   = M1/(M1+M2);                      % equimolar
                w2_F(i,j)   = 1 - w1_F(i,j);
                [x,   y]                        =   refpropm('X','T',T(i,j)   +
273.15,'P',p,'methanol','water',[w1_F(i,j) w2_F(i,j)]);
                w1_L(i,j)   = x(1);
                w2_L(i,j)   = x(2);
                w1_V(i,j)   = y(1);
                w2_V(i,j)   = y(2);
                x1(i,j) = w1_L(i,j)/M1 / ( w1_L(i,j)/M1 + w2_L(i,j)/M2 );
                x2(i,j) = w2_L(i,j)/M2 / ( w1_L(i,j)/M1 + w2_L(i,j)/M2 );
                y1(i,j) = w1_V(i,j)/M1 / ( w1_V(i,j)/M1 + w2_V(i,j)/M2 );
                y2(i,j) = w2_V(i,j)/M2 / ( w1_V(i,j)/M1 + w2_V(i,j)/M2 );
            end
        end

        %% Steady state calculation
        for j = 2:jmax             % increase number until a stable solution
is obtained
            for i = 1:n
                %%% feed flow | mass balance
                if i==1             % evaporator end cell
                    V_rflx(j)   = rflx_evap*L(i,j-1);
                    F(i,j)     = V_rflx(j) + V(i,j-1)*(1 - mtf_V)  +  L(i+1,j-
1)*mtf_L;
                    z1(i,j)      = ( V_rflx(j)*y1(i,j-1) + V(i,j-1)*y1(i,j-
1)*(1 - mtf_V)  +  L(i+1,j-1)*x1(i+1,j-1)*mtf_L ) / F(i,j);
                elseif i==feed      % column inlet
                    F(i,j)      = V(i-1,j-1)*mtf_V + V(i,j-1)*(1 - mtf_V)  +
L(i+1,j-1)*mtf_L + L(i,j-1)*(1 - mtf_L)  +  F_ex;
                    z1(i,j)       = ( V(i-1,j-1)*y1(i-1,j-1)*mtf_V + V(i,j-
1)*y1(i,j-1)*(1 - mtf_V)  +  L(i+1,j-1)*x1(i+1,j-1)*mtf_L + L(i,j-1)*x1(i,j-
1)*(1 - mtf_L)  +  F_ex*z1_ex ) / F(i,j);
                elseif i==n         % condenser end cell
                    L_rflx(j)   = rflx_cond*V(i,j-1);
                    F(i,j)       = V(i-1,j-1)*mtf_V  +  L_rflx(j) + L(i,j-
1)*(1 - mtf_L);
                    z1(i,j)          =  ( V(i-1,j-1)*y1(i-1,j-1)*mtf_V    +
L_rflx(j)*x1(i,j-1) + L(i,j-1)*x1(i,j-1)*(1 - mtf_L) ) / F(i,j);
                else                % regular cells
                    F(i,j)      = V(i-1,j-1)*mtf_V + V(i,j-1)*(1 - mtf_V)  +
L(i+1,j-1)*mtf_L + L(i,j-1)*(1 - mtf_L);
                    z1(i,j)       = ( V(i-1,j-1)*y1(i-1,j-1)*mtf_V + V(i,j-
1)*y1(i,j-1)*(1 - mtf_V)  +  L(i+1,j-1)*x1(i+1,j-1)*mtf_L + L(i,j-1)*x1(i,j-
1)*(1 - mtf_L) ) / F(i,j);
                end
                z2(i,j)     = 1 - z1(i,j);
```

```
                %%% mass fractions calculations | required for enthalpies
                if i==1
                w1_L(i,j)    = x1(i,j-1)*M1 / (x1(i,j-1)*M1 + x2(i,j-1)*M2);
% convert mole fraction to mass fraction
                w2_L(i,j)    = 1 - w1_L(i,j);
                end
                if i~=n              % for H_L calculations
                    w1_L(i+1,j)   =   x1(i+1,j-1)*M1   /   (x1(i+1,j-1)*M1   +
x2(i+1,j-1)*M2);
                    w2_L(i+1,j) = 1 - w1_L(i+1,j);
                end
                w1_V(i,j)    = y1(i,j-1)*M1 / (y1(i,j-1)*M1 + y2(i,j-1)*M2);
                w2_V(i,j)    = 1 - w1_V(i,j);

                if i==1
                    w1_F(i,j)          =    (   w1_L(i,j)*(   L(i+1,j-1)*mtf_L
)   +  w1_V(i,j)*( V_rflx(j)         + V(i,j-1)*(1 - mtf_V) ) ) / F(i,j);
                    w2_F(i,j)    = 1 - w1_F(i,j);
                elseif i==n
                    w1_F(i,j)    = ( w1_L(i,j)*( L_rflx(j)          + L(i,j-
1)*(1 - mtf_L) )   +  w1_V(i,j)*( V(i-1,j-1)*mtf_V                        ) )
/ F(i,j);
                    w2_F(i,j)    = 1 - w1_F(i,j);
                else
                    w1_F(i,j)     = ( w1_L(i,j)*( L(i+1,j-1)*mtf_L + L(i,j-
1)*(1 - mtf_L) )   +  w1_V(i,j)*( V(i-1,j-1)*mtf_V + V(i,j-1)*(1 - mtf_V) ) )
/ F(i,j);
                    w2_F(i,j)    = 1 - w1_F(i,j);
                end
                %%% temperature calculations | energy balance
                if i==1              % reboiler | water extraction side
                    H_Lo(i,j)           =    refpropm('H','T',T(i+1,j-1)    +
273.15,'Q',0,'methanol','water',[w1_L(i+1,j) w2_L(i+1,j)]);
                    H_Li(i,j)          =   refpropm('H','T',T(i,j-1)         +
273.15,'Q',0,'methanol','water',[w1_L(i,j)   w2_L(i,j)  ]);
                    H_Vo(i,j)                        =       refpropm('H','P',p
,'Q',1,'methanol','water',[w1_L(i,j)   w2_L(i,j)  ]);
                    H_Vi(i,j)          =   refpropm('H','T',T(i,j-1)         +
273.15,'Q',1,'methanol','water',[w1_V(i,j)   w2_V(i,j)  ]);
                    H_F(i,j)           =   (  H_Lo(i,j)*L(i+1,j-1)*mtf_L     +
H_Vo(i,j)*V_rflx(j) + H_Vi(i,j)*V(i,j-1)*(1 - mtf_V) ) / F(i,j);
                elseif i==feed
                    H_Lo(i,j)           =    refpropm('H','T',T(i+1,j-1)    +
273.15,'Q',0,'methanol','water',[w1_L(i+1,j) w2_L(i+1,j)]);
                    H_Li(i,j)          =   refpropm('H','T',T(i,j-1)         +
273.15,'Q',0,'methanol','water',[w1_L(i,j)   w2_L(i,j)  ]);
                    H_Vo(i,j)           =    refpropm('H','T',T(i-1,j-1)    +
273.15,'Q',1,'methanol','water',[w1_V(i-1,j) w2_V(i-1,j)]);
                    H_Vi(i,j)          =   refpropm('H','T',T(i,j-1)         +
273.15,'Q',1,'methanol','water',[w1_V(i,j)   w2_V(i,j)  ]);
                    H_F(i,j)            =   (   H_Lo(i,j)*L(i+1,j-1)*mtf_L   +
H_Li(i,j)*L(i,j-1)*(1   -   mtf_L)      +      H_Vo(i,j)*V(i-1,j-1)*mtf_V   +
H_Vi(i,j)*V(i,j-1)*(1 - mtf_V)  +  H_Fex*F_ex ) / F(i,j);
                elseif i==n          % condenser | methanol extraction side
                    H_Lo(i,j)                        =       refpropm('H','P',p
,'Q',0,'methanol','water',[w1_V(i,j)   w2_V(i,j)  ]);
                    H_Li(i,j)          =   refpropm('H','T',T(i,j-1)         +
273.15,'Q',0,'methanol','water',[w1_L(i,j)   w2_L(i,j)  ]);
                    H_Vo(i,j)           =    refpropm('H','T',T(i-1,j-1)    +
273.15,'Q',1,'methanol','water',[w1_V(i-1,j) w2_V(i-1,j)]);
                    H_Vi(i,j)          =   refpropm('H','T',T(i,j-1)         +
273.15,'Q',1,'methanol','water',[w1_V(i,j)   w2_V(i,j)  ]);
```

```
                    H_F(i,j)     = ( H_Lo(i,j)*L_rflx(j) + H_Li(i,j)*L(i,j-
1)*(1 - mtf_L)  +  H_Vo(i,j)*V(i-1,j-1)*mtf_V ) / F(i,j);
                else
                    H_Lo(i,j)           =    refpropm('H','T',T(i+1,j-1)    +
273.15,'Q',0,'methanol','water',[w1_L(i+1,j) w2_L(i+1,j)]);
                    H_Li(i,j)         =   refpropm('H','T',T(i,j-1)         +
273.15,'Q',0,'methanol','water',[w1_L(i,j)   w2_L(i,j)  ]);
                    H_Vo(i,j)           =    refpropm('H','T',T(i-1,j-1)    +
273.15,'Q',1,'methanol','water',[w1_V(i-1,j) w2_V(i-1,j)]);
                    H_Vi(i,j)         =   refpropm('H','T',T(i,j-1)         +
273.15,'Q',1,'methanol','water',[w1_V(i,j)   w2_V(i,j)  ]);
                    H_F(i,j)           =   (   H_Lo(i,j)*L(i+1,j-1)*mtf_L   +
H_Li(i,j)*L(i,j-1)*(1   -   mtf_L)      +      H_Vo(i,j)*V(i-1,j-1)*mtf_V   +
H_Vi(i,j)*V(i,j-1)*(1 - mtf_V) ) / F(i,j);
                end
                T(i,j)                                                      =
refpropm('T','H',H_F(i,j),'P',p,'methanol','water',[w1_F(i,j)  w2_F(i,j)])  -
273.15;
                %%% flash
                [x,      y]            =      refpropm('X','T',T(i,j)      +
273.15,'P',p,'methanol','water',[w1_F(i,j) w2_F(i,j)]);
                w1_L(i,j)   = x(1);
                w2_L(i,j)   = x(2);
                w1_V(i,j)   = y(1);
                w2_V(i,j)   = y(2);
                x1(i,j) = w1_L(i,j)/M1 / ( w1_L(i,j)/M1 + w2_L(i,j)/M2 );
                x2(i,j) = w2_L(i,j)/M2 / ( w1_L(i,j)/M1 + w2_L(i,j)/M2 );
                y1(i,j) = w1_V(i,j)/M1 / ( w1_V(i,j)/M1 + w2_V(i,j)/M2 );
                y2(i,j) = w2_V(i,j)/M2 / ( w1_V(i,j)/M1 + w2_V(i,j)/M2 );
                K1(i,j) = y1(i,j)/x1(i,j);
                K2(i,j) = y2(i,j)/x2(i,j);
                alpha(i,j)  =  ( z1(i,j)  +  z2(i,j)  -  z1(i,j)*K1(i,j)  -
z2(i,j)*K2(i,j) ) / ...
                                ( z1(i,j)*K1(i,j)*K2(i,j) - z1(i,j)*K1(i,j) -
z1(i,j)*K2(i,j)  +  z1(i,j)  +  z2(i,j)*K1(i,j)*K2(i,j)  -  z2(i,j)*K1(i,j)  -
z2(i,j)*K2(i,j) + z2(i,j) );
                V(i,j)  = alpha(i,j)*F(i,j);
                L(i,j)  = F(i,j) - V(i,j);

            end
            %conservation of mass
            if h==0
            m_corr(j) = ( sum(L(:,j-1).*x1(:,j-1)) + sum(V(:,j-1).*y1(:,j-
1)) )/( sum(L(:,j).*x1(:,j)) + sum(V(:,j).*y1(:,j)) );
            else
                m_corr(j) = 1;
            end
            for i=1:n
                x1(i,j) = m_corr(j)*x1(i,j);
                y1(i,j) = m_corr(j)*y1(i,j);
                x2(i,j) = 1 - x1(i,j);
                y2(i,j) = 1 - y1(i,j);
            end

            % stability check
            T_profile = T(:,j);
            T_profile_old = T(:,j-1);
            T_change = T_profile - T_profile_old;

            if sum(T_change.^2) < 1e-10
                fprintf('Number of iterations:'),disp(j)
                break
```

```
            end
        end          % ending j

        %results
        Temperature_profile(:,h+1+(gmax+1)*g) = T(:,j);
        Concentration_profile(:,h+1+(gmax+1)*g) = z1(:,j);
        gh(1,h+1+(gmax+1)*g) = mtf_L;
        gh(2,h+1+(gmax+1)*g) = mtf_V;

        M_L_evap     = x1(1,j)*M1 + x2(1,j)*M2;
        M_V_cond     = y1(n,j)*M1 + y2(n,j)*M2;
        dH_in        = H_Vo(1,j) - H_Li(1,j-1)*rflx_evap;
        dH_out       = H_Vi(n,j) - H_Lo(n,j-1)*rflx_cond;
        m_evap       = L(1,j)*M_L_evap;
        m_cond       = V(n,j)*M_V_cond;
        Q(1,h+1+(gmax+1)*g) = dH_in*m_evap;      %Q in
        Q(2,h+1+(gmax+1)*g) = dH_out*m_cond;     %Q_out

    end          %ending h
end          %ending g
```

Appendix F – Reactor design

As determined in the basis of design, the reactor type is Lurgi. This reactor type is in essence equal to a shell and tube heat exchanger. The reactor consists of multiple parallel tubes in which the catalyst is placed. The tubes are bundled together in the shell through which the coolant flows. The coolant is a liquid vapor mixture that is held at a pressure for which the boiling point is 250 °C, in order to have optimal temperature control. In order to have an equal temperature at all catalyst sites, the tubes have to be sufficiently small. Since the methanol synthesis operates in the gas phase, a wall thickness of 2.2 mm is selected (Swagelok, 2017). The inner diameter of the tubes is set to 2 cm to obtain a constant temperature level of the reacting fluids. The larger the diameter, the larger the temperature gradient will become inside the reactor since the reaction is exothermic. To calculate the number of tubes inside the reactor, a clearance of 0.25*D in a square pitch is used (Edwards, 2008) as shown in figure F.1.

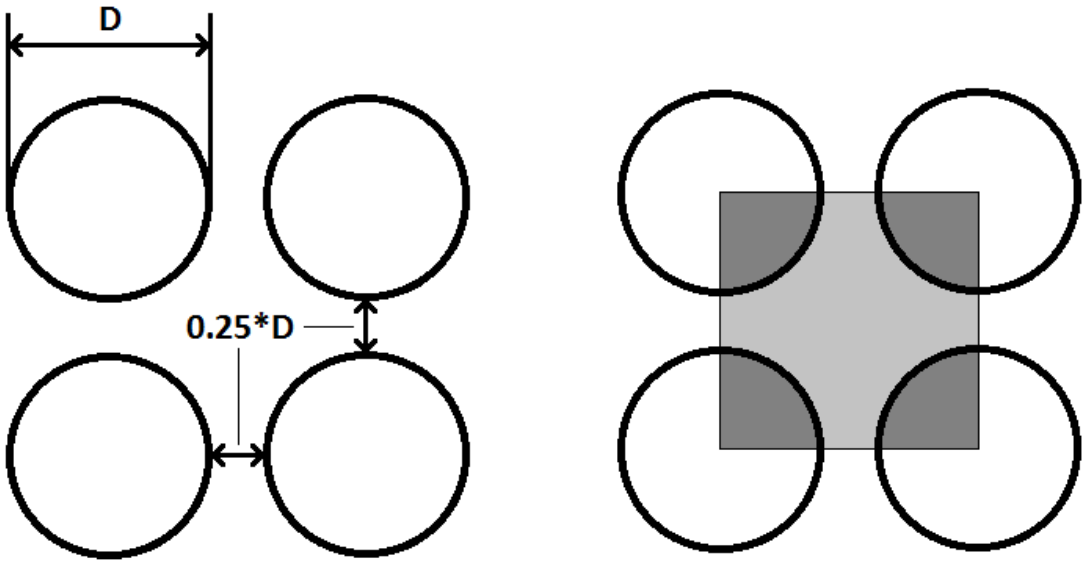

Figure 14 – Reactor tube configuration

The percentage of cross-sectional area that is covered by tubes is calculated using equation F.1, a visual representation of the occupied area is shown in figure F.1.

$$\frac{\frac{\pi}{4}D^2}{(1.25*D)^2} = \frac{\frac{\pi}{4}}{1.25^2} = 0.50 \tag{F.1}$$

In reality, this percentage will be lower due to space inefficiencies at the shell wall. Therefore, a percentage of 45% is assumed for the area covered by tubes.

The. The cross sectional area of the reactor shell is calculated using equation F.2

$$\frac{A_{tube}}{\eta_{tube}} * n_{tubes} \tag{F.2}$$

Where A_{tube} is the cross sectional area of one tube, η_{tubes} is the special efficiency and n_{tubes} is the number of tubes. Using the 45% calculated in equation F.1 and using the length and the diameter of the tubes from the optimization section in table 15, the total cross-sectional area can be calculated.

$$\frac{\frac{\pi}{4}*0.0244^2}{0.45} * 500 = 0.520\ m^2 \tag{F.3}$$

The pressure in the shell is set so that the boiling temperature of the steam is at 250 °C. In that way, the constant temperature of the reaction can be regulated well since the energy that is produced in the reaction will increase the quality of the steam and not the temperature. According to REFPROP, water has a boiling temperature of 250 °C at a pressure of 40 bar. The required wall thickness of the shell is calculated using equation F.4 (ASME Section VIII division 1 2011 edition code book, paragraph UG-27)

$$t = \frac{PR}{SE - 0.6P} \tag{F.4}$$

Where t is the wall thickness in mm, P is the pressure in MPa, R is the inside shell radius in mm, S is the maximum allowable stress value of the material in MPa and E is the joint efficiency, a dimensionless number to account for weakness in welds or other joints. A yield strength of the steel of 200 MPa and a joint efficiency of 0.7 is assumed. The radius of the shell is calculated from the cross-sectional area and is 0.407 m

$$t_{shell} = \frac{4 * 407}{200 * 0.7 - 0.6 * 4} = 11.8\, mm \tag{F.5}$$

For this design, a wall thickness of the shell of 15 mm is selected.

The same calculation is done for the tubes in the reactor to check whether the value of 2.2 mm is sufficient for the given pressure.

$$t_{tubes} = \frac{5.5 * 10}{200 * 0.7 - 0.6 * 5.5} = 0.4\, mm \tag{F.6}$$

Using a wall thickness of 2.2 mm, this is easily satisfied.

Appendix G – Reactor optimization

Table 42 – Reactor optimization configurations and results

	Base case	**Long tubes (eq. Loading)**	**Short tubes (eq. Loading)**	**More tubes (eq. Loading)**	**Fewer tubes (eq. Loading)**
Variables					
Length (m)	0.3	0.4	0.2	0.3	0.3
Number of tubes	650	650	650	800	500
Tube diameter (m)	0.02	0.02	0.02	0.02	0.02
Catalyst loading (kg)	70.7	94.27	47.13	87.02	54.38
Checks					
Max. catalyst loading (kg)	108.738	144.984	72.492	133.832	83.645
Total reactor volume (m3)	0.0613	0.0817	0.0408	0.0754	0.0471
Flow speed (m/s)	0.0189	0.0189	0.0194	0.0152	0.0249
Reactant dwelling time (s)	15.888	21.199	10.320	19.759	12.061
Reynolds number	190.12	189.99	195.14	152.87	250.45
Auxiliary constants					
Catalyst bulk density (kg/m3)	1775	1775	1775	1775	1775
Pi	3.14	3.14	3.14	3.14	3.14
Reactor volume flow (m3/s)	3.86E-03	3.85E-03	3.96E-03	3.82E-03	3.91E-03
Viscosity (Pa-s)	2.01E-05	2.01E-05	2.01E-05	2.01E-05	2.01E-05
Gas density (kg/m3)	10.097	10.097	10.097	10.097	10.097
	Base case	**Long tubes (eq. Loading)**	**Short tubes (eq. Loading)**	**More tubes (eq. Loading)**	**Fewer tubes (eq. Loading)**
Recycle stream mass flow	144.67	142.98	150.35	143.61	148.07
Reactor outlet mass flows					
WATER	13.59	13.592	13.576	13.588	13.579
CO2	69.106	67.938	73.122	68.526	71.607
HYDROGEN	24.631	24.344	25.323	24.329	24.968
METHANOL	26.214	26.194	26.252	26.188	26.229
CO	8.361	8.083	9.238	8.159	8.86
OXYGEN	0.629	0.627	0.63	0.626	0.629
NITROGEN	2.202	2.198	2.206	2.196	2.203
Product stream flow					
WATER	13.22	13.227	13.194	13.224	13.204
CO2	0.65	0.649	0.662	0.652	0.658
HYDROGEN	trace	trace	trace	trace	trace
METHANOL	23.243	23.258	23.183	23.252	23.207
CO	0.002	0.002	0.002	0.002	0.002
OXYGEN	< 0,001	< 0,001	< 0,001	< 0,001	< 0,001
NITROGEN	< 0,001	< 0,001	< 0,001	< 0,001	< 0,001

	Larger diameter	Smaller diameter	Higher catalyst loading	Lower catalyst loading	Optimized case
Variables					
Length (m)	0.3	0.3	0.3	0.3	0.2
Number of tubes	650	650	650	650	500
Tube diameter (m)	0.025	0.015	0.02	0.02	0.02
Catalyst loading (kg)	110.47	39.77	90	55	36.26
Checks					
Max. catalyst loading (kg)	169.904	61.165	108.738	108.738	55.763
Total reactor volume (m3)	0.0957	0.0345	0.0613	0.0613	0.0314
Flow speed (m/s)	0.0119	0.0351	0.0187	0.0192	0.0261
Reactant dwelling time (s)	25.177	8.553	16.050	15.639	7.677
Reynolds number	149.97	264.87	188.20	193.15	262.31
Auxiliary constants					
Catalyst bulk density (kg/m3)	1775	1775	1775	1775	1775
Pi	3.14	3.14	3.14	3.14	3.14
Reactor volume flow (m3/s)	3.80E-03	4.03E-03	3.82E-03	3.92E-03	4.09E-03
Viscosity (Pa-s)	2.01E-05	2.01E-05	2.01E-05	2.01E-05	2.01E-05
Gas density (kg/m3)	10.097	10.097	10.097	10.097	10.097

	Larger diameter (eq. Loading	Smaller diameter (eq. Loading)	Higher catalyst loading	Lower catalyst loading	Optimized case
Recycle stream mass flow	142.59	153.84	143.53	147.45	155.472
Reactor outlet mass flows					
WATER	13.592	13.57	13.588	13.587	13.576
CO2	67.745	75.502	68.443	70.891	76.193
HYDROGEN	24.235	25.815	24.34	25.088	26.327
METHANOL	26.184	26.284	26.188	26.246	26.331
CO	8.015	9.825	8.149	8.807	10.18
OXYGEN	0.626	0.634	0.626	0.629	0.639
NITROGEN	2.194	2.214	2.195	2.202	2.227
Product stream flow					
WATER	13.229	13.181	13.224	13.211	13.18
CO2	0.648	0.665	0.651	0.652	0.66
HYDROGEN	trace	trace	trace	trace	trace
METHANOL	23.263	23.151	23.251	23.219	23.144
CO	0.002	0.002	0.002	0.002	0.002
OXYGEN	< 0,001	< 0,001	< 0,001	< 0,001	< 0,001
NITROGEN	< 0,001	< 0,001	< 0,001	< 0,001	< 0,001

Table 43 – Base case

Mass flows	Before reactor	After reactor	After flash and purge	product stream	product after flash
WATER	0.346	13.59	0.346	13.24	13.22
CO2	101.459	69.106	67.124	1.304	0.65
HYDROGEN	29.062	24.631	24.342	0.043	trace
METHANOL	2.775	26.214	2.775	23.411	23.243
CO	8.259	8.361	8.259	0.018	0.002
OXYGEN	0.629	0.629	0.621	0.002	< 0,001
NITROGEN	2.202	2.202	2.176	0.004	< 0,001

Table 44 – Longer tubes

Mass flows	Before reactor	After reactor	After flash and purge	product stream	product after flash
WATER	0.342	13.592	0.342	13.247	13.227
CO2	100.308	67.938	65.973	1.299	0.649
HYDROGEN	28.777	24.344	24.058	0.043	trace
METHANOL	2.739	26.194	2.739	23.427	23.258
CO	7.985	8.083	7.985	0.018	0.002
OXYGEN	0.627	0.627	0.619	0.002	< 0,001
NITROGEN	2.198	2.198	2.172	0.004	< 0,001

Table 45 – Shorter tubes

Mass flows	Before reactor	After reactor	After flash and purge	product stream	product after flash
WATER	0.358	13.576	0.358	13.214	13.194
CO2	105.413	73.122	71.07	1.337	0.662
HYDROGEN	29.744	25.323	25.028	0.043	trace
METHANOL	2.87	26.252	2.87	23.351	23.183
CO	9.126	9.238	9.126	0.02	0.002
OXYGEN	0.63	0.63	0.622	0.002	< 0,001
NITROGEN	2.206	2.206	2.18	0.004	< 0,001

Table 46 – More tubes

Mass flows	Before reactor	After reactor	After flash and purge	product stream	product after flash
WATER	0.342	13.588	0.342	13.243	13.224
CO2	100.885	68.526	66.545	1.309	0.652
HYDROGEN	28.762	24.329	24.043	0.043	trace
METHANOL	2.742	26.188	2.742	23.419	23.252
CO	8.06	8.159	8.06	0.018	0.002
OXYGEN	0.626	0.626	0.618	0.002	< 0,001
NITROGEN	2.196	2.196	2.17	0.004	< 0,001

Table 47 – Fewer tubes

Mass flows	Before reactor	After reactor	After flash and purge	product stream	product after flash
WATER	0.352	13.579	0.352	13.223	13.204
CO2	103.919	71.607	69.576	1.327	0.658
HYDROGEN	29.393	24.968	24.676	0.043	trace
METHANOL	2.825	26.229	2.825	23.375	23.207
CO	8.753	8.86	8.753	0.019	0.002
OXYGEN	0.629	0.629	0.621	0.002	< 0,001
NITROGEN	2.203	2.203	2.177	0.004	< 0,001

Table 48 – Larger diameter

Mass flows	Before reactor	After reactor	After flash and purge	product stream	product after flash
WATER	0.34	13.592	0.34	13.248	13.229
CO2	100.117	67.745	65.78	1.301	0.648
HYDROGEN	28.669	24.235	23.95	0.043	trace
METHANOL	2.727	26.184	2.727	23.429	23.263
CO	7.916	8.015	7.917	0.018	0.002
OXYGEN	0.626	0.626	0.618	0.002	< 0,001
NITROGEN	2.194	2.194	2.168	0.004	< 0,001

Table 49 – Smaller diameter

Mass flows	Before reactor	After reactor	After flash and purge	product stream	product after flash
WATER	0.366	13.57	0.366	13.201	13.181
CO2	107.759	75.502	73.413	1.347	0.665
HYDROGEN	30.231	25.815	25.515	0.042	trace
METHANOL	2.934	26.284	2.934	23.32	23.151
CO	9.707	9.825	9.707	0.02	0.002
OXYGEN	0.634	0.634	0.626	0.002	< 0,001
NITROGEN	2.214	2.214	2.188	0.004	< 0,001

Table 50 – Higher catalyst loading

Mass flows	Before reactor	After reactor	After flash and purge	product stream	product after flash
WATER	0.342	13.588	0.342	13.243	13.224
CO2	100.802	68.443	66.465	1.307	0.651
HYDROGEN	28.772	24.34	24.054	0.043	trace
METHANOL	2.743	26.188	2.743	23.418	23.251
CO	8.049	8.149	8.049	0.018	0.002
OXYGEN	0.626	0.626	0.618	0.002	< 0,001
NITROGEN	2.195	2.195	2.169	0.004	< 0,001

Table 51 – Lower catalyst loading

Mass flows	Before reactor	After reactor	After flash and purge	product stream	product after flash
WATER	0.353	13.587	0.353	13.23	13.211
CO2	103.219	70.891	68.885	1.311	0.652
HYDROGEN	29.515	25.088	24.795	0.043	trace
METHANOL	2.831	26.246	2.831	23.386	23.219
CO	8.7	8.807	8.7	0.019	0.002
OXYGEN	0.629	0.629	0.621	0.002	< 0,001
NITROGEN	2.202	2.202	2.176	0.004	< 0,001

Table 52 – Optimized case

Mass flows	Before reactor	After reactor	After flash and purge	product stream	product after flash
WATER	0.373	13.576	0.373	13.199	13.18
CO2	108.446	76.193	74.111	1.334	0.66
HYDROGEN	30.741	26.327	26.022	0.042	trace
METHANOL	2.989	26.331	2.989	23.312	23.144
CO	10.058	10.18	10.057	0.021	0.002
OXYGEN	0.639	0.639	0.631	0.002	< 0,001
NITROGEN	2.227	2.227	2.201	0.004	< 0,001

Appendix H – Reactor pressure drop validation

The pressure drop over the reactor is 5 mbar. To validate this low result, the Reynolds number of the flow in the reactor tubes is calculated. The density and the dynamic viscosity are obtained from REFPROP. The relatively low amounts of water and methanol which accounts for only 1.7% of the mass is neglected in the calculation because REFPROP can't calculate reliable data using these substances. With the obtained density and viscosity, the Reynolds number can be calculated using the diameter of the tubes and the flow velocity.

$$Re_D = \frac{\rho v D}{\mu} \tag{H.1}$$

Table G.1 in appendix G shows the values for reactant velocity and the diameter of the tubes. The Reynolds number for these values is approximately 260. This means that the flow is well within the laminar region and a low pressure drop is expected. The presence of catalyst in the tube will negatively affect the pressure drop since pressure drop is correlated to the amount of friction the liquid experiences. This effect is not studied, but since the Reynolds number is well below the turbulence transition (2500-4000), it is concluded that the low pressure drop is still plausible.

Appendix I – K-value comparison

On comparing the K-values obtained from REFPROP with experimental data (Kiyofumi Kurihara, 1993), a significant difference between the two is found. Additional experimental data (J. Soujanya, 2010) at a comparable pressure matches better with the experimental data from (Kiyofumi Kurihara, 1993) than with the values found in REFPROP, further confirming the validity of the experiments. Figure I.1 shows the difference between the experimental data and the data obtained from REFPROP.

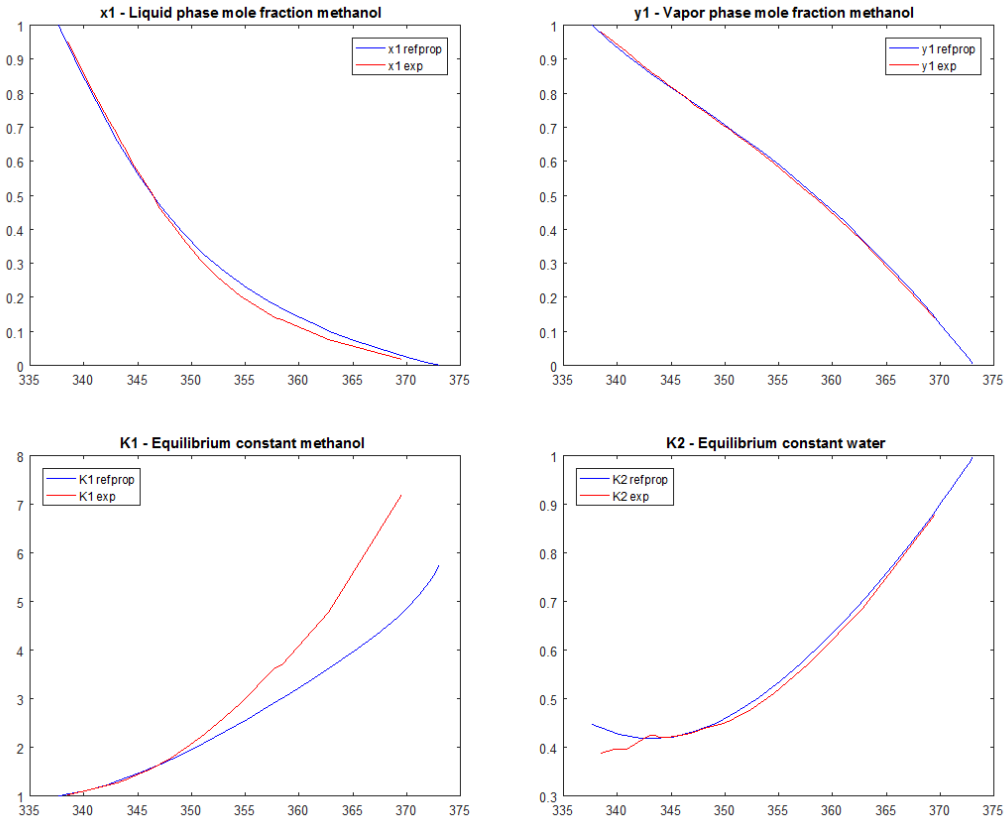

Figure 15 – Experimental and REFPROP data comparison

The REFPROP values for x_1 and y_1 only deviate little from experimental values, but since the K-values are calculated by dividing y_1 by x_1, the error is amplified significantly. Especially when the mole fractions approach 0 or 1, the error in the K-values increase.

Table 53 – K-values methanol/water mixture (Kiyofumi Kurihara, 1993)

Temperature (°C)	K value (methanol)	K value (water)	Temperature (°C)	K value (methanol)	K value (water)
64.5	1.001135	0.381668	74.92	1.776190	0.437931
65.31	1.031546	0.387755	76.39	1.991620	0.447040
66.51	1.083049	0.396694	77.43	2.156250	0.455882
67.74	1.148194	0.395939	77.71	2.203226	0.459420
69.26	1.230126	0.416961	79.3	2.488462	0.477027
69.96	1.272459	0.423676	81.36	2.897561	0.510692
70.44	1.308756	0.424069	84.61	3.628571	0.572093
70.68	1.329154	0.419890	85.23	3.699248	0.585928
71.55	1.409556	0.420290	89.57	4.779221	0.684724
73.23	1.570858	0.426854	96.41	7.210526	0.879715
73.94	1.662338	0.431227	99.9	8.794850	0.997727